STRUCTURE AND TECTONICS OF THE KEBAN METAMORPHICS IN

THE NORTHERN MARGIN OF THE BİTLİS SUTURE ZONE,

SOUTHEASTERN TURKEY

A thesis presented to the Faculty

of the State University of New York

at Albany

in partial fulfillment of the requirements

for the degree of

Master of Science

College of Science and Mathematics

Department of Geological Sciences

Gültekin Savcı

1983

State University of New York at Albany

College of Science and Mathematics

Department of Geological Sciences

The thesis for the master's degree submitted by

GÜLTEKİN SAVCI

Under the title

STRUCTURE AND TECTONICS OF THE KEBAN METAMORPHICS IN

THE NORTHERN MARGIN OF THE BİTLİS SUTURE ZONE,

SOUTHEASTERN TURKEY

has been read by the undersigned. It is hereby recommended

for acceptance by the faculty with credit to the amount of

6 semester hours.

(Signed) _W.S. Kidd_

(Date) _6ᵗʰ June 1983_

(Signed) _W. D. Means_

(Date) _6 / 6 / 83_

(Signed) _Kevin Burke_

(Date) _6 / 6 / 83_

Recommendation accepted by the Dean of Graduate for

the Graduate Academic Council.

(Signed) _R.H. Farrell_

(Date) _25 July 83_

STRUCTURE AND TECTONICS OF THE KEBAN METAMORPHICS IN

THE NORTHERN MARGIN OF THE BİTLİS SUTURE ZONE,

SOUTHEASTERN TURKEY

Abstract of

A thesis presented to the Faculty

of the State University of New York

at Albany

in partial fulfillment of the requirements

for the degree of

Master of Science

College of Science and Mathematics

Department of Geological Sciences

Gültekin Savcı

1983

ABSTRACT

The study area near Keban consists of the allochthonous Keban
division of the Keban-Malatya crystalline complex and the Yuksekova
island-arc rocks of the Bitlis-Puturge Complex in the northern margin
of the Bitlis Suture Zone. Detailed mapping shows that the Palaeozoic-
Triassic Keban Metamorphics are composed of the following formations:
(1) white, massive, karstic Kirklar Marble; (s) phyllitic psammite with
calcschist interlayers Calik Formation; and (3) semi-crystallized gray
Koyunatlayan Limestone. These formations define a tectonostratigraphy
with the Kirklar Marble at the base and the Koyunatlayan Limestone at
the top. The detailed lithological description of the Keban Metamor-
phic rock assemblages suggest that they represent a deformed continental
margin sedimentary sequence that has been metamorphosed to lower
greenschist facies sometime in Jurassic to early Cretaceous times.
The Keban crystalline rock units were cut by a group of hypabyssal
igneous rocks (syenite porphyry) which were produced during an exten-
sional regime (rifting) in late Cretaceous. In the map area, the
Campanian-Lower Maastrichtian Yuksekova Volcanic rocks are represented
by mafic extrusives and mafic volcaniclastics. They have experienced a
low grade greenschist metamorphism.

In the Keban Metamorphics, structural data indicate at least two
phases of penetrative deformational events (D_1 and D_2). There is also
evidence for two non-penetrative tectonic deformations (T_{oo} and T_3).
The contacts between the metamorphic rock units are folded thrust
faults (post-early Paleocene Pertek thrusting: T_{oo}) marked by fault
rocks; no associated folding has been seen. Along the fault zones,
a number of major mylonite and/or high-strain zones occur in the form

i

of ductile shear zone, each up to few thousands of meters long and several meters wide. Besides the foliated mylonites, the fault rocks of the Keban Metamorphics are represented by fault breccias and gouge zones which display an incohesive random-fabric. Detailed structural analysis shows that the deformation mechanisms in each fault rock depends largely on its main mineral constituent. In the map area, from east to west, the N-S striking fault zones change from brittle-ductile shear zones into brittle zones with the western side of the zone showing less ductile features (eg. the Corik and Bezirgandere Faults) than the eastern side (eg. the Hirsiz and Gelintas Faults). D_1 deformation phase is marked by tight to isoclinal folds (F_1); associated foliation (S_1: slaty cleavage and/or schistosity) and mineral elongation lineation (L_1). D_1 does not overprint any earlier deformation phase, but it does overprint the earlier tectonic structure (T_{oo}). It is overprinted by later D_2 deformation phase. D_2 is marked by open folds (F_2); a crenulation cleavage (S_2) and an intersection lineation (L_2). They overprint both the earlier tectonic structure (T_{oo}) and the earlier deformation phase (D_1).

In the study area, the contact between the Keban Metamorphics and the Yuksekova Volcanic Complex is a fault contact which strikes in N-S direction (the Keban Fault: T_3). The structural analysis conducted along the Keban Fault shows that this is a sinistral strike-slip fault with a large thrust component. The age of the fault is determined as post-early Paleocene to medial Eocene. The Keban Fault is marked by brittle fault rocks, slickensides, mylonite and other foliated highly-strained ductile fault rocks. No folds associated with this tectonic structure have been seen.

DEDICATION :

To my parents whose love

encouraged my research

and

To John F. Dewey

". . .The silver-shod goddess Tethys was
subject to Peleus and brought forth lion-
hearted Achilles, the destroyer of men."

Hesiod, Theogony, 1006-1007;
translated by Hugh, G., Evelyn-
White in Hesiod, the Homeric
Hymus and Homerica (London,
1959) p. 152-3.

TABLE OF CONTENTS

LIST OF TABLE

PLATES (located in back pocket)

1. Geological Map (1:12,000 scale)

2. Geological Cross Section

3. Profile sketches and locations of folds in the Keban Metamorphics,
   near Keban. (a) Regional geological map showing major tectonic
   setting of the western part of southeastern Turkey (see also
   Figure 1.4); (b) Outcrop map showing locations of sketched folds
   in the map   area.

4. Detailed structural map showing the relationship between the
   Keban Metamorphics and the Yuksekova Volcanic Complex (1:80
   and 1:2 scale), Locality 11 in Plate 5

5. Simplified Form Surface and Tectonic Map of the Keban
   Metamorphics, near Keban (1:35,000 scale).

ACKNOWLEDGEMENTS

CHAPTER 1

INTRODUCTION

Southeastern Turkey is an area of special interest from the point
of view of plate tectonics. It contains the Bitlis Suture Zone, a
tectonic feature that is a critical region in the evolution of the
Alpine-Himalayan orogenic belt.

The Bitlis Suture Zone is a consequence of the development of Neo-
Tethys. It connects the Taurus belt in the west and Zagros belt in the
east and forms the northern boundary of the shelf domain of the Arabian
continent. It extends for about 900 km from Hatay in the west to the
vicinity of the city of Hakkari in the east and ranges from about 100
to 300 km wide (Figure 1.1). The Suture Zone was formed as a consequence
of multiple opening and closing of parts of the Neo-Tethys ocean between
Lias and early Miocene epochs (Sengor and Yilmaz, 1981). It contains
mainly of Palaeozoic-Mesozoic crystalline basements (Bitlis, Puturge,
Keban and Malatya metamorphics: Figure 1.3), Jurassic-Cretaceous
ophiolites (Kocali ophiolite: Sungurlu, 1974; and Guleman ophiolite:
Erdogan, 1977), Maastrichtian-early Eocene flysch deposition (Hazar
complex: Perincek, 1979a), Campanian-Maastrichtian island arc volcanic
complex (Yuksekova complex: Perincek, 1978; Hempton, 1982; Hempton and
Savci, 1981, 1982), Maastrichtian sediments on top of the island arc
volcanic complex (Harami Formation: Perincek, 1979a), middle Eocene
Maden strike slip basin (Aktas, 1982) and/or marginal basin (Sengor and
Yilmaz, 1981) sediments and volcanics, Eocene-Miocene (Cungus basin:
Sungurlu, 1974; Sengor and Yilmaz, 1981) marginal basin sediments and
volcanics.

Figure 1.1.   Distribution of the Bitlis Suture Zone.   The
Bitlis Suture Zone connects the Taurus belt in the west and
Zagros belt in the east, and forms the northern boundary of
the shelf domain of the Arabian continent .   It extends for
about 900 km in length from Hatay in the west to the vicinity
of city of Hakkari in the east, and is between 100 to 300 km
wide.

Key:

Bitlis-Puturge Complex
(including the Kocali slices)

Keban-Malatya Complex

⎫
⎬ (Bitlis Suture Zone)
⎭

Munzur limestone (a segment
    of Anatolide-Tauride platform)

Key to abbreviations: EAF=East Anatolian fault zone,
K=Keban Metamorphics,   M=Malatya Metamorphics, m=Munzur
limestone, NAF=North Anatolian fault zone.
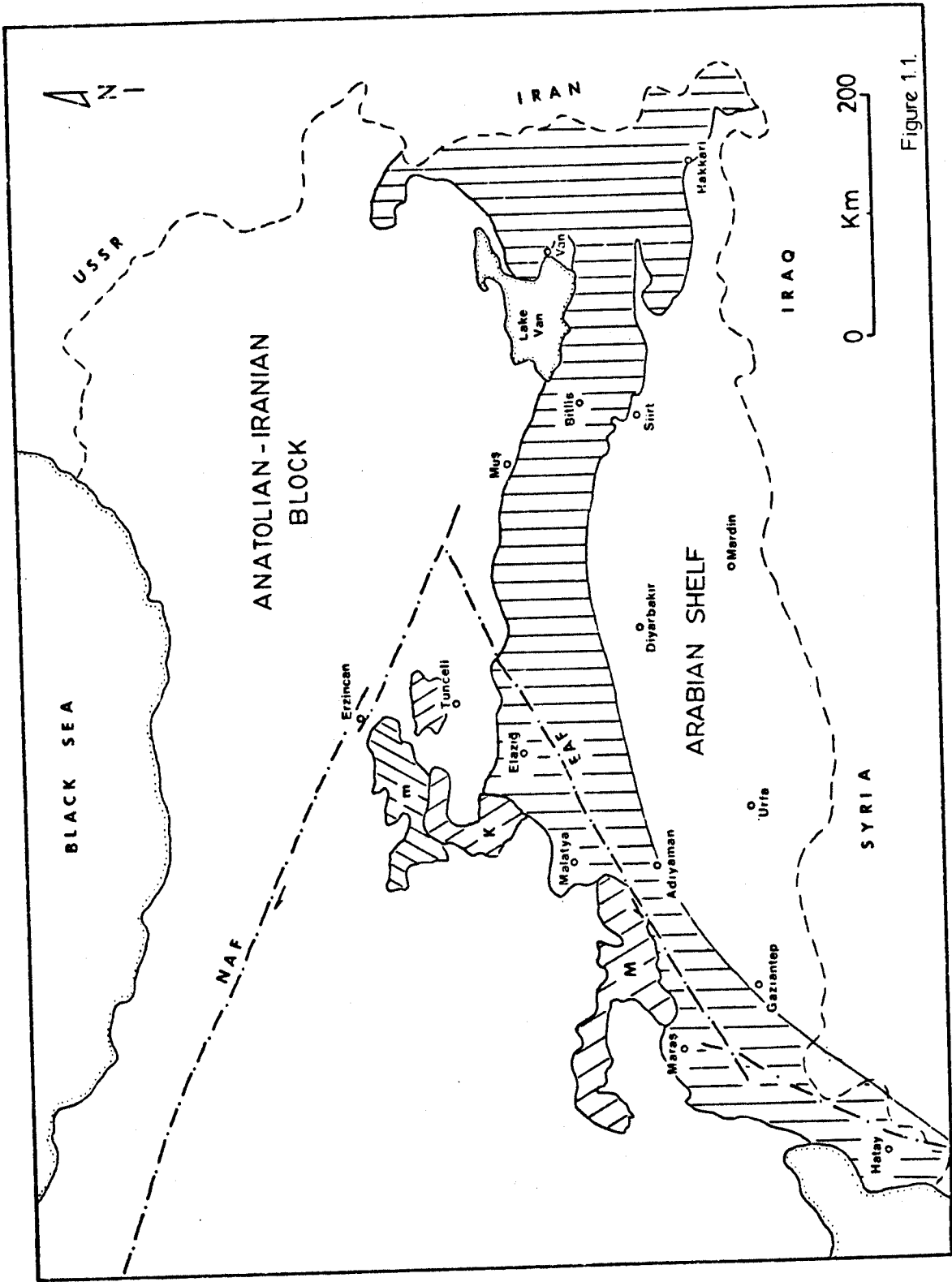
Figure 1.1.

The Bitilis Suture Zone consists structurally of four main slices (Sungurlu, 1974; Perincek, 1979a, 1980; Sengor and Yilmaz, 1981). They are named as follows (Figure 1.2):

1. Late Campanian-early Maastrichtian Kocali slices,

2. Early Paleocene Keban slices,

3. Post medial Eocene Yuksekova slices,

4. Post early Miocene Cungus slices.

Four segments of crystalline basement can be recognized within the suture zone. They are Bitlis, Puturge, Keban and Malatya metamorphics (Figure 1.3). Although Keban-Malatya metamorphics are similar to the Bitlis-Puturge metamorphics, they differ from the Bitlis-Puturge metamorphics because of their distinct lithology and structural position and of the absence of Jurassic and Cretaceous sediments on top of them unlike the stratigraphic succession present on top of Bitlis-Puturge metamorphics (eg. the Maastrichtian-early Eocene Hazar Complex). Another distinct property of the Keban-Malatya metamorphics is the syenite igneous activity (due to rifting) in late Cretaceous time (see Chapter 2). The differences of the nature, distribution and relative lithologic proportions of the Keban-Malatya Metamorphics and Bitlis-Puturge Metamorphics are discussed in Chapters 2 and 4.

The study area, near Keban, is located to the south of Keban Dam-Lake in the vicinity of the city of Elazig (Figure 1.4). It is under-lain by unfossiliferous greenschist facies crystalline rock series (Keban Metamorphics) and by mafic extrusives, volcaniclastics, tuff and granodioritic intrusions (Yuksekova Volcanic Complex). The crystal-line series mentioned above formed between Palaeozoic and Triassic (Kipman, 1981; Perincek and Ozkaya, 1981) and are cut by syenite group

Figure 1.2. Map illustrates the four main tectonic slices in the Bitlis Suture Zone.

1. Late Campanian-early Maastrichtian Kocali slices
2. Early Paleocene Keban slices
3. Post medial Eocene Yuksekova slices
4. Post early Miocene Cungus slices

(They are numbered in the order of emplacement with number 1 having been emplaced first.)

Abbreviations are same as those in Figure 1.1. The map is drawn according to author's interpretation of the data reported by Sungurlu (1974, personal communication in March 1982); Perincek (1979a, 1979b); Sengor and Yilmaz (1981). For detailed explanation of the Keban fault, see Chapters 2 and 3.

Figure 1.2.

Legend:

- post early Miocene Cüngüs Slices
- post middle Eocene Yüksekova Slices
- early Paleocene Keban Slices
- late Campanian-early Maastrichtian Koçali Slices
- post early Paleocene-medial Eocene Keban fault
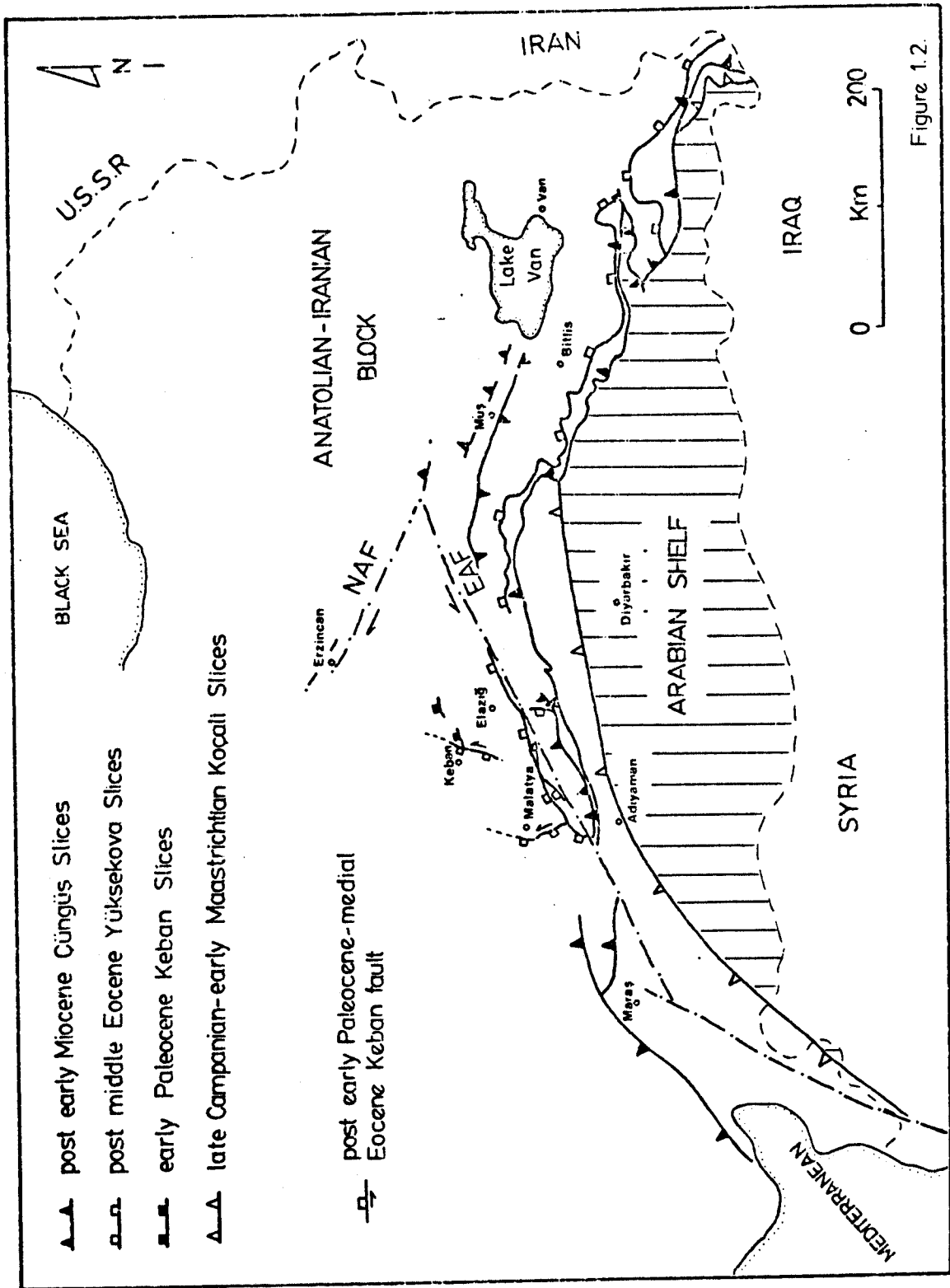
Figure 1.3.   Distribution of the crystalline basement within
the Bitlis Suture Zone.   The map is compiled from Geological
Map of Turkey, 1/500,000 (1961-1964);   Adamia et al. (1980).
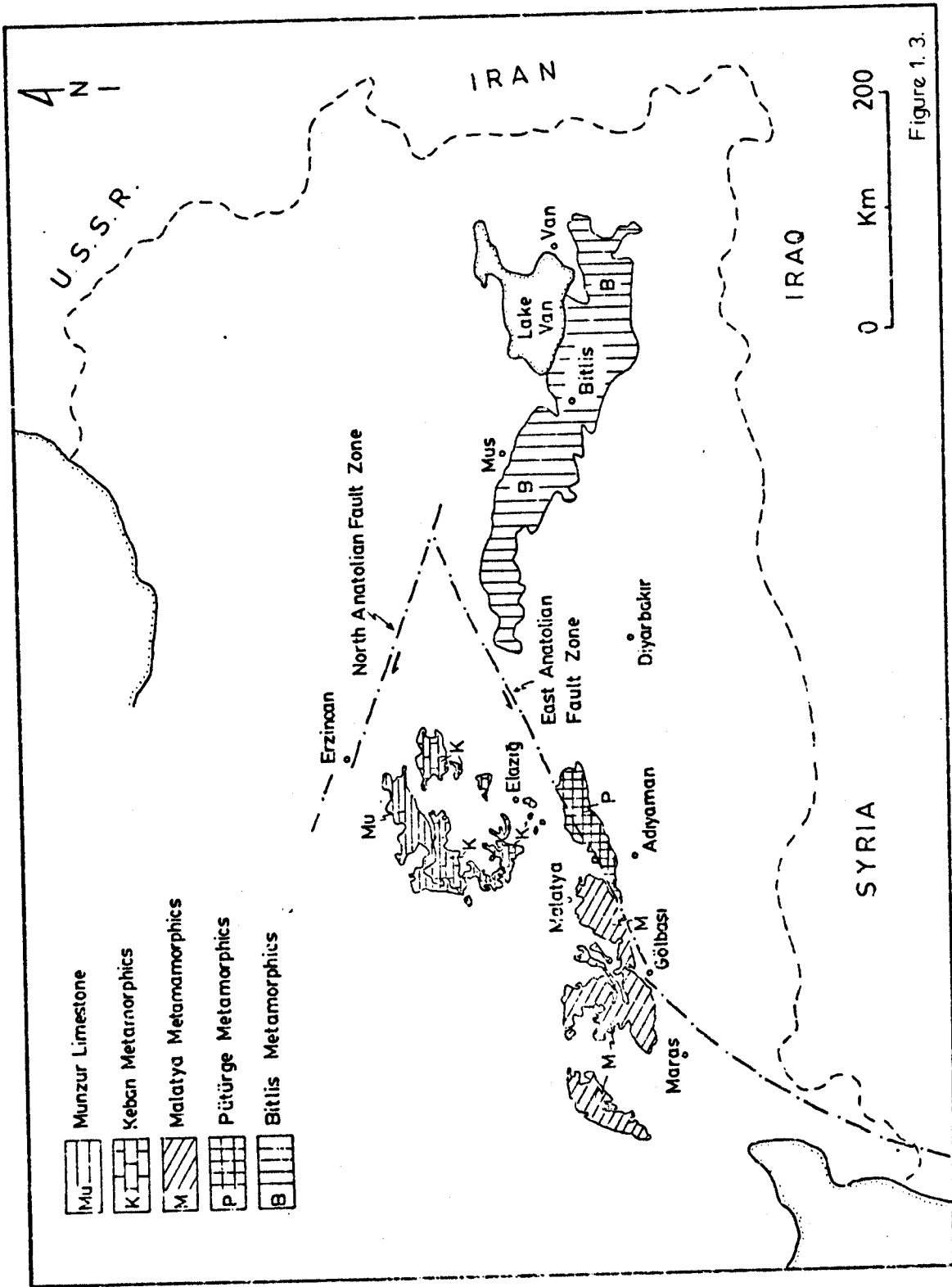
Figure 1.3.

hypabyssal rocks (syenite porphyries) intruded during the late Cretaceous.
The Keban Metamorphics are tectonically restricted by the Mesozoic
Munzur limestone and ophiolites of Ovacik Unit (Ozgul et. al, 1982) both
in the north, where the contact roughly strikes in an east-west direction,
and by the Yuksekova Volcanic Complex in the south whose contacts
roughly strike both in east-west (in the vicinity of the town of Pertek)
and north-south (in the study area, Keban) directions (Figure 1.4).
Farther south, the Malatya Metamorphics, lie tectonically on both Maden
Complex to the northeast of Celikhan, and on Yuksekova Volcanic Complex(?)
in the southeast of Malatya city (Figure 1.4).

Two different crystalline formations (Puturge Metamorphics and
Keban-Malatya Metamorphics), distinct with respect to their strati-
graphical and structural characteristics are shown in figure 1.4. The
Puturge Metamorphics which lie to the south are an extension of the
Bitlis Metamorphics which are found to the east (Figure 1.3). These
are derived from Palaeozoic-Mesozoic sequences. Jurassic-Cretaceous
Guleman Ophiolites, Maastrichtian-early Eocene flysch type sediments
(Hazar Complex), medial Eocene Maden strike-slip and/or marginal basin
and Eocene-Miocene Cungus marginal basin sediments and volcanics
(these four complexes are named as Ergani Complex by Sengor and Yilmaz,
1981; see Figure 1.4), and Campanian-early Maastrichtian Yuksekova
Volcanic Complex are all placed on Puturge Metamorphics (Sungurlu, 1974;
Perincek and Ozkaya, 1981; Sengor and Yilmaz, 1981). These complexes
and formations outlined above are named as "Bitlis'Puturge Complex" in
this thesis for ease of explanation (Figure 1.1). The non-fossiliferous
Keban and Malatya Metamorphics were formed between Palaeozoic and Triassic
(Kipman, 1981; Perincek and Ozkaya, 1981). The Keban Metamorphics are

Figure 1.4.   Simplified geological map and tectonic setting
of the area between Cungus in the south and south of Erzincan
city in the north shows the location of the study area (details
are discussed in the text).   The Elazig Fault in the map, first
recognized and named by the author in his 1980-field work,
is completed from the landsat image.   The faults are the same
as those shown in Figure 1.2.   In conjunction with the author's
own observations, the map is compiled and somewhat reinter-
preted from M.T.A.   (1961a, 1961b); Perincek (1979a, 1979b);
Sengor and Yilmaz (1981); Yazgan (1981).

Figure 1. 4.

cut by a group of hypabyssal igneous rocks (syenite porphyries), and no
sedimentary deposition has occurred (or been preserved) on the Malatya
and Keban Metamorphics during the whole of Jurassic and Cretaceous times
(Perincek and Ozkaya, 1981; Yazgan, 1981). This complex, which lies to
the north of the Bitlis-Puturge Complex, is names "Keban-Malatya Complex"
(Figure 1.1). The contact between these two complexes is a faulted
contact, partially covered with seidmentary and volcanic formations
(such as Seske, Kirkgecit and Karabakir Formations) deposited in late
Paleocene and late Miocene (Perincek, 1979a). The Mesozoic Munzur
limestones are a part of the Anatolide-Tauride platform (Ketin, 1966;
Sengor and Yilmaz, 1981) and are placed on the Keban Metamorphics with
tectonic contacts. The northern branch of the ophiolites of the Neo-
Tethys which are found next to the northern and southern parts of the
Munzur limestones are defined as Ovacik Unit by Ozgul et al. (1982).
The emplacement age of the ophiolites and Munzur limestones over the
Keban Metamorphics was determined as late Campanian-early Maastrichtian
by the same authors.

Keban is a town in the study area, linked to Elazig city by a
54 km (35 mile) long highway which was constructed in the early 70's
while the dam construction as in process. A 16 km (10 mile) long
portion of this highway cuts the study area in NW-SE direction parallel
to Keban Cayi (stream in Turkish = cay) (Figure 1.5). As is shown in
figure 1.5, besides the main Keban-Elazig highway, four secondary
stabilized roads link this highway to the villages in the vicinity.
The present field study was carried out in two separate sessions in the
summer and autumn-winter of 1981 with a total of eight weeks in the field.
The first session was completed between June 1st and July 1st prior to
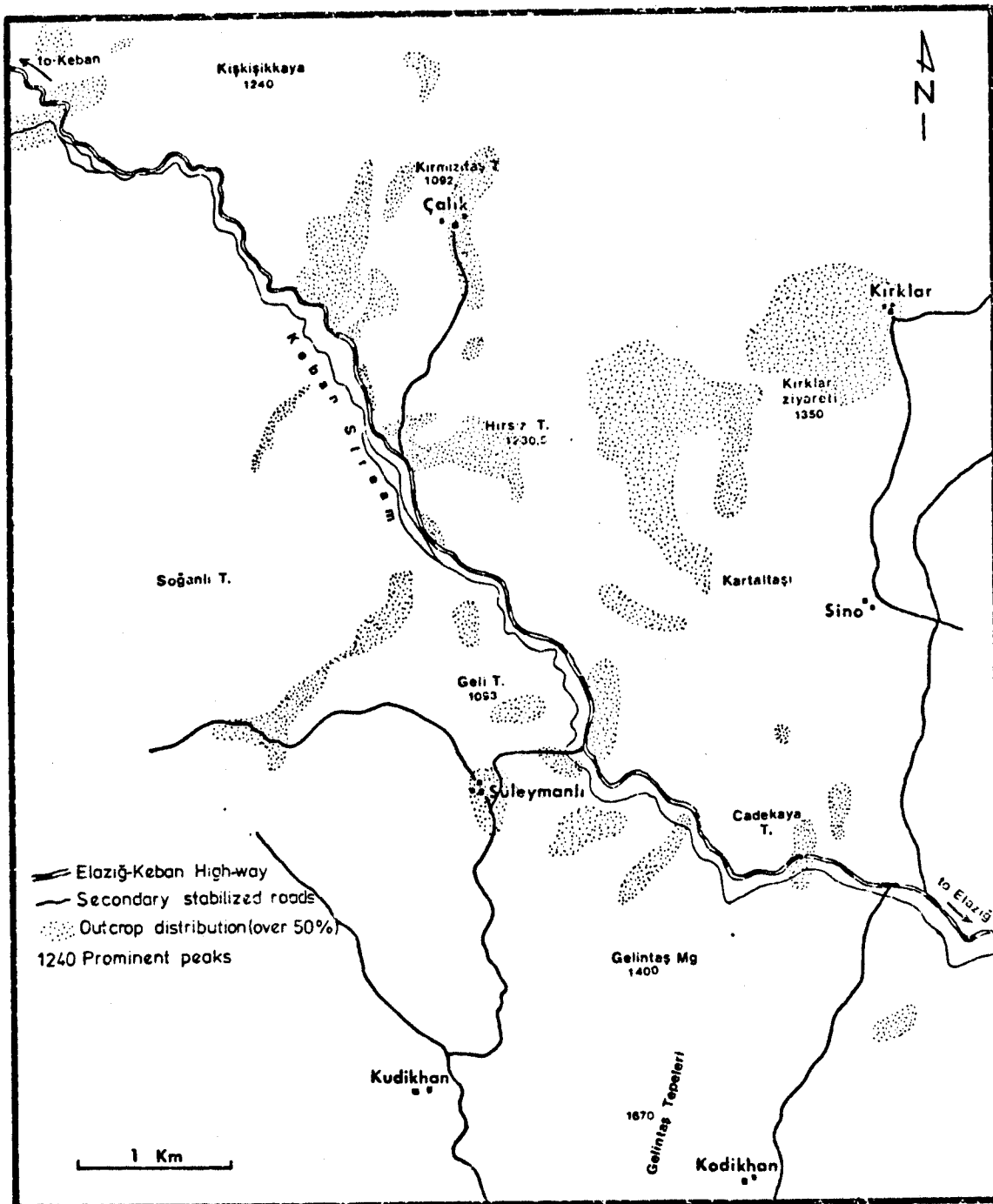
Figure 1.5. Distribution of the well-exposed outcrops and the roads in the map area.

compulsory military service, and the second session was completed between November 1st and December 1st after the completion of the military service.

From the study a 1:12,000 scale outcrop map of an area of 40 km^2 was drawn (Plate 1) involving a detailed structural mapping and analysis of folds and faults within the Keban greenschist facies rocks, in order to identify the internal structure of the metamorphics. Moreover, the contact relationship of Keban Metamorphics with Yuksekova Volcanic Complex was analyzed in detail (Plate 4). (A short lithological description of Yuksekova Volcanic Complex based on a 1:25,000 scale geological mapping conducted in a 40 km^2 area south of Elazig city (Figure 2.23), by the author in his five weeks of field work in 1980 summer is also given in this volume). From the new data obtained, a new plate tectonic model was developed to describe Neo-Tethyan evolution for eastern and southeastern Turkey emphasizing the tectonic importance of the Keban-Malatya Complex. During the geological mapping (Plate 1) all the outcrops in the area were individually observed, and they are shown on the map as dots with their characteristics. The area contains almost no trees enabling all the outcrops to be easily seen (for the distribution of the outcrops in the area, see Figure 1.5). The outcrops were mapped at a larger scale (eg. 1:3,200; 1:2 etc.) in parts where it was useful to do so (for example, to elucidate contact relationships: Plates 3 and 4).

It is generally very hot and dry in summer and extremely cold in winter in the area. The town of Keban which is 1.5 km from the NW corner of the study area is at an altitude of 730 meters. The highest points of the study area are Gelintas Tepe (hill in Turkish = tepe)

(1670 m), Gelintas Magara (cave in Turkish = magara) (1400 m), Kirklarziyareti Mevki (site in Turkish = mevki) (1350 m), Kiskisikkaya (1240 m), Hirsiz Tepe (1230.5 m), Geli Tepe (1093 m) and Kirmizitas Tepe (1092 m) (Figure 1.5). While the majority of the population in the area is occupied with agriculture and herding, a considerable portion works in the Keban Dam complex.

The reasons for the selection of the location as a study area are as follows:

Turkish Petroleum Corporation (T.P.A.O.) in the area from Hakkari in the east to Adiyaman-Golbasi in the west (Figure 1.1) has completed a 1:50,000 scale geological map in ten years of research both on Arabian Shelf Platform and the Bitlis-Puturge Complex. Also, in the same area various Ph.D studies has been completed (eg. Boray, 1972; Ozkaya, 1972; Hall, 1974; Erodogan, 1977; Perincek, 1978; Yalcin, 1979; Bastug, 1980; Hempton, 1982 etc.) as well as some projects (eg. the Bitlis project of Geological Survey of Turkey: M.T.A. and Turkish Universities projects). However, the lack of information on the general structural characteristics and importance of Keban and Malatya Metamorphics prevents a well-constrained general geotectonic interpretation of the east and southeast Turkey. Also, the insufficienty of serious geological and engineering studies in the early 60's before the dam construction started has caused concern to the author. In the selection of the study area a great deal of help has been received by the author from Dogan Perincek and Ozan Sungurlu.

The intentions of the study were six fold:

1) Detailed outcrop mapping in order to understand the structural and stratigraphic features of the Keban Metamorphics.

2) To obtain deformation phases of volcanics and crystalline formations and layering-cleavage relations. To this end, microstructural analysis of foliations and different generations of folds and faults were studied in specimens. Outcrop photos were extensively used for the recording and later analyzing minor structural relations. All outcrop maps and sketches (Plates 3 and 4) used as illustrations in this volume are map and/or cross section view.

3) To determine the metamorphic grade of the crystalline formations and the volcanics.

4) To comprehend the relationship between Keban Metamorphics and Yuksekova Volcanic Complex in the Keban area.

5) To determine the intrusion age of the syenite prophyries that cut across the metamorphics, and from this to better understand their geotectonic significance. However, I believe that a reliable age determination for these igneous rocks will only be obtained by Isotope Geochemistry.

6) To build a new plate tectonic model of the Keban and Malatya Metamorphics and their implications for Neo-Tethyan evolution, based on the data obtained and on the comparison of the microstructural and regional findings of the study with that of the findings of data from the larger region.

Method:

The field season of this research was supported by Turkish Petroleum Corporation (T.P.A.O.) during the summer and autumn-winter 1981. This organization provided base maps. Base maps consisted of 1:12,000 scale enlargements of 1:25,000 scale topographic maps. Air photos were not used because they were not available at the time the mapping was

in progress. Because topographic maps are top secret in Turkey, the topographic contours are not shown on the geological map (Plate 1) but are indicated on a small scale map (Plate 3).

This study attempted to cover an area small enough to be mapped in detail in the period of time available and large enough to be representative of the northern boundary of the Bitlis Suture Zone. Most field work consisted of outcrop mapping on a scale of 1:12,000 (Plate 1) and in parts where it was necessary (to show contact relationships of fold generations etc.) small areas were mapped on larger scale (1:3,200 to 1:2; for example, Figure 4 in Plate 3 and Plate 4). Since terraces and alluvial fans are not large or abundant in the map area, they are not shown on the geological map. Where the contact between the map units are covered by the small alluvial fans, they are drawn with dashed lines on the map.

A cross section (Plate 2) was drawn WSW-ENE (A-A' portion of the section) and NW-SE (B-B' portion) (i.e. cross strike) through the best exposure of the field area.

Approximately 210 kg of rock samples were shipped from the field area to Albany. Numbers of polished slabs and about 55 thin sections were described in detail. Some of the detailed petrographic and microstructural descriptions were not included in this thesis but are in my possession. They will be available upon request. The thin sections and rock samples are in the possession of the Department of Geological Sciences, State University of New York at Albany and will also be available upon request.

CHAPTER 2

LITHOSTRATIGRAPHY

2.1 Introduction

The area of this study is entirely underlain by the allochthonous

Keban division of the Keban-Malatya crystalline complex and the Yuksekova

island-arc rocks of the Bitlis-Puturge Complex in the northern margin

of the Bitlis Suture Zone. The Campanian-Lower Maastrichtian Yuksekova

Volcanic Complex outcrops in the eastern one-fifth part of the map area,

and the Keban metamorphic rocks occupy rest of the map area. The contact

between these two complexes is a contact which roughly strikes both in

east-west (in the vicinity of the town of Pertek) and north-south (in

the map area, Keban) directions (Figure 1.4 and Plate 1). The contact

that strikes in the east-west direction, named the Pertek Fault, is

partially covered with the Upper Paleocene-Lower Eocene Seske Formation

around Pertek (Perincek, 1979a, 1979b, 1980) and also to the north of

Elazig city. This implies that a major episode of thrusting of Keban-

Malatya Complex over the Bitlis-Puturge Complex had been completed by

early Paleocene. The structural analysis conducted along the north-

south directed faulted contact (Keban Fault), which this research is

concerned with, shows that this is a strike-slip fault with a large

thrust component (Plate 4). The sense of strike-slip motion of the

fault is determined as left lateral (Plate 4) (detailed features of

the Keban Fault are discussed in Chapter 3). In the map area, the

absence of any sediments along the fault contact does not allow determi-

nation of the age of the fault. However, those alluvial fans that

partially cover the contact (Plate 1) are unaffected by the fault,

implying that the fault has not been active very recently. Also, the north-south directed Keban Fault cuts the east-west directed Pertek early Paleocene thrust. This is clearly seen both on 1:500,000 scale Geological Map of Turkey (M.T.A., 1961a, 1961b) and the landsat image of this region (see Figure 3.44). Putting together the data in T.P.A.O's unpublished geological map of the region (1:50,000 scale), Perincek (1979a), and with reevaluation, it is seen that the Keban Fault has not affected the post-Eocene sediments near its south end, nor does it cut the post-medial Eocene Yuksekova thrusts further south (see Figure 1.4). The age of Keban Fault is therefore assumed to be post-early Paleocene to medial Eocene in this thesis.

Within the study area, the Palaeozoic-Triassic Keban Metamorphics consist of the following formations: 1. white, massive, karstic marble (Kirklar Formation), 2. phyllitic psammite with calcschist interlayers (Calik Formation), 3. semi-crystallized gray limestone (Koyunatlayan Formation). In the largest exposures these formations define a tectono-stratigraphy with the Kirklar Formation at the base and the Koyunatlayan Formation at the top (Plate 2). The crystalline formations were meta-morphosed to lower greenschist facies in Jurassic to early Cretaceous time and were intruded by a group of syenite hypabyssal rocks (syenite porphyries) during the late Cretaceous time. Also present in the area are terraces and alluvial fans. The terraces indicate the ancient level of the Keban Stream, in the map area. The Campanian-Lower Maastrichtian Yuksekova Volcanic rocks which are in the east of the map area are tectonically restricted from Keban Metamorphics by the Keban Fault. In the map area, these volcanics are represented by mafic

extrusives and mafic volcaniclastics. Besides the mafic extrusives
and mafic volcaniclastics, some gronodioritic intrusions have been
observed within the mafic extrusives, and pelagic limestone lenses,
along the Elazig-Keban highway.

The purpose of this chapter is to review previous work, to
describe lithological detail and metamorphic features of the units of
the Keban Metamorphics and the Yuksekova Volcanic Complex near Keban.
The detailed structural description and its genetic interpretation
is discussed in Chapter 3. The structural relationships of the Yukse-
kova Volcanic Complex with the Keban Metamorphics are also considered
in Chapter 3. Ideas concerning the tectonic implication of these two
complexes for the tectonic evolution of the northern margin of the
Bitlis Suture Zone are discussed in Chapter 4.

2.2. Keban Metamorphics

The Keban-Malatya Complex, which crops out in the western four-fifths of the map area, forms the northern margin of the Bitlis-Puturge Complex. It extends for about 400 km from northeast of Tunceli in the northeast to Maras in the southwest, and ranges for about 200 km from Munzur Mountain in the north to Golbasi in the south (Figure 1.3). In the map area, the metamorphic terrain occupies approximately 30 km^2. The highest point with an altitude of 1,820 m (Kusakli Tepe, which is 2 km south of Gelintas Tepe: see Figure 1.5) and the lowest point with an altitude of 730 m (the town of Keban) give the maximum relief of 1,090 meters. Since these two points are separated by approximately 12 km from each other, a minimum structural thickness of at least 1,100 meters can be safely assumed for the Keban Metamorphics in the map area. The area of the metamorphic terrain contains almost no trees so the rock exposures are abundant. Outcrop mapping at a scale of 1:12,000 was conducted within the map area in the summer and autumn-winter of 1981 with a total of 8 weeks in the field. Some outcrops were mapped and sketched at a larger scale (1:60 to 1:2) in places where it was useful to show fold generations, and contact relationships of the metamorphics.

2.2.1. Previous Work

Until now, there has not been any detailed geological study on the Keban Metamorphics. Geologists have made studies and comparisons in the Bitlis-Puturge Complex and Arabian shelf terrains. They have thought of the Keban-Malatya Metamorphics as a part of the Bitlis-Puturge Metamorphics.

The Keban region has been of interest, at the end of the 19th

century and the beginning of the 20th century, to mining geologists, because of the presence of lead-zinc mineralization formed at the contact of the syenite porphyry intrusions in the metamorphics of the Keban region. The first geological report on the region was done by Fischbach (1900). From his 1877 study, he reports the operation of the lead-zinc mines and the existence of mines and old workings. Later, the lead reserve researches by M.T.A. between 1934 and 1940 were summarized in a report by Yener (1935). After this date the foreign and Turkish researchers who worked in the Keban region gave conflicting lithological descriptions and stratigraphical sequences. Some of these are outlined here.

Yener (1935) described the Keban Metamorphics as calcphyllite at the base and crystallized limestone at the top. Maucher's (1937) and Oelsner's (1938) main concern was with the mineralization of the Keban region. Oelsner (1938) claimed that the metamorphics are composed of crystallized limestone at the base and schists at the top. Kovenko (1941) reported from his 1938 study that the metamorphics consist of green-gray calcschist with limestone interlayers at the top and marbles at the base. He further claimed that the contact relationships between these two units are tectonic. Borchert (1952) described two units; phyllite and calcareous schist. He asserted that the marbles that Kovenko (1941) described are interlayers within the phyllite unit. He further noted an Alpine type deformation which formed the tectonic frame of this region. Sagiroglu (1952) describes two phases of deformation in the region. He suggests that the schist unit is younger than the crystal-lized limestone which he defined in the Keban region. Tolun (1955) mapped

at a scale of 1:5,000 in the Keban area. He describes the crystalline rocks bottom to top as follows: micaschist; calcschist; sericite-schist; and marble. He claims that the complication in the stratigraphic position among the crystalline rock units is a consequence of a Paleozoic deformation. He also claims that the syenite porphyries are folded together with the metamorphic rock formations. Gawlik (1958) divided the metamorphics into three units. They are bottom to top: psammitic schists-mica rich calcschist; crystallized limestone; and phyllite. Zuesman's (1969) and Kines' (1971) work are based on the mineralization of the Keban region.

M.T.A. (The Geological Survey of Turkey) has completed a 1:500,000 scale Geological Map of Turkey and has published them under the editor-ship of Cahit Erentoz in 21 separate sheets with accompanying texts. The sheets which deal with the Keban Metamorphics were compiled by Altinli (1963) and Baykal (1966). Their 1:500,000 scale maps show the general boundaries of the Keban Metamorphic rock series. For the Keban Metamorphics, their map shows an "undifferentiated metamorphic series" of Palaeozoic age. It contains some large irregular marble bodies. However, they show that they thought of the Keban-Malatya metamorphic rock series as a part of the Bitlis-Puturge Metamorphics in the accom-panying text. In the accompanying tectonic map of Baykal (1966), the Keban Metamorphics are marked as a single large anticlinorium in NNE-SSW direction. He also illustrates the syenite porphyries as a part of an "Upper Cretaceous (occasionally with ophiolite and Paleocene)" map unit in the geological map.

Kumbasar (1964) describes the Keban Metamorphics from bottom to top: graphitic sericitic calcschists; semi-crystallized dolomitic

limestones; calc-phyllites; and crystallized limestones. She describes

the petrography of the syenite porphyries in detail. Based on her

petrographic and geochemical study, she concludes that the syenite

porphyries were formed from a granosyenitic and syenite granitic magmas.

Kipman (1981) states that the metamorphics around the Keban area

consist of marble, recrystallized limestone-calcschist and metaconglo-

merate-calcphyllite. He determined some Permo-Carboniferous fossils

(Glomospira, Ammediscus) in the recrystallized limestone-calcschist

unit. He specifies the age of the metamorphics as Permo-Carboniferous

to Triassic. He describes the syenitic igneous rocks which cut across

the metamorphics as syenomonzonitic-syenitic subvolcanics (Kipman, 1982).

He claims that these were formed from the salic and alkalic rich magma

in four different phases in the following order: (a) Pyroxene trachy-

latite, (b) Pyroxene-Hornblende trachylatite, (c) Hornblende biotite

trachyte and (d) Alkali trachyte. He suggests the late Cretaceous-

Paleocene for the volcanic activity.

Before and after the construction of the Keban Dam, the State

Power Consultants (E.I.E.I.) and the State Waterworks Company (D.S.I.)

have conducted a series of studies on the engineering geology in

relation to the dam. Besides the danger of the dam site being very

close to the active East Anatolian Fault, this group has always denied

the severe tectonism for southeastern Turkey. They stated this in their

reports related to the dam saying that the town of Keban is a convenient

area for the dam construction. But after the construction had started,

noticing that the construction site lies on a big fault (the Bezirgan

Fault), this group reports that they have moved the site slightly to

the north (Tilford and Ciloglu, 1969). Unfortunately in the report by

E.I.E.I.(1972) it is observed that these researchers still take the same view of the seismic hazard of the area.

Most of the researchers mentioned above gave conflicting results about the region. The almost total absence of fossil control in the metamorphic units as well as the severe tectonism makes it virtually impossible to establish the original stratigraphy among the lithologic units. Because of this fact all the researchers who worked in the area, depending on the particular part they worked on, reported different stratigraphic sequences.

In the southeastern Turkey, modern studies began with the work of Turkish Petroleum Corporation (T.P.A.O.) geologists. T.P.A.O., in the area from Hakkari in the east to Malayta in the west (Figure 1.1), completed a 1:50,000 scale geological map in 1978. The result of this research has published by Perincek (1979a, 1980). Perincek (1979a) describes the Keban Metamorphics as marble with amphibolite interlayers around the Pertek area. Perincek (1979a, 1980) observed that the east-west directed thrust contact (Pertek Fault: see Figure 1.4) between the Keban Metamorphics and Yuksekova Volcanics is overlain by Upper Paleocene-Lower Eocene Seske Formation and Upper Eocene-Oligocene Kirkgecit Formation. This suggests that a major episode of thrusting of the Keban-Malatya Complex over the Bitlis-Puturge Complex had been completed by early Paleocene. However, Hempton (1982), misinterpreting findings of Perincek, concludes that the thrusting between the two complex had completed by early Eocene: "In the northern part of the suture zone, the Seske Formation (Upper Paleocene-Lower Eocene) overlies and seals a north-dipping thrust contact between the Keban Metamorphics and the

Elazig-Yuksekova Complex. This implies that a major episode of thrusting had been completed by the early Eocene." (Hempton, 1982, p. 266)

Ozgul (1976), based on his field studies between 1967 and 1975 in the Central and Eastern Taurus belt, classifies the basic geological characteristics of the Taurus belt into six units. He defines the Bolkardagi, Aladag, Geyikdagi and Alanya Units as shelf type carbonates and detritic sediments; Bozkir and Antalya units as deep sea sediments, ophiolites and basic volcanics. He adds the Keban Complex to the Alanya Unit, and the Munzur Limestone to the Geyikdagi, and the ophiolites to the Bozkir Unit. Noticing the differences among these, Ozgul et al. (1982) renamed the Alanya Unit as Keban Unit, Bozkir Unit as Ovacik Unit and Geyikdagi Unit as Munzur Limestone for the eastern Taurus region. These units are separated from each other by tectonic contacts. The emplacement age of the ophiolites of Ovacik Unit and Munzur Limestone over the Keban Metamorphics was determined as late Campanian-early Maastrichtian by the same authors. They also state that the Munzur Limestones are unmetamorphosed and are composed of Upper Campanian pelagic micrites. They define the Ovacik Unit as mainly of ophiolitic melange and partially Lower Maastrichtian and younger detritic resific limestone.

Sengor and Yilmaz (1981) state that the Bitlis, Puturge, Malatya and Keban Metamorphics represent a continental fragments of the Cimmerian continent (Sengor, 1979a) disintegrated in early Jurassic and define these as Bitlis/Puturge Massifs. They suggest that the Bitlis/Puturge Massifs were Late Pre-Cambrian basements upon which

Palaeozoic and Mesozoic sediments were deposited without any major break. Objections to the Bitlis/Puturge Massifs definition of Sengor and Yilmaz (1981) emerged later on such as Bergougnan and Fourguin (1982), Perincek and Ozkaya (1982), Ozkaya (1982).

Perincek and Ozkaya (1982) and Ozkaya (1982) compare the Keban-Malatya Metamorphics with the Bitlis-Puturge Metamorphics and suggest that there could be an oceanic basin between them. They claim that they are different in their structural position. These authors also compare the Bitlis-Puturge Metamorphics with Arabian Shelf sediments and interpret that these could merely be the fragments of Arabian Continent. Based on this assumption, they drawn a potential boundaries of a "Keban Micro-plate" which they locate to the north of the Bitlis-Puturge Metamorphics and theArabian Platform. Their structural and lithological correlation criteria are not very convincing.

2.2.2. Lithology

The age of Keban Metamorphics were specified by Kipman (1981) as Permo-Carboniferous to Triassic based on fossils (_Glomospina_, _Ammedicus_) found in the equivalent to the Koyunatlayan limestone defined below, around Zeryan Stream which is to the northwest of the map area. In general, however, the metamorphics are unfossiliferous. The absence of fossil control in the metamorphic formations as well as the severe tectonism makes it difficult to establish the original stratigraphy among the lithologic units. However, in the studies done so far, almost all of the researchers mentioned above in the "Previous Work," designate different stratigraphic sequences in different areas. Besides, the necessary stratigraphic criteria, or structural criteria

such as vergence (Bell, 1961), have not been found to determine the younging direction of these formations. For these reasons, the lithologic units described in the map area, are defined from the bottom to top according to their tectonostratigraphic positions. Since the units previously defined appear not to be applicable to this area, at least in the way they were originally defined the units are given geographical names from the region in this study. The following descriptions of the tectonostratigraphy from base to top and all field identification of rocks are based entirely on lithologic definitions and the structural position of the lithologies.

A. Kırklar Formation

This unit consists of cracked and highly karsted marbles (Figure 2.1), with weathered surfaces pale grayish dull white, and fresh surfaces pinkish white, dull reddish white and generally white. These hard and massive, jointed rocks outcrop in the cores of antiforms, which have roughly north-south oriented fold axes, located in the east and west parts of the map area (Plates 1 and 2). The State Power Consultants (E.I.E.I.) (1972) names this unit the Keban Marbles. Since the whole metamorphic mass is referred to by the same name, it is renamed the Kırklar Formation in this study. The best reference localities within the study area are continuous outcrops on the Kiskisikkaya at the northwestern part of the map area and the Gelintas Tepeleri at the southeastern part of the map area. Its minimum structural thickness is estimated 600 meters. The nature of its contact with other units of the metamorphics is defined below.

The sparitic (Pettijohn, 1957; AGI Glossary, 1972) Kırklar marbles

Figure 2.1 A view of the Kirklar Formation, looking southwest toward the Gelintas Tepeleri from Elazig-Keban highway.
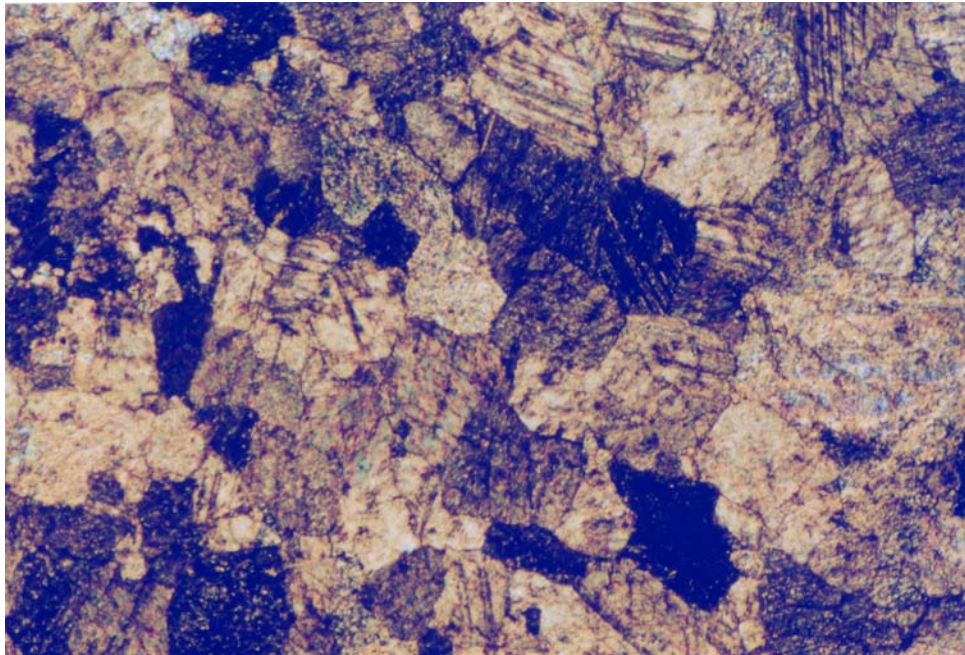
Figure 2.2 A microscopic view of sparitic Kirklar Marble (x40, crossed Nicols)..

are composed of both clear and brownish calcite crystals which comprise 95-98 % of the rock. These show a granoblastic, mosaic texture. Closer to the fault zones, the characteristics of the texture starts to change and a lepidoblastic texture can sometimes be observed. The calcite crystals which are the fundamental elements of the marbles show a high degree of twinning. In between the calcite crystals some muscovite (1-2%) and epidote (2-3%) crystals can be seen. In this type of marble, the muscovite crystals define foliation, but this foliation can only be seen under the microscope and is not obviously visible in hand specimen or outcrop. In between and also inside the calcite crystals are 1 to 2% of opaque minerals. Iron-Oxide appears to be the dominant opaque. Figure 2.2 illustrates a microscopic view of the Kirklar Marble.

The Kirklar Marble is the lowest of the tectonostratigraphic formations in the map area. On top of these, Calik and Koyunatlayan Formations, which will be defined below, occur above a thrust contact. Along the Kirklar-Calik contact, partly in Kirklar but mainly in the Calik Formation, there is a mylonite zone (see Chapter 3) which is 3 to 5 meters thick (in Corik Dere-Asi Dere: Figure 2.3). Along the contact of the Kirklar and Koyunatlayan Formations, about 5 meters thick mylonite zone (western edge of the Gelintas Magrasi) and about 35 meters thick gouge zone are observed in the north of Gelintas Tepeleri (Figure 2.4). After the faulting that juxtaposed the units that form the metamorphics, they were all folded together. The result of folding because of the massive and hard characteristics of the Kirklar Formation, are only seen at a small scale in a couple of places. Two generations of folds have been identified (detail structural features of the metamorphic units are discussed in Chapter 3).

Figure 2.3   A 3 meter thick mylonitic zone formed in the Calik Formation along the Corik Fault; Locality 1 in Plate 5.

Figure 2.4   A view of the contact between Kirklar and Koyunatlayan Formations (Gelintas Fault), looking southeast toward Gelintas Tepeleri from the Elazig-Keban highway; Locality 5 in Plate 5. Key to abbreviations: K=Kirklar Marble, Ko= Koyunatlayan Limestone, m=mylonite zone, G=Gouge zone, ---=Traces of the fault contact

On the geological map (Plate 1), the tectonic map (Plate 5), and in the cross section (Plate 2), the Kirklar Formation forms the core of anti-forms having roughly north-south axes (see Chapter 3).

In the Kirklar Formation whithin the eastern part of the map area a very fine grain mylonitic foliation (Figure 2.5) is also observed at the faulted contact (Keban Fault) with the mafic extrusives of Yuksekova Volcanic Complex.

In the mylonites, depending on the physical characteristics of the rocks, different scales of mylonitic and shear band foliations can be seen (Berthe et al., 1979 a, b; Watts and Williams, 1979; Platt and Vissers, 1980; Vauchez, 1980; White et al., 1980; Gapais and White, 1982). The details of these are discussed in Chapter 3.

A 3 m thick metamorphosed microdiorite dike, with chilled margins, cuts across the Kirklar Marble in one place along the southeastern part of the Elazig-Keban highway (Figure 2.6A and see also Plate 1). Apophyses of meta-microdiorite are injected from the meta-microdiorite body into adjacent marble (Figure 2.6B). The strongly foliated meta-microdiorite dike is a dark, blackish gray to yellowish green, generally dark green colour, with a mafic mineral composition: (in decreasing order of abundance) albite; green biotite; clinozoisite; epidote; opaque minerals; sphene; some calcite, apatite and very rare quartz have been identified (Figure 2.7). This metamorphic mineral assemblage, except apatite which may represent one of the original mineral constituents, shows that the microdiorite dike experienced low grade greenschist meta-morphism into a biotite-epidote subfacies (Miyashiro, 1973). None of the previous workers in various areas of the Keban Metamorphics have mentioned such dikes cutting across the metamorphics. The metamicrodiorite

Figure 2.5 A very fine grained mylonite zone formed in the Kirklar Marble along the Keban Fault. The mylonite is characterized by compositional layering (see also Chapter 3 and Figure 3.41).

Figure 2.6   A meta-microdiorite dike (A) with chilled margins (B) cuts across the Kirklar Formation; Locality 10 in Plate 5.
Apophyses of meta-microdiorite are injected from the meta-microdiorite body into adjacent marble (B).
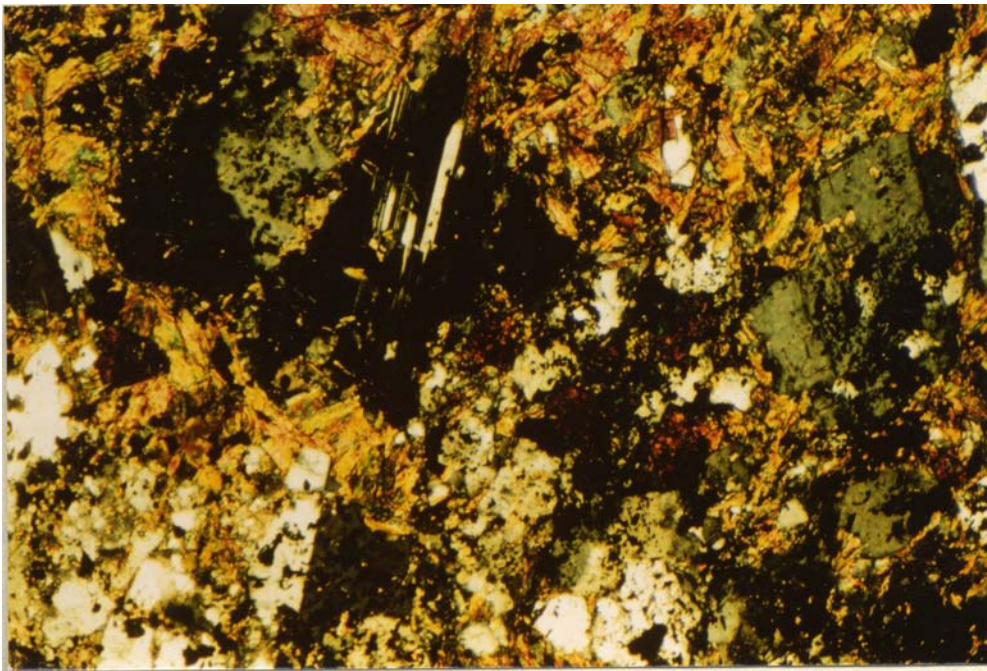
Figure 2.7   Optical micrograph of the meta-microdiorite (x40, crossed Nicols).

is not observed in any other places in the map area.

Perincek (1979a) first described a 1 to 150 m thick amphibolite interlayer within the equivalent to the Kirklar Marble around Singec Koprusu (kopru is bridge in Turkish), which is about 50 km east of the map area. I participated in a one-day field trip organized to the area mentioned above with Fevzi Bingol who is a professor at the Firat University at Elazig. He is carrying out a research on this important aspect of the metamorphics around the town of Pertek. In the study area, however, no amphibolite interlayers have been found either in the Kirklar Formation or in the other metamorphic units.

B. Çalık Formation

The Calik Formation consists of generally dark gray phyllitic psammite with pale greenish-yellow gray weathered surfaces. The phyllitic psammites are interlayered with mostly gray calcschist from 1 cm to 20 cm thick which are in places grayish dull white to reddish-pinkish gray. The best exposures of the Calik Formation is seen around Calik and north of Hirsiz Dere. Its minimum structural thickness is estimated 250 meters. This unit overlies the Kirklar Formation with a thrust contact and represents the second tectonostratigraphic formation in the map area among the crystalline rocks. Figure 2.8 illustrates a typical outcrop appearance of the Calik Formation. One mm to 20 cm thick quartz and calcite veins are also commonly observed within the Calik Formation (see Figure 3.27). The Calik Formation outcrops in a zone of low relief up to 700-1000 m wide in the middle of the map area. This strip is controlled by the north-south oriented fold system (Plate 1 and 5).

40 to 45% calcite, and 25 to 30% quartz form the dominant mineral composition of the calcschist interlayers of Calik Formation. It also

Figure 2.8   Typical Calik Formation outcrop in Calik Koyu (koy is village in Turkish).

contains 10 to 15% muscovite-sericite, about 10% iron-oxide, 5% chlorite and very rare feldspar (plagioclase). The calcite crystals are both clear and brownish, showing a lepidoblastic texture (Figure 2.9); the long axes of the lepidoblastic calcite crystals are usually subparallel to the preferred orientation of muscovite and chlorite. They also show a high degree of twinning. The quartz crystals, on the other hand, show granoblastic texture (Figure 2.9). A weak foliation (S_1=schistosity) and mineral elongation lineation (L_1) are developed, manifested by lenses and rod shaped grains of muscovite-sericite, chlorite aggregates on a mm to cm scale, and a preferred orientation of muscovite-sericite and chlorite. A second generation of foliation (S_2) is weak in calcschist layers (See Chapter 3 for detail).

The phyllitic psammite of Calik Formation is a dark gray, fine grained rock with mineral composition: 75 to 80% quartz, 10 to 15% muscovite-sericite, 5% iron-oxide, 4% chlorite, 4% calcite, 2% epidote and very rare graphite and feldspar (plagioclase). Figure 2.10 shows a microscopic view of the phyllitic psammite. Two generation of foliations (S_1=slaty cleavage—sometimes transposed foliation (Hobbs et al. 1976): Figures 1 and 6 in plate 3—, and S_2=crenulation cleavage) and two lineations (L_1=mineral elongation lineation, L_2=intersection of the foliations) are very well developed. The earlier foliation (S_1=slaty cleavage) is defined by preferred orientation of layer quartz, muscovite-sericite and chlorite, and is crenulated on a microscale (S_2=crenulation cleavage). All those foliation and lineation elements are subparallel to each other in most places. Details of these structures and layering-cleavage relationship and their structural implications are discussed in Chapter 3.
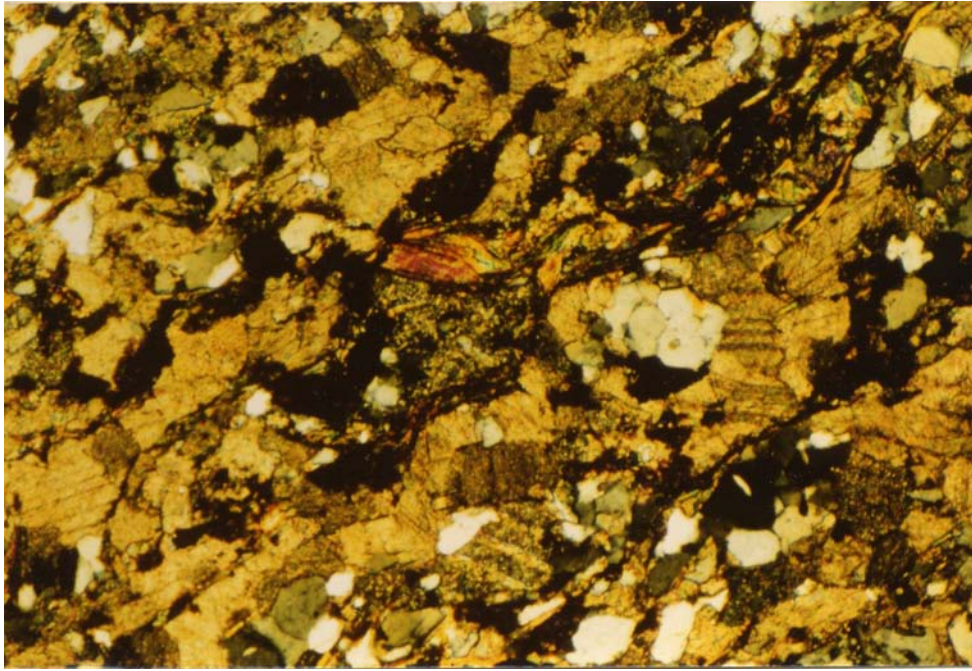
Figure 2.9   Microscopic view of calcschist of the Calik Formation (x40, crossed Nicols).
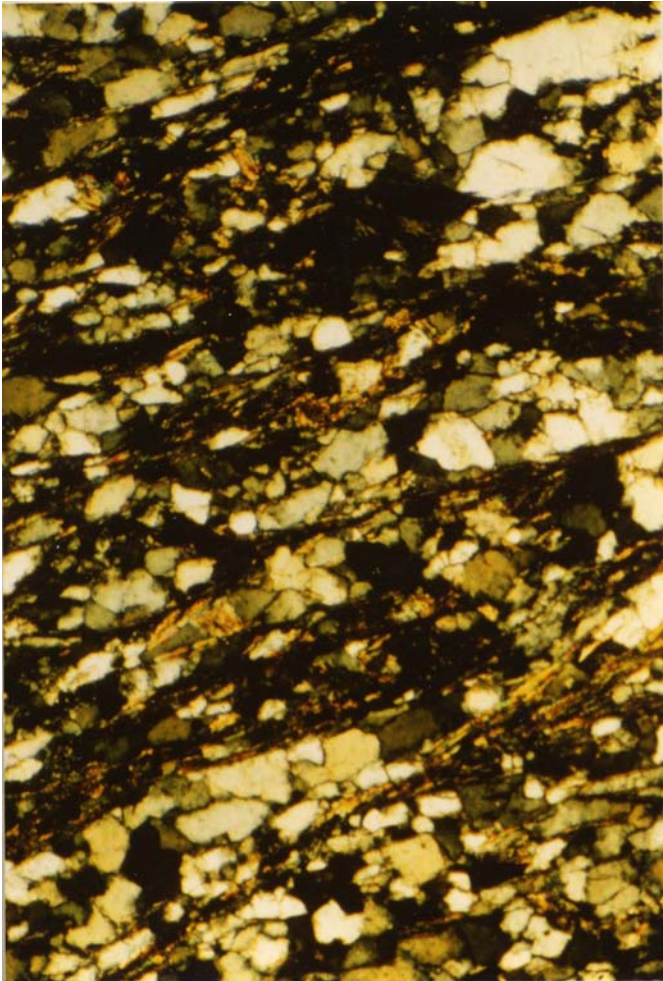
Figure 2.10   Optical micrograph of phyllitic psammite of the Calik Formation (x40, crossed Nicols).

C.   Koyunatlayan Formation

The structurally highest metamorphic unit in the map area consists
of semi-crystallized light, dull brown, light gray and usually dark gray
limestone which has a dull yellow-brown, yellowish gray, white-gray
weathered surfaces.   In this thesis it is defined as the Koyunatlayan
Formation.   It tectonically overlies both Calik and Kirklar Formations
(Plate 1 and 2), and outcrops in a zone up to 2,000 m wide in the western
part, and also in a zone 900 m wide in the eastern part of the map area
(see Plate 1).   Both zones are in the cores of synforms of the roughly
north-south oriented fold system (Plate 2).   The best outcrops of the
Koyunatlayan Formation is seen along the Koyunatlayan Dere.   The
estimated minimum structural thickness of this unit is at least 300
meters.   Figure 2.11 illustrates the typical outcrop appearance of the
Koyunatlayan Formation.

The Koyunatlayan limestone shows generally granoblastic (Figure
2.12), but in places lepidoblastic (Figure 2.13) texture.   The mineral
composition is 85 to 95% calcite, 2 to 5% iron-oxide, 2% plagioclase,
3% quartz, and some muscovite-sericite minerals which are common on
the surface of the limestone layers.   2 to 3% epidote also represents
one of the mineral constituents of the Koyunatlayan limestone.   Muscovite
rods in length up to several mm often exist on layer surfaces and define
a mineral elongation lineation which is parallel with hinge lines of
folds where they are observed together (see fold 14 in Plate 3).
However, the rock shows very weak schistosity, and it can be classified
as sparitic limestone (Pettijohn, 1976; AGI Glossary, 1972) (Figure 2.14).
It differs from the Kirklar Formation by its distinct colour and from
the Calik Formation by its lithological features and mineral composition.

Figure 2.11   An outcrop appearance of the Koyunatlayan Formation, north of Karaagac Dere.
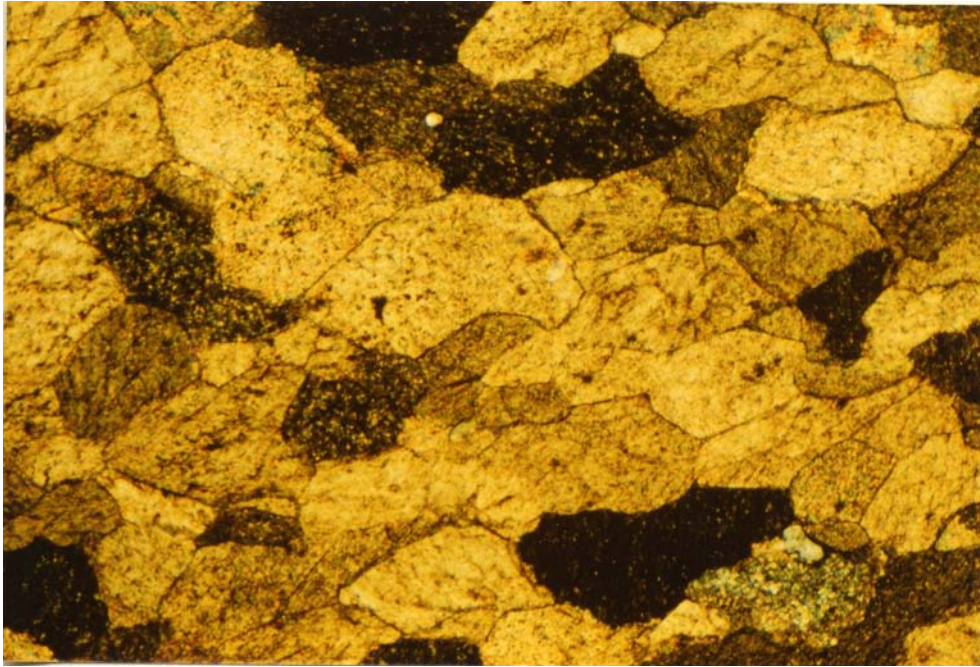
Figure 2.12 Microscopic view of the Koyunatlayan Limestone showing granoblastic texture (x40, crossed Nicols).
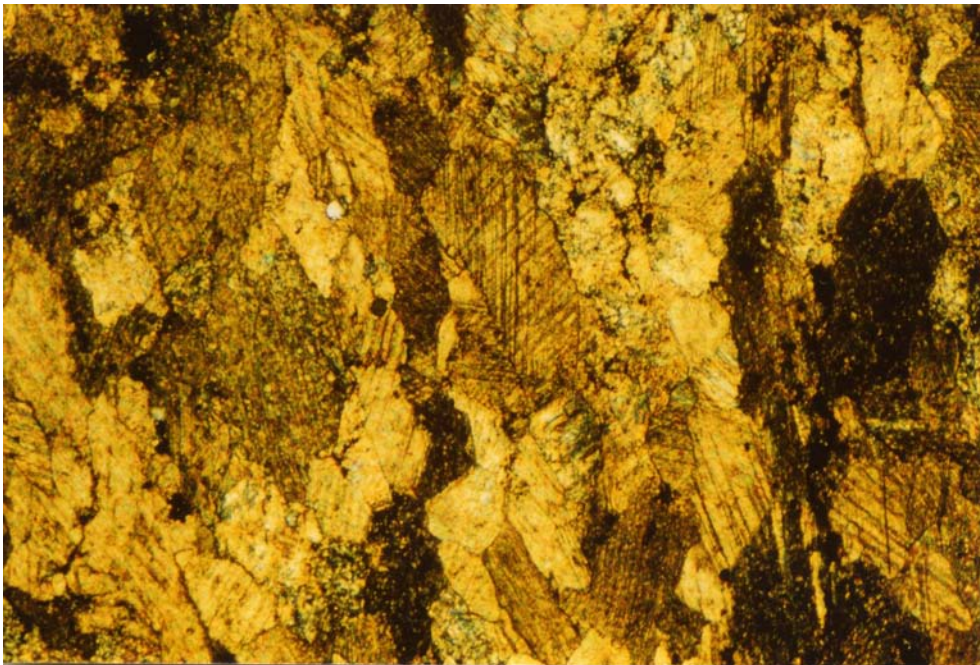
Figure 2.13 Microscopic view of the Koyunatlayan Limestone showing lepidoblastic texture (x40, crossed Nicols).

```
size    >50% CLASTICS   >50% CHEMICAL
                        PRECIPITAE
  ∞
            Calcirudite

  2 mm                    Sparite or
                          Sparrudite
            Calcarenite
 1/16mm
                                          1/100mm
            Calcisiltite                  1/250mm
                          Transitional?
1/256mm
            Calcilutite   Micrite or
                          Micrudite
 1/∞
```
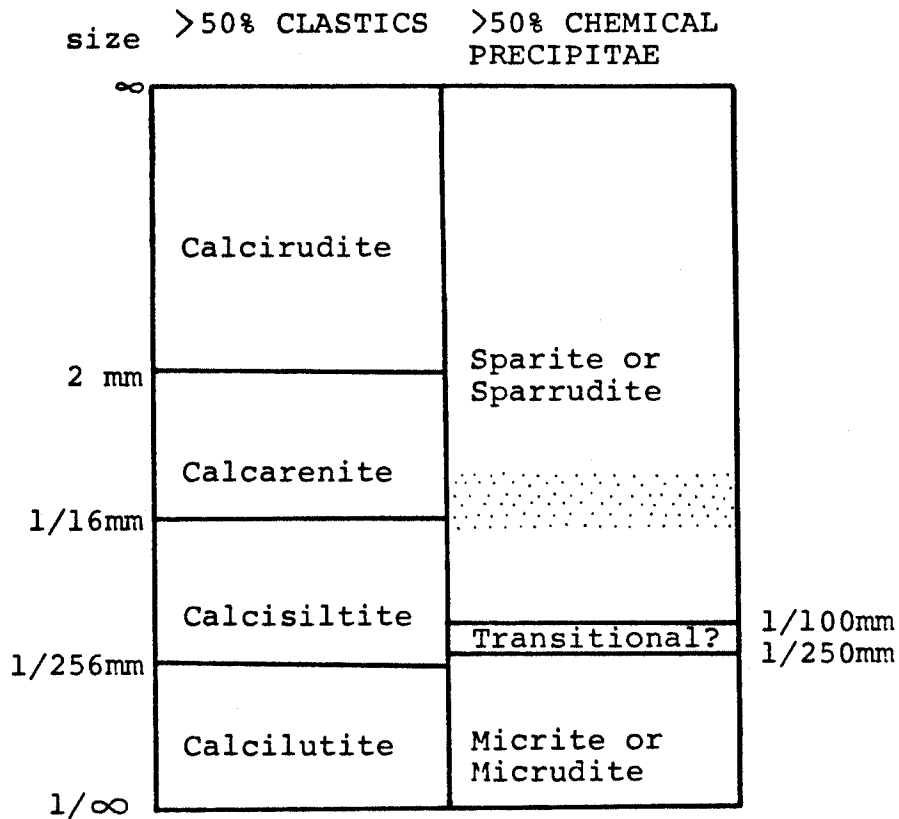
Figure 2.14.   Limestone classification diagram based on Pettijohn
(1957) and the AGI Glossary's (1972) definitions.   In the absence
of extensive fossil debris the distinction between chemical and
detrital carbonate can be very difficult, especially when
textures suggest recrystallization.   Therefore, the rocks studied
were assigned almost exclusively to the right side of the chart
(after Jacobi, 1977 (figure 50), Stratigraphy, Depositional
Enviroment and Structure of the Taconic Allochthon, Central
Washington County, NY : Master Thesis, SUNY-Albany, 191 pp.).

         Distribution of the calcite crystals in the Koyunatlayan
         and Kirklar Formations.

In the Koyunatlayan Formation, two generation of folds are well defined on the basis of overprinting relationships. Since no younging criteria have been found, they named as synforms or antiforms on the basis of their field occurence (see Chapter 3 for detail).

2.2.3. Igneous Activity

A group of hypabyssal igneous rocks which cut across the crystalline rock series in the Keban region are called "syenite porphyry." They have received various names for the syenitic magma such as "trachyte" for extrusive rocks, and "microsyenitic" or "syenite porphyry" for hypabyssal rocks (Nockolds et al., 1978). In general, the mineralogy of the syenite porphyry is more like that of the syenites than of the trachytes. It differs from the trachyte by its phaneritic groundmass texture (Travis, 1955) (see Figure 2.16).

Several apophyses of syenite porphyry outcrop in the map area, cutting across the Calik Formation (Figure 2.15) (see Plate 1 for the distribution of the syenite porphyry outcrops in the map), but they cut across all the crystalline units to the west and northwest of the study area. The main igneous body is situated around Siftiltepe and Nalliziyaret Tepe (Tolun, 1955; Kumbasar, 1964; Kipman, 1982) to the northwest of the map area. Tolun (1955) mapped at a scale of 1:5,000 to the northwest of my field area. He shows that the syenite porphyries were folded together with the metamorphic rock units. This is also clearly seen in his map pattern.

The yellowish white to pinkish brown syenite porphyries have yellowish brown to yellow weathered surfaces. They are composed of K-feldspar (45-50%), plagioclase (10%), and hornblende, augite and

Figure 2.15 Typical syenite porphyry outcrop to the west of Bezirgan Dere.

Figure 2.16 Optical micrograph of the syenite porphyry showing phaneritic groundmass texture (picture width 3.25cm).

very rare opaque minerals, sphene, quartz (in decreasing order of abundance). These porphyritic rocks show phaneritic groundmass texture. K-feldspars which are the dominant elements of the rock are determined as sanidine and orthoclase based on their 2V angle. Idiomorphic prismatic sanidine phenocrysts which are parallel with the igneous lamination of the rock are up to 1.5 to 2 cm long (Figure 2.16). Dull pinkish orthoclase phenocrysts represent the second dominant minerals in the rock composition. They differ from the sanidine by their larger 2V angle. Moreover, the idiomorphic orthoclase phenocrysts are smaller than the sanidine phenocrysts. Xenomorphic K-feldspar crystals are the dominant minerals in the groundmass as well. Idiomorphic plagioclase phenocrysts, usually showing albite twinning, are also found. Very rare xenomorphic quartz crystals can be seen in the groundmass. The rest of the mineral constituents of the syenite porphyry such as brown hornblende, sphene and augite are observed in the groundmass in xenomorphic form. Figure 2.16 illustrates a representative microscopic view of the syenite porphyry.

In general, the syenite porphyries are unmetamorphosed, but they caused contact metamorphism of the surrounding crystalline rocks including the development of mineralization such as scheelite, magnetite, chalcophyrite and valadinite (Kumbasar, 1964).

The igneous activity has not affected the Tertiary sediments which cover the metamorphics such as Upper Paleocene-Lower Eocene Seske, and Upper Eocene-Oligocene Kirkgecit Formations. This implies that the igneous activity was completed before the late Paleocene. Moreover, the thrust faults observed in the map area cut the syenite porphyry. Their tectonic significance is discussed in section 2.2.6 and Chapter 4.

2.2.4. Major Mylonite Zones

The crystalline rock formations described in 2.2.2. have faulted contact (thrust) relationships with each other. In the thrust contact between the Calik and Kirklar Formations (along the Corik Fault: locality 1 in Plate 5, and Bezirgan Fault: locality 2), the Koyunatlayan and Calik Formation (along the Hirsiz Fault: locality 3), the Kirklar and Koyunatlayan Formations (along the Corik Fault: locality 4, and Gelintas Fault: locality 5) a number of major mylonite and/or high strain zones occur, in the form of ductile shear zone (Ramsay, 1980), each up to few thousands of meters long and several meters wide. In the study area, besides the foliated mylonites, the fault rocks of the Keban Metamorphics are represented by fault breccias and gouge zones which display incohesive random-fabric (Sibson, 1977). The mineralogy and microstructural features of these fault rocks are discussed in Chapter 3. It is believed that the deformation mechanisms in each fault rock depends largely on its main mineral constituent (White et al., 1982). From this point of view, the mylonitic and/or highly strained rocks along the Asi and Hirsiz Faults are depend largely on the behaviour of quartz, mica, and some feldspar and clacite as these fault rocks consist largely of these minerals, and mylonites along the Gelintas Fault, on the other hand, will depend largely on the behaviour of calcite and mica, feldspar since the mylonitic rock consists of calcite, feldspar and mica.

In the east, another mylonite zone is also observed in the contact zone between the Kirklar Formation and Yuksekova Volcanics (along the Keban Fault: locality 6 in Plate 5).

The mineralogy and microstructural details of each mylonite zone and their structural significance are considered in Chapter 3.

2.2.5. Metamorphism

The mineral assemblage of the "phyllitic psammite-calcschist" Calik Formation

quartz + muscovite + chlorite + epidote ± calcite ± plagioclase

suggests that the Calik Formation experienced low grade greenschist metamorphism (Miyashiro, 1973; Winkler, 1979). Since the metamorphic mineral assemblage contains no biotite, it is safe (Miyashiro, 1973) to name this as belonging to a "chlorite subfacies" in low grade greenschist metamorphism. It presumably was a medium pressure, low temperature event such as would happen in regional metamorphism (Miyashiro, 1973, p. 90).

The mineral assemblage of the Kirklar and Koyunatlayan carbonate Formations is

calcite + muscovite + quartz + epidote + plagioclase.

The above assemblage is also interpreted as low grade greenschist metamorphism such as Miyashiro (1973) describes from the Central Abukuma Plateau, Japan. He states that "the most limestone in the Central Abukuma Plateau are rather pure $CaCO_3$ rocks (such as Kirklar and Koyunatlayan Formations in this volume) and show only a progressive increase in grain size with rising temperature. In low temperature zones, most grains of calcite measure 0.005 - 0.1 mm in diameter, whereas in higher temperature zones they measure 1 - 10 mm" (Miyashiro, 1973, p. 268). The grain size of the sparitic Kirklar and Koyunatlayan carbonates in the study area, range from about 0.04 mm to 0.7 mm (see Figure 2.14).

The above statements suggest that the Keban Metamorphic rocks, near Keban, experienced a low grade greenschist metamorphism into a chlorite zone subfacies, probably in medium pressure, low temperature conditions. The age of the metamorphism is discussed in 2.2.6 below.

The syenite porphyries which cut across the metamorphic rocks are unmetamorphosed, and mostly have preserved their original igneous texture. At the contact with crystalline rocks, they show an associated contact metamorphism. The contact metamorphic rocks are not well exposed in the map area, and hence they are not considered in this research. For the detailed description of the contact metamorphic rocks and the mineralization, which was caused by the contact meta-morphism, see Kumbasar (1964).

2.2.6. Discussion

The lithological data from this study show that the Keban Metamor-phics are composed mostly of carbonate rocks (about 85% of the map area: Kirklar Marble and Koyunatlayan semi-crystallized limestone). These sparitic carbonate facies imply that those sediments were formed on a continental shelf (Selley,1978; Mitchell and Reading, 1969; Dewey and Bird, 1970). The rest of the lithology of the Keban metamorphics (phyllitic psammite with calcschist interlayering Calik Formation with about 15% of the map area) is more indicative of continental shelf which might be very close to the continental slope. Hence, the detailed lithologic description of these metamorphic rock assemblages which formed the Keban Metamorphics suggest that they represent original continental margin sedimentary sequences. They were probably formed mainly on the continental shelf and perhaps partially on the continental slope.

In the studies done so far, almost all of the researchers have thought that the Keban Metamorphic rocks are an extension of the more southerly Puturge Metamorphics (Sengor and Yilmaz, 1981). Hempton (1982) shows that the Puturge Metamorphics consist of 80% metapelite, 15% metaquartzite, and only about 5% recrystallized limestone. Boray (1975) describes the Bitlis Metamorphics in the vicinity of city of Bitlis as metapelites (Upper Unit) and marbles (Lower Unit). Hempton's (1982) lithological description of Puturge Metamorphics corroborates Boray's Upper Unit of the Bitlis Metamorphics (R. Mason, personal communication, 1982).

This study shows that the Keban Metamorphic rocks consist of a higher percentage of carbonate (over 85%) and almost no pelite. Moreover, the Keban Metamorphics are cut by a distinctive group of hypabyasal syenites, which often indicate rifting phenomenon (Burke and Dewey, 1973). They are inferred to have been intruded during the late Cretaceous. No sedimentary deposition has occurred on the Keban Metamorphic basement during the whole of Jurassic and Cretaceous times, whereas sedimentary deposition has occurred on the Puturge massif; the Maastrichtian sediments (Simaki flysch: Perincek, 1979b). Moreover, the ensimatic Yuksekova (=Elazig) island arc complex (Hempton and Savci, 1982) always occupies an intermediate position between the Keban and Puturge Metamorphics. The above discussion is based mainly on the lithological features and implies that the Keban metamorphic rocks do not resemble the Puturge metamorphic rocks. They represent segments of different continental margins which were situated north and south of the Yuksekova Ocean (more detailed discussion on their

tectonic setting throughout the Neo-Tethyan evolution will be considered

in Chapter 4). Although their structural position suggests that the

Malatya metamorphic rocks which lie in the south resemble the Keban

metamorphic rocks which are found in the north, the lithologic

relationship between these two metamorphic complexes is still obscure.

The mineral assemblages (given 2.2.5.) in the metamorphics

indicate that they experienced a low grade greenschist metamorphism.

The age of the metamorphic rocks are specified by Kipman (1981), and

Perincek and Ozkaya (1981) as Palaeozoic-Triassic based on the fossils

found in them in the Keban and Pertek areas, respectively. As was

mentioned above, there is no known sedimentary deposition on the Palaeo-

zoic-Triassic metamorphic basement until the Paleocene (Seske Formation).

The late Cretaceous igneous rocks which are considered below, preserve

their igneous texture and are unmetamorphosed. These data suggest that

the Keban continental margin sediments underwent low grade greenschist

metamorphism sometime in Jurassic to Lower Cretaceous times.

Those Tertiary sediments such as the Upper Paleocene-Lower Eocene

Seske Formation, and the Upper Eocene-Oligocene Kirkgecit Formation

that partially cover both the metamorphic rocks and the unmetamorphosed

syenite porphyry, implies that the syenite igneous activity is older

than the Upper Paleocene and younger than the metamorphism of Keban

sediments. In accordance with the data discussed above and also with

conformity to the geotectonic explanation of Sengor and Yilmaz (1981)

(see Chapter 4), the age of the intrusion is assumed to be as late

Cretaceous. However, I believe that a reliable age determination for

the igneous rocks will only be obtained by Isotope Geochemistry. The

above assumption, of course, suggests that the age of the contact meta-

morphism is also late Cretaceous.

2.3. Yuksekova Volcanic Complex

The Yuksekova Complex (Perincek, 1978) is found along the southern
margin of the Keban-Malatya Complex. It extends for about 200 km near
Palu-Malatya-Adiyaman regions in the western Yuksekova terrain, extending
for about 350 km from Agri to Hakkari in the eastern Yuksekova terrain
(see Figure 2.17 and Sengor and Yilmaz's (1981) figure 2 at page 189-
190, for the distribution of the Yuksekova Complex in the southeastern
Turkey). They are represented by large thrust slices of ophiolitic
rocks near Hakkari in the eastern Yuksekova terrain (Sengor and Yilmaz,
1981; O. Sungurlu, personal communication, 1982), and by a large thrust
slice of island arc rocks near Elazig and Malatya in the western
Yuksekova terrain (Hempton and Savci, 1982).

The Yuksekova Volcanic Complex crops out in the eastern one-fifth
part of the map area (Plate 1). Within the map area, rocks belonging
to this suite do not exhibit as much topographic relief compared with
the crystalline rocks to the west and are generally easily accessible
(Figure 2.18). The lithological description and structural detail of
volcanics is not considered as much as the crystalline rocks in this
research. Much lithological and structural detail of the Yuksekova
Volcanic Complex in the Sivrice-Elazig area which is about 65 km south
of the map area, has recently been published by Hempton and Savci (1981,
1982). This thesis is more concerned with the original and present
contact relationships between the Yuksekova Volcanic Complex and the
Keban Metamorphics. About 7 km^2 outcrop mapping was conducted in
volcanics on a scale of 1:12,000 along the Keban Fault (Plate 1). The
contact relationship between the volcanics and the crystalline rock
series are also mapped on a larger scale of 1:80 and 1:2 (Plate 4).
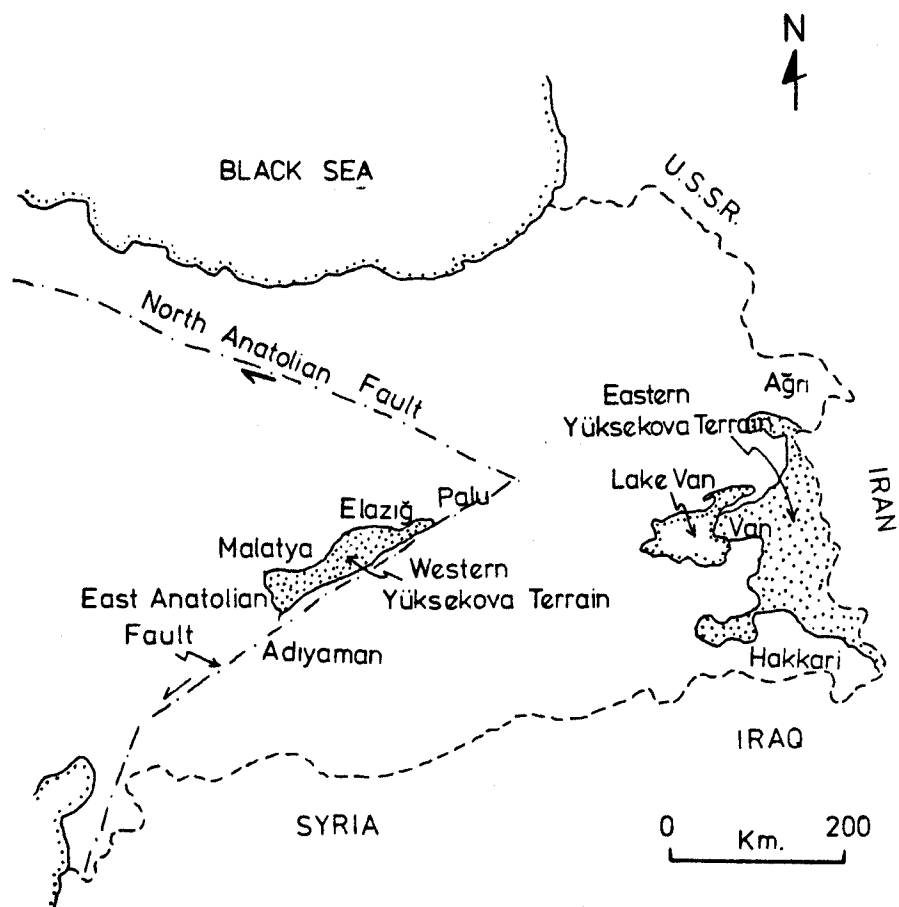
Figure 2.17. Map illustrates outcrop distribution of the Yuksekova Complex. The Yuksekova Complex extends for about 200 Km near Palu-Malatya-Adiyaman regions in the western Yuksekova terrain, extending for about 350 km from Agri to Hakkari in the eastern Yuksekova terrain.

Figure 2.18 A view of the Yuksekova Volcanic Complex along the Keban Fault, looking northeast toward Sino Mahallesi from the Sino road (see Figure 1.5).

Within the study area, the Yuksekova Volcanic Complex consists
of mafic extrusives and mafic volcaniclastics. Also, some granodioritic
rocks which cut across the mafic extrusives of the Yuksekova Complex
are also observed at the eastern edge of the map area along the Keban-
Elazig highway.

2.3.1. Previous Work

The Campanian-early Maastrichtian Yuksekova Volcanic Complex was
first named by Perincek (1978, 1979b) for the volcanic rocks in the
vicinity of the town of Yuksekova around Hakkari city.

The 1:500,000 scale geological map of M.T.A. (1961-1964) shows
the general boundaries of the Bitlis, Puturge, Keban and Malatya Meta-
morphic rock series in the Bitlis Suture Zone. They also illustrate
an "Upper Cretaceous (occasionally with ophiolite and Paleocene)" map
unit which refers to the rest of the units of the Bitlis Suture Zone
including the Yuksekova Volcanic Complex.

Erdogan's work (1977) is concerned with the geological and geochemi-
cal characteristics of the massive sulphide deposits which occur in the
Guleman Ophiolites in the Maden-Ergani area. He mapped at a scale of
1:25,000 in this area. He also describes basalt and gabbro units
farther east in the Helezur area where he conducted 1:2,000 scale
geological mapping. Erdogan (1977) correlated the Helezur basalts with
Guleman basalts and proposed that the Helezur basalts represented a
portion of the same oceanic crust with the Guleman Ophiolites. Hempton
(1982) objects to Erdogan's (1977) interpretation for the Helezur
basalts. He mapped the same area at a scale of 1:12,000, and suggests
that the Helezur basalts belong to the Yuksekova Volcanic Complex.

Perincek (1978, 1979b) states that the Yuksekova Complex consists
of red-greenish-grey-light grey limestone, shale, sandstone, volcanic
sandstone, tuff, agglomerate, basalt, diabase, gabbro, serpentinite,
granite and granodiorite, pillow lava and pyroclastics around Yuksekova
town in the province of Hakkari. Perincek (1979b) observed some red
limestone lenses in the volcanics and determined Campanian-Maastrichtian
fossils (Globotruncana stuarti, Globotruncana lapparenti, Globotruncana
arca, Heterohelix sp.) from them. Perincek (1979b), and Perincek and
Ozkaya (1981) show that some granodioritic rocks cut across the volcanics
of the Yuksekova volcanics north of Elazig city. Perincek further
noted weak metamorphism in the volcanic complex.

Sengor and Yilmaz (1981) suggest that the Yuksekova volcanic
rocks have island-arc affinities based on Hempton (1982) and Hempton
and Savci's (1982) data, and contemplate that it was related to south-
dipping subduction in Senonian time.

Yazgan's work (1981) deals with major and minor chemical elements
and the initial isotopic ratio of strontium of the volcanics of the
Yuksekova and medial Eocene Maden Complexes. He asserts that the
Yuksekova volcanics were situated on an active continental margin
existing in late Cretaceous time. He further noted that an existence
of ophiolitic complex (Komurhan) within the Hempton and Savci's (1982)
Yuksekova (=Elazig) Volcanic Complex. His interpretation of the struc-
tural and geochemical data are not generally accepted.

Hempton and Savci (1981, 1982) first describe the Yuksekova
Volcanic Complex in great structural and lithological detail for a 120
km^2 portion of the western Yuksekova terrain. Since Hempton and Savci's
(1982) description is only relevant to the area between Sivrice and

Elazig, the Yuksekova Volcanic Complex is renamed as Elazig Volcanic Complex for the area mentioned above. They described the Elazig Volcanic Complex as comprising large north dipping, internally imbricated thrust slices composed of three units from base to top: 1. gabbro, diabase, and basalt with siliceous intrusives metamorphosed to the lower green-schist facies, 2. augite andesite volcanics and volcaniclastics with siliceous dikes metamorphosed to the prehnite-pumpellyite facies, 3. unmetamorphosed andesite, and hornblende andesite flows cut by mafic dikes, andesitic volcaniclastics, and pillow basalt cut by sileceous dikes. To the north, the volcanic rocks of unit 3 are unconformably covered by the Upper Maastrichtian Harami Formation and also structurally overlain by north-dipping thrust sliver of the Keban Metamorphics. The Upper Paleocene-Lower Eocene Seske carbonates, Upper Eocene-Oligocene clastics of the Kirkgecit Formations and Upper Miocene Karabakir basalts unconformably overlie the Elazig Volcanic Complex (including the Harami Formation on top of it), and the Keban Metamorphics. The nature, distribution, and relative lithological proportions of the volcanic lithologies induce Hempton and Savci (1982) to suggest that unit 1, 2 and 3 of the Elazig Volcanic Complex represented succesively deeper levels within a primitive ensimatic island arc developed where oceanic crust was subducted beneath other oceanic crust.

Hempton (1982) mapped at a scale of 1:12,000 in the Sivrice area (locally at a scale of 1:1,000). His primary concern was with the structure of the northern margin of the Bitlis Suture Zone and the East Anatolian Fault zone around Sivrice area. He describes the first two units of Hempton and Savci's (1982) Elazig Volcanic Complex in

greater detail and concludes with same interpretation for the volcanic rock units.

Perincek and Ozkaya (1981) assert that the Yuksekova Complex might be either an ensialic island arc complex developed on the Keban Metamorphics or an island arc complex which has both an ensimatic and an ensialic characteristic. They suggest that the Guleman ophiolites may be the base of the ensimatic island arc complex. The structural and lithological criteria they employed are only assumption and are not generally acceptable. Ozkaya (1982) describes the Yuksekova Volcanic Complex around Palu area and claims that the Yuksekova Complex of the Palu belt occupies an intermediate position between Bitlis and Keban continental crust wedges and possibly represents an arc-trench complex. He further noted that the relationship between the Keban metamorphic rocks and Yuksekova Complex is obscure around Keban area.

2.3.2. Lithology

The eastern one-fifth part of the map area is occupied by the Yuksekova volcanic rocks. In the map area, they are represented by mafic extrusives and volcaniclastic interlayers. The volcanics and volcaniclastics have been intruded by granodioritic dikes (Perincek, 1979b) and quartz veins.

The lithological description of the volcanics in the map area is restricted here with only the description of the mafic extrusives. Moreover, a short lithological description of the Hempton and Savci's (1982) Unit 3 of the Elazig Volcanic Complex is given below (from 1:25,000 scale geological mapping conducted by the author in the summer of 1980: Figure 2.23).

In the map area (Plate 1), the weathered surface is usually grayish-green, greenish-brown and bluish-gray, fresh surface is dark reddish-brown and mostly dull bluish-gray vesicular mafic extrusives which show a hyalopilitic texture (Nockolds, 1978) (Figure 2.19) are composed mainly of plagioclase (probably labrodorite?), and some quartz and clinopyroxene that has altered to epidote and calcite. The vesicles are filled with secondary calcite minerals and therefore it shows an amygdaloidal (Nockolds et al., 1978) texture (Figure 2.20). They show many brittle structural features such as joints, small faults, and fracture cleavage (Figure 2.21). As is shown in figure 2.21, spaces between the fractures are filled by a white, soft, fine grained sili- ceous material that exhibits no structure and is not coherent. It usually contains small angular fragments of mafic extrusive. Strike and dip measurements from the fracture cleavages along the Keban fault seem to be between N10W and N10E; 50-75 NE and/or SW orientations (see Plate 1). This may reflect the influence of the N-S directed Keban fault. The mafic extrusive rocks also contain joints. In some outcrops there has been observed a single joint plane orientation whereas most volcanic outcrops show a set of joint planes (usually two) (Figure 2.21). Since the purpose of this study mostly focuses on the contact relation- ship between the metamorphics and volcanics and on internal structural features of the metamorphics, a very small portion of the volcanics in the Keban area was mapped. Therefore, only a few measurements from the volcanics have been collected.

Although the volcanic rocks have preserved their igneous texture, they contain some metamorphic minerals such as altered plagioclase
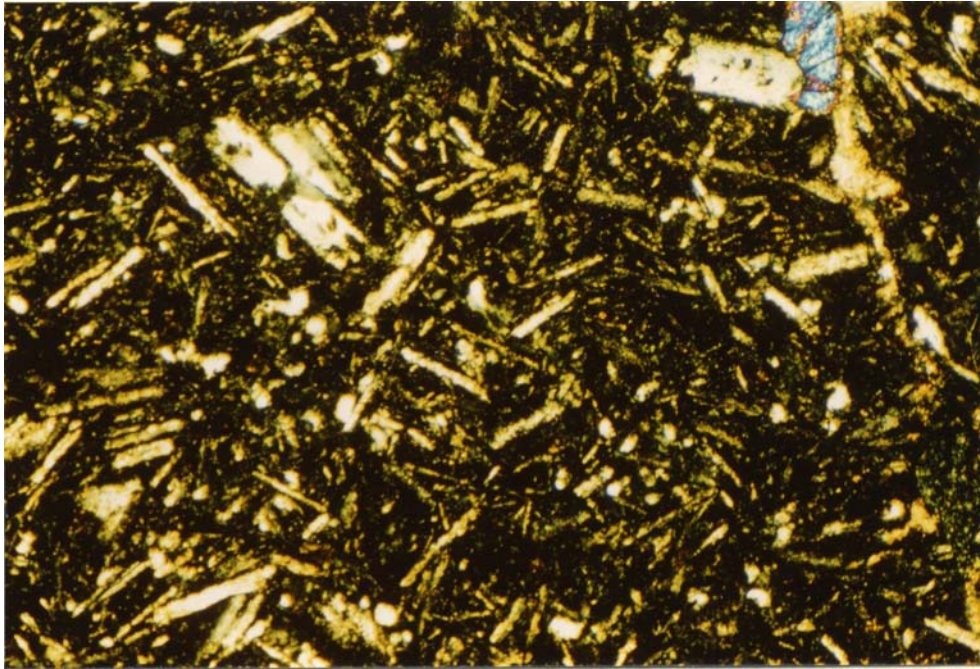
Figure 2.19 Optical micrograph of the Yuksekova mafic extrusive, showing a hyalopilitic texture (x40, crossed Nicols).
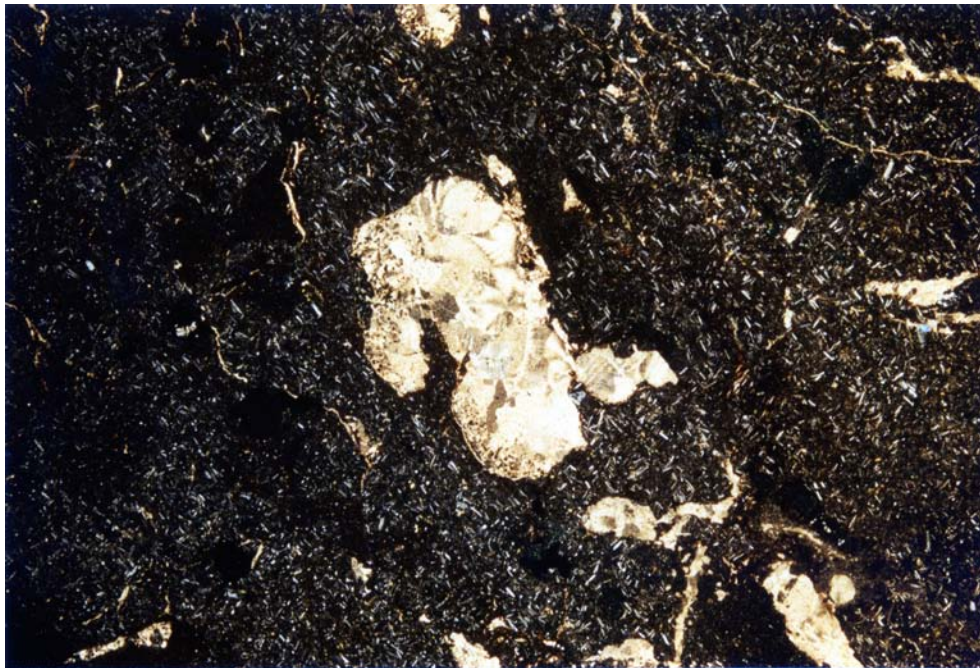
Figure 2.20 Microscopic view of the Yuksekova mafic extrusive, showing an amygdaloidal texture (picture width 1.9 cm, crossed Nicols).

Figure 2.21   Typical Yuksekova mafic extrusive outcrop in south of Kirklar Koyu. Note well-developed fracture cleavage (parallel with pencil) and two sets of joint planes.

which contains chiefly of epidote (saussurite: AGI Glossary, 1972),

and calcite. These metamorphic mineral assemblage suggests that they

experienced very low grade greenschist metamorphism (Miyashiro, 1973;

Winkler, 1979).

In the vicinity of Tadim Koy (koy is village in Turkish) (Figure

2.23), south of Elazig city, the Yuksekova volcanics consist of basaltic-

andesitic pillow lavas (Figure 2.22) in the south, and hornblende-

andesite, andesite and volcaniclastic interlayers within the volcanic

assemblage in the north (Figure 2.23). They are unmetamorphosed, and

cut by siliceous dikes in the south and mafic dikes in the north (Figure

2.25). This volcanic unit was recently defined by Hempton and Savci

(1982) as the upper unit of the Elazig Volcanic Complex.

The basaltic-andesitic pillows (Figure 2.22) cut by siliceous

dikes are located in about 3.5 km south of the geological map shown in

figure 2.23. The best exposures of the pillows outcrop along the Elazig-

Sivrice highway.

The hornblende andesitic flows which partially show a spheroidal

weathering (Figure 2.24) outcrop in the western and northern part of

Tadim Koy (Figure 2.23) and cut by mafic dikes (Figure 2.25). They

consist mostly of idiomorphic hornblende and plagioclase with some

augite, magnetite and apatite (Figure 2.26). The c axis of the greenish-

brown hornblende phenocrysts is up to 2-6 mm long. The plagioclases

are determined as andesine by using the Michel-Levy method (Kerr, 1977).

Hipidiomorphic to xenomorphic plagioclase and hornblende crystals

are also the basic elements of the matrix. To the north the amount of

hornblende phenocrysts gradually decrease and then can only be found in

the matrix. In these andesitic flows which outcrop around Tepekoy and

Figure 2.22 Basaltic-andesitic pillow lavas from the Elazig-Diyarbakir highway.

Figure 2.24 Hornblende andesite of the Yuksekova (=Elazig) Volcanic Complex, showing spheroidal weathering; Tadim Koyu (see Figure 2.23 for its location).
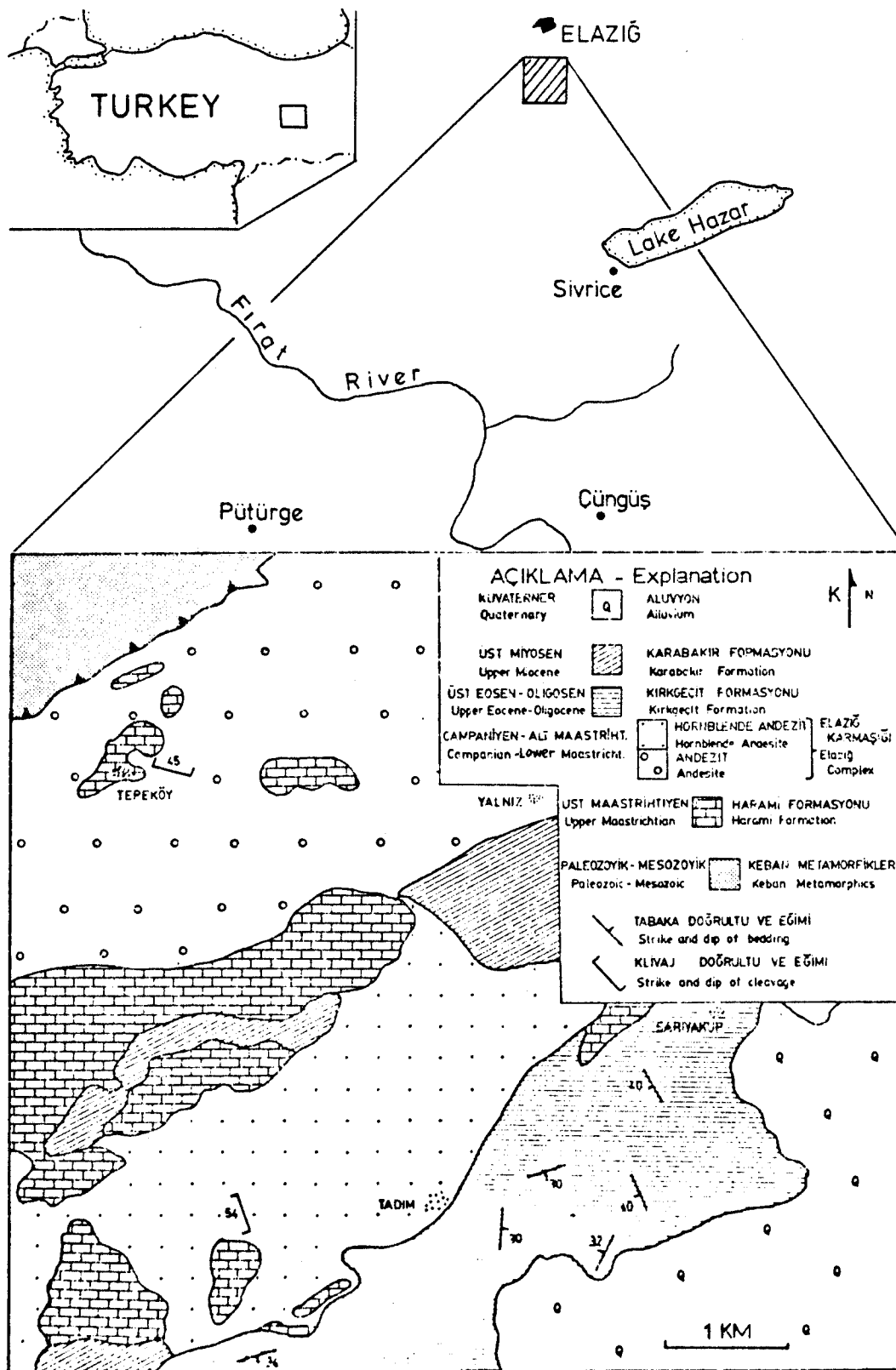
Figure 2.23. Generalized geological map of the south of Elazig area based on much more detailed 1:25,000 scale mapping showing the upper unit of Elazig Volcanic Complex (after Hempton and Savci, 1982; Figure 4, p. 147).

Figure 2.25 A mafic dike cutting across the hornblende andesite unit of the Yuksekova (=Elazig) Volcanic Complex; 2 km west of Tadim Koyu.
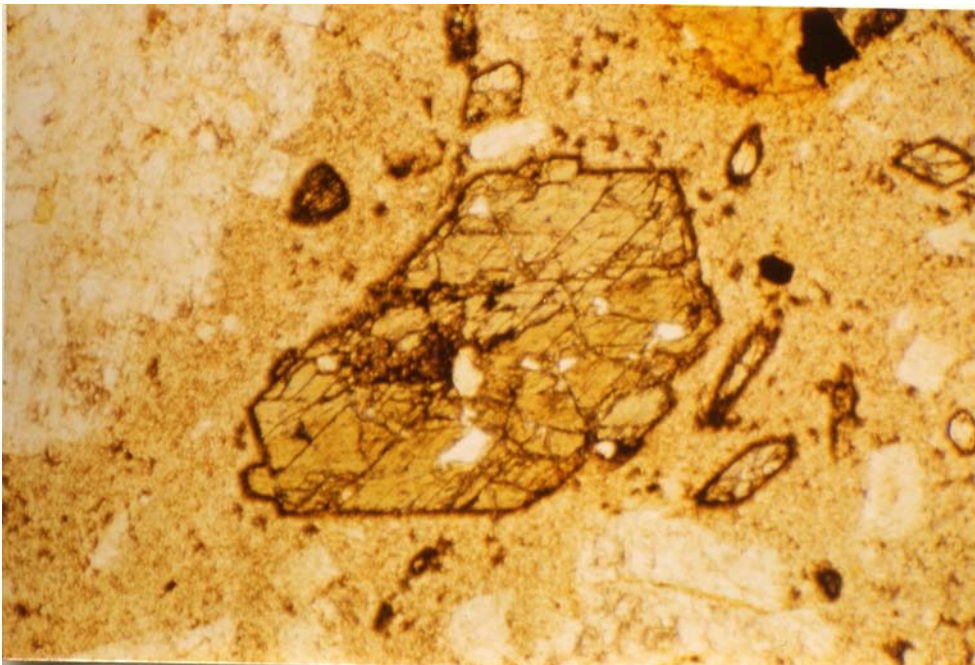
Figure 2.26 Microscopic view of hornblende andesite (x40, polarised light).

Yaliniz, the plagioclase phenocrysts show a larger c axis, up to 5 mm. Between 50 cm and 1 m thick volcaniclastic layers are also observed within the volcanics (Figure 2.27). Hempton and Savci (1982) suggest that the above volcanic unit represents the last stage of the primitive ensimatic Elazig volcanic island arc activity. For detailed petrographic description and their tectonic implications, see Hempton and Savci (1982).

The Yuksekova Volcanic Complex is covered by Upper Maastrichtian Harami Formation with an angular unconformity mostly around Elazig area (Perincek, 1979b; Hempton and Savci, 1982). Perincek (1979b) describes the Harami Formation as follow: "The Harami Formation is represented by limestones which are white coloured, recrystallized occasionally, fossiliferous and 50 m thick bedded. . . . The Formation sometimes contains basal conglomerates whose materials are derived from the Yuksekova Complex. The thickness of Harami Formation varies between 50 to 200 m." Perincek (1979b) also determined the age of the Harami Formation as Upper Maastrichtian based on fossils (Siderolites cf. vidalis, Siderolites calcistropoides, Orbitoides media, Omphalocyclus sp., Lepidorbitoides sp.,Pseudosiderolites sp., Loffitenia sp.) found in it.

The Harami Formation only covers the Yuksekova Volcanic Complex and is unmetamorphosed. It shows very gentle folding around Harput-Elazig (Figure 2.28). Both the Yuksekova Volcanic Complex and Harami Formation are structurally overlain by north-dipping thrust slivers of the Keban Metamorphics around the Elazig area (Hempton and Savci, 1982) and around Pertek area (Perincek, 1979a). The Keban Metamorphics, Yuksekova Volcanic Complex and Harami Formation, and, in part, the thrust contact between Keban and Yuksekova-Harami, are covered by Upper Paleocene-Lower Eocene Seske, Upper Eocene-Oligocene Kirkgecit, Lower

Figure 2.27 A 50 cm thick volcaniclastic layer within the Yuksekova Volcanic Complex; Tepekoy.

Figure 2.28 A view of the Harami Formation, looking north toward Harput from Elazig city.

Miocene Alibonca and Upper Miocene Karabakir Formations (see also Chapter 4). This implies that the major episode of thrusting of Keban Metamorphics over the Yuksekova Volcanic Complex and Harami Formation had been completed by early Paleocene.

The age of the volcanics, partially metamorphosed to the low grade greenschist and prehnite-pumpellyite facies, (Hempton, 1982; Hempton and Savci, 1982) was specified by Perincek (1979b) as Campanian-Lower Maastrichtian based on the fossils found in the limestone lenses within the volcanics. The volcanic complex is disconformably covered by unmetamorphosed Upper Maastrichtian Harami Limestones. This suggests that the metamorphism of the volcanic rocks was synchronous with the volcanic activity.

CHAPTER 3

STRUCTURE

3.1. Introduction

The structure of the Keban Metamorphic rocks, like other features in the Bitlis Suture Zone, is quite spectacular because of the existence of well-exposed outcrops; although some hard, massive, karstic marble outcrops show few structural features. The rocks, in the study area, vary greatly in physical and mechanical properties so that the same generation of deformation may have different forms (eg. a slaty cleavage is well-developed in phyllitic psammite Calik Formation, whereas a schistosity of the same generation is well-developed in calcschist interlayers of the Calik Formation and only weakly developed in the limestone of the Koyunatlayan Formation). Evidence of at least two phases of deformation (D_1, D_2) has been observed. This analysis will employ the tecniques of structural analysis (Weiss and McIntyre, 1957; Turner and Weiss, 1963) and emphasize the equal-area stereographic projection of significant structural features in order to show the patterns of preferred orientation of these structural features. Foliation, particularly slaty and crenulation cleavage in phyllitic psammite, and schistosity in the calcschist interlayers of Calik Formation and in the Koyunatlayan limestones, is beautifully displayed in the study area. These foliations are developed parallel to axial surfaces of folds. Within the metamorphics, there has also been observed two generations of folds which are related to the foliations mentioned above, on the basis of overprinting relationship. Along the thrust contact between the metamorphic rock units described in the

previous chapter, a number of major mylonite bodies are observed in the form of ductile deformation zones (Ramsay, 1980), each up to few thousands of meters long and several meters wide. Such rocks show mylonitic foliations (Sm: White et al., 1980) which are subparallel to the fault zone, and shear band foliations (Ss: White et al., 1980) which were formed oblique to the mylonitic foliation at a low angle (less than 45°). The average preferred orientation of grain shapes defines the mylonitic foliation (Sm). The compositional lamination in the mylonites is also a common feature in some places. In the same zone, besides the foliated mylonites, there has been observed some random-fabric fault rocks (Sibson, 1977) such as fault breccias and fault gouge, and fault planes (brittle shear zone: Ramsay, 1980) (see Figure 3.7). In other words, it is observed that brittle shear zones (faults) in the Keban region show some ductile deformation such as foliated mylonites up to 20 meters wide on one and/or on either side of the brittle fault break. This type of shear zone described above is defined as "brittle-ductile shear zone" by Ramsay (1980). Ramsay (1980) states that in the brittle-ductile shear zones it is quite possible that the ductile part of the deformation history occurred at a different time from the brittle faulting. He also notes that the behaviour of regional shear zones passes from ductile type at deep levels to brittle types at higher crystal levels (Figure 3.1). Ramsay further states that at higher levels the ductile shear zone is transformed into a brittle-ductile zone with the higher level of the zone showing less ductile features than the lower (see Figure 3.1). These generalizations are considered later in this chapter.
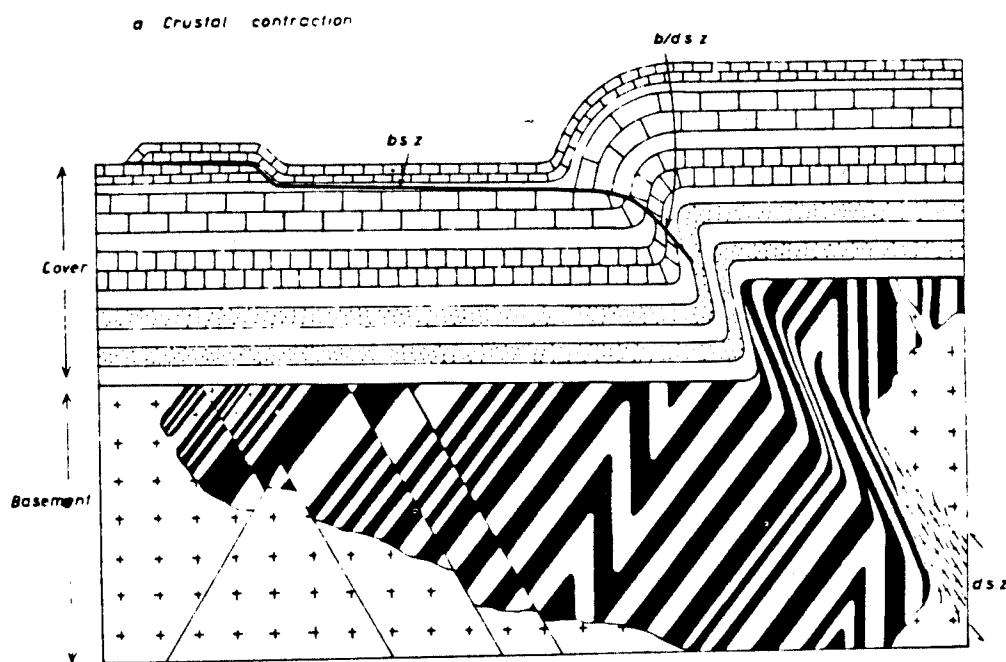
Figure 3.1. Relationship between deep level ductile shear
zones and high level brittle shear zones in the regional
development of shear zones: crustal contraction (after Ramsay,
1980, figure 22, p. 98). Key to abbreviations; b.s.z.=brittle
shear zone, b/d.s.z.=brittle-ductile shear zone, d.s.z.=ductile
shear zone.

The deformation mechanism in each fault rock in Keban region is dependent largely on their major mineral content. All these structural features, including linear structures, are discussed below in this chapter.

The prupose of this chapter is to describe structural features of each fault, the fault rocks (eg. fault breccia, mylonite, fault gouge), and to present a structural analysis of the different generations of foliations and folds. At the end, I discuss in detail the contact relationship between the Keban Metamorphics and the Yuksekova Volcanic Complex, and the deformation history of the study area, near Keban.

3.2. Observation: Megascopic and Microscopic

3.2.1. Faults and Fault Rocks in the Keban Metamorphics

As is mentioned in Chapter 2, throughout the map area, the contacts between the metamorphic rock units are thrust contacts (see Plates 1 and 5). This part of the chapter describes the megascopic and microscopic features of the selected fault rocks and their deformation history. Four major rock types give rise to fault rocks in the Keban area; they are Kirklar marble, Koyunatlayan limestone, Calik phyllitic psammite and Yuksekova mafic extrusives. The mineralogy and detailed structural significance of the first three of these fault rocks mentioned above are discussed below. The contact relationship between the Keban Metamorphics of the Keban-Malatya Complex (see Chapter 1 and Figure 1.1) and the Yuksekova Volcanics of the Bitlis-Puturge Complex in the study area (the Keban Fault: see Figure 1.4 and Plate 4) is considered later in this chapter (3.2.5.).

In the study area, the fault rocks of the Keban Metamorphics are recognized by their distinct appearance such as fault breccias, fault gouge which show incohesive random-fabric (Sibson, 1977), and foliated mylonites and/or highly strained rocks. Figure 3.2 shows Sibson's (1977) textural classification of fault rocks, and structural features of the fault rocks in the Keban area. In the map area, fault planes can also be easily seen along the fault zones (see Figure 3.7). After the faulting that juxtaposed the metamorphic units described in Chapter 2, they were folded together (see Plates 1, 5, and Figures 3.3, 3.6, 3.7, 3.11).

Figure 3.2. Sibson's (1977; table 1, p. 192) textural classification of fault rocks (A), and structural features of the fault rocks in the Keban area (B).

A. Çörik Fault

The type locality for the Çorik Fault is located in Çorik Dere (locality 4 in Plate 5, Figure 3.3) and a road outcrop on the Keban-Elazig highway (locality 1 in Plate 5, Figure 2.3). This fault extends for about 4 km in the map area, roughly in the north-south direction. It was formed mainly between the Kirklar and Koyunatlayan Formations, and between the Kirklar and Calik Formations where the topographic relief is not so high (Locality 1 in Plate 5; see also Plate 2). This implies that the western part of the Koyunatlayan Formation (see Chapter 2) does not have a very great structural thickness.

The fault zone is characterized by fault rocks such as fault breccias derived from parts of the Kirklar Formation. In two specific localities, a 5 m thick and 40-50 m long mylonitic zone was formed in the Calik Formation at Locality 1 in Plate 5, and the fault is characterized mainly by fault breccias of the Kirklar Marble at Locality 4 in Plate 5. These fault rocks are typical examples for almost all the fault zones observed in the map area. The mineralogy and microstructural features of the fault breccia are given below in the section on the Bezirgan Fault.

The mylonitic zone along the Çorik Fault can be traced only on the contact between the Calik and Kirklar Formations (Locality 1 in Plate 5). This part of the contact represents a structurally lower level of the Çorik Fault (see Plate 2). Since the fault shows some ductile deformation (highly strained rocks: see Figure 3.4) in the hangingwall, it is named as a brittle-ductile shear zone (Ramsay, 1980). The contact between the Kirklar and Koyunatlayan Formations (Locality 4 in Plate 5) is represented by a fault or brittle shear zone, with no mylonite nor highly strained rocks present. This may imply that the

Figure 3.3   A view of the southern part of the Corik Fault, looking south toward Corik Dere from Sorenktasi Sirti. Note folded contact along the stream. Key to abbreviations: K=Kirklar Marble, Ko=Koyunatlayan Limestone.
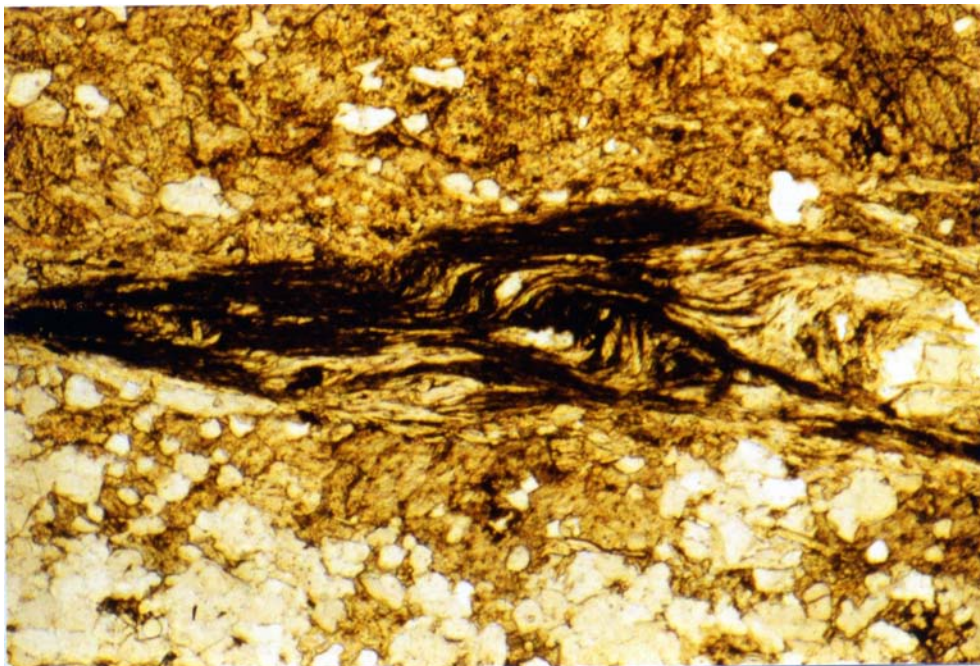
Figure 3.4   Optical micrograph of a fault rock from the Calik Formation, showing intrafolial folds (x40, polarized light). The direction of shearing in this view is horizontal and of left-lateral shear sense.

Corik Fault is represented by its deeper crustal level brittle-ductile shear zone around the structurally lowest exposed part of the fault zone (Locality 1 in Plate 5) and by its higher level brittle shear zone around Corik Dere (Locality 4 in Plate 5).

Closer to the fault, the mylonitic zone becomes progressively finer grained. Quartz, calcite, mica (muscovite-sericite) and some graphite are the main mineral constituents of the Corik mylonite. In the mylonitic zone, the average preferred orientation of grain shapes of calcite and quartz, and mineral elongation of muscovite-sericite define a weak mylonitic foliation (Sm) under the microscope (Figure 3.4). Some intrafolial folds (Cobbold and Quinquis, 1980; White et al., 1982) can also be seen under the microscope. According toe Cobbold and Quinquis, 1980; White et al., 1982, "the axial surfaces of intrafolial folds always face in the direction of movement" (Figure 3.5a). Using this criterion the sense of movement in this sheared rock is determined as sinistral (Figure 3.4). The microscopic results based on the remnant relatively unsheared pods of quartz and calcite surrounded by sheared and foliated mica-rich phyllitic psammite (Figure 3.5c) corroborate the field observation. A similar type of deformation observed in the Hirsiz Fault (Locality 3 in Plate 5) is discussed in detail below. The average orientation of the fault, varies between N5E; 55-60 SE and N10W; 40-50 NE. After the faulting, the faults describe in this chapter were all folded together with the metamorphic units defined in previous chapter. In large exposures, the folding is easily recognizable along the Corik Fault (see Figures 3.3. and 3.6). Because of folding phenomenon, the strike and more prominently the dip of the fault contact vary within short distances. As is shown in Figure 3.3, the fault

Figure 3.5. A cartoon illustrating the use of some micro-structural features to determine the sense of movement in sheared rocks.

    (a) Asymmetry of intrafolial folds (White et al., 1982; figure 10 a).
    (b) Asymmetry of augen structure within foliation planes (Simpson and Schmid, in press; figure 4 a).
    (c) Remnant unsheared pods surrounded by sheared, foliated rock (Simpson, 1983; figure 2).
    (d) Rotated garnet porphyroblast (Powell and Vernon, 1979; figure 9).
    (e) Rotated feldspars with associated pressure shadows (Simpson and Schmid, in press, figure 4 f).
    (f) Rotated rigid inclusion and passive marker lines (Gosh and Ramberg, 1976; figure 26).
    (g) Broken and displaced hard grains such as feldspars in ductile matrix (Simpson and Schmid, in press; figure 9 B).
    (h) Shear bands (White et al., 1980; Platt and Vissers, 1980). See also Figure 3.19.

(a)

(b)

"tails" of fine grained
material of same composition
as the porphyroclast

(c)

(d)

(e)

pressure-shadow
infilling

(f)

(g)

broken and displaced
feldspar grains

(h)

Sm

S_s
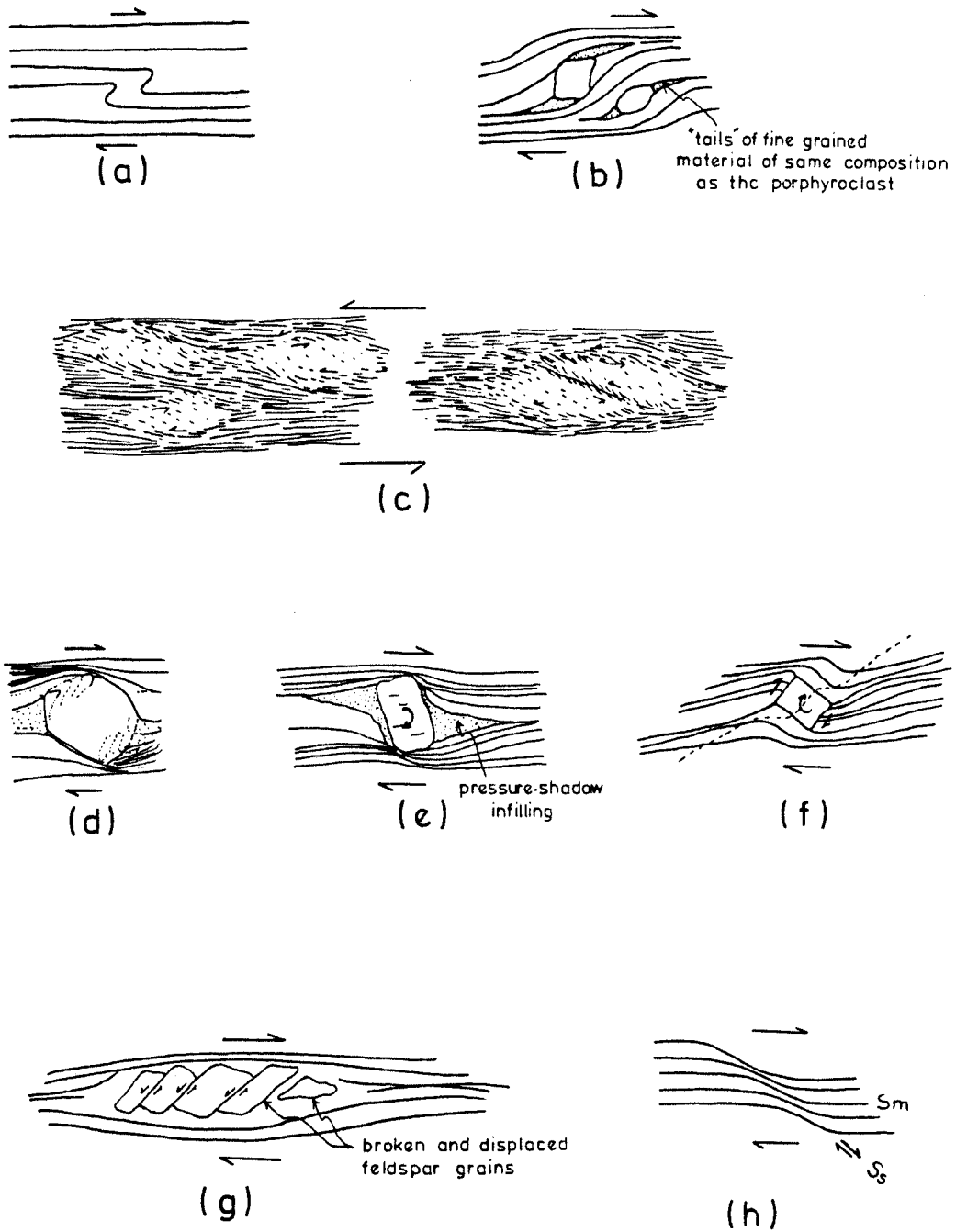
Figure 3.5.

Figure 3.6   A view of the northern part of the Corik Fault, looking west toward Kiskisikkaya from north of Sulu Dere. Note folded thrust contact around the Kiskisikkaya.

contact is found steeply dipping where it is close to the hinges of the folds and is found gently dipping where it is located on one of the limbs of the folds. The best locality to see the variation of the fault dips is in the western slope of the Corik Dere (Figure 3.3).

B. Bezirgan Fault

Within the study area, the best reference locality of the Bezirgan Fault is along the eastern slope of the Bezirgan Dere which is about 2.5 km away from the town of Keban (Plate 5, Figure 3.7). In previous work, all researchers determined this to be a normal fault formed between Calik and Kirklar Formations, which represent the hangingwall and footwall of the normal fault respectively (E.I.E.I., 1972; Kipman, 1981). Detailed mapping and microstructural analysis were conducted on the Bezirgan Fault. From these, it is observed that this is a folded thrust fault.

About a 2.5 km long portion of the Bezirgan Fault was mapped in this study (Plates 1 and 5). The fault zone is characterized by the fault plane which is clearly observable to the north of the Keban-Elazig highway (Figure 3.7). Other characteristics of the fault zone are fault breccias, about a 3 m thick fault gouge on the footwall (Kirklar Marble), and a narrow (about 60 cm thick) high-strain zone on the hangingwall (Calik Phyllitic Psammite) (see Figure 3.8 for the distribution of these fault rocks on a road outcrop at locality 2 in Plate 5).

The fault breccias, which probably formed by crushing, shattering and grinding during the thrusting, are common features in the Kirklar Marble along the fault zone (the type locality for the fault rocks
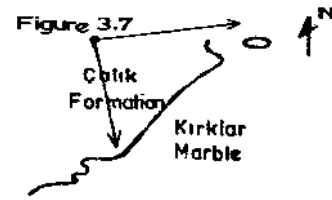
Figure 3.7   A panoramic view of the Bezirgan Fault, looking east from the hill, northern slope of the Bezirgan Dere. The location of Figure 3.8 is marked on the photograph.

A

Figure 3.8   A) A cross section view of the Bezirgan Fault on the Keban-Elazig highway, Locality 2 in Plate 5. Note the distribution of fault rocks in the cross section view. B) (on next page) A sketch of Figure 3.8A indicates the direction of movement as sinistral (looking northeast) based on structures in a strongly foliated high strain zone. Key to abbreviation: m=marble lens
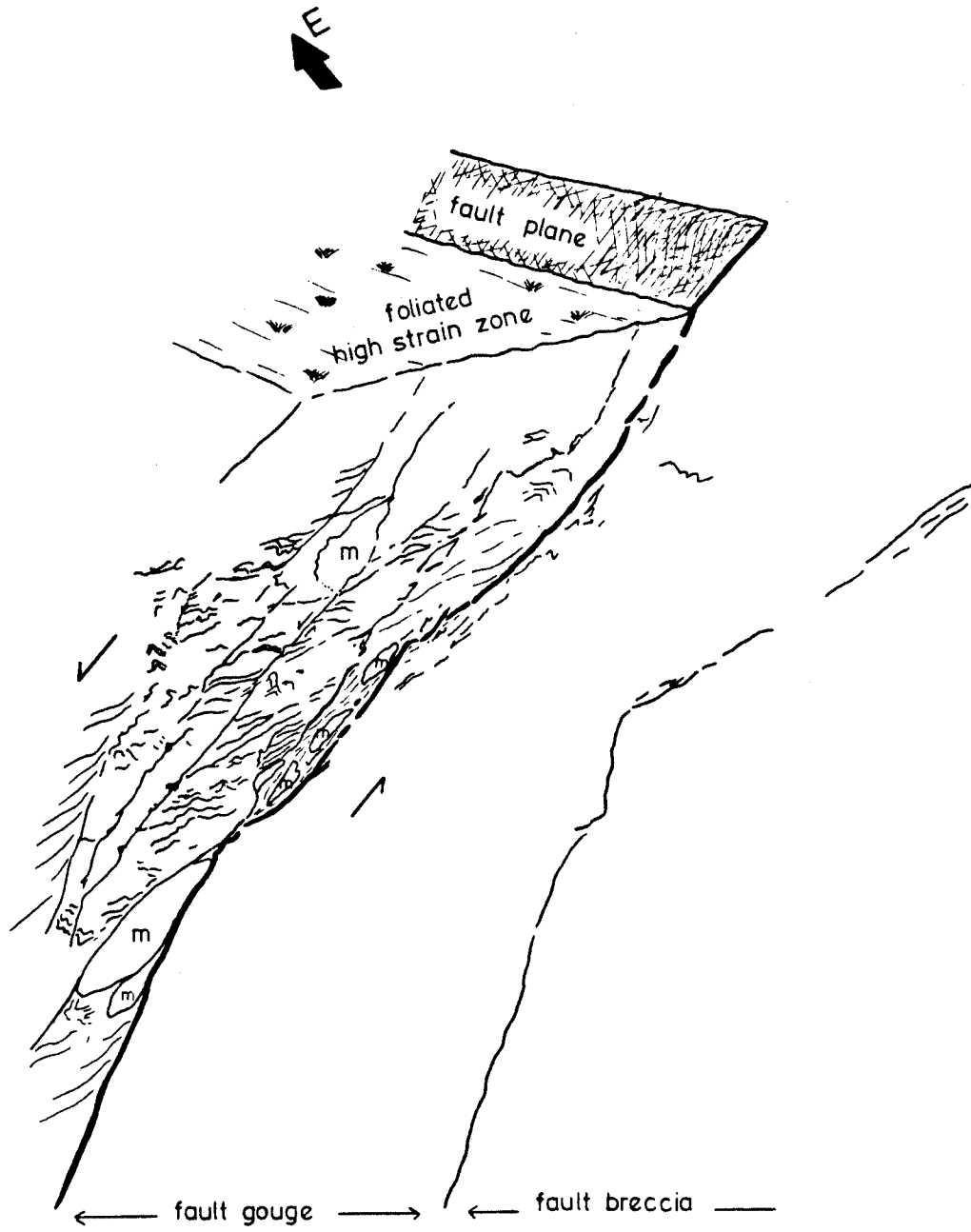
Figure 3.8 B

discussed here are from Locality 2 in Plate 5). Figure 3.9 illustrates

a typical microscopic view of fault breccia. It usually shows highly

angular coarse marble fragments up to 3 cm across. Although these

angular marble fragments consist of calcite, and do not show any signi-

ficant shape orientation, they show scratching marks which may be the

indications for crushing and grinding during thrusting. The matrix of

the fault breccia (Figure 3.9) is composed mostly of calcite and iron-

oxide. Some xenomorphic epidote crystals are also found in the matrix.

The edge of the marble fragments are coated by iron-oxide. Under the

microscope, no significant recrystallization product which might replace

calcite crystals has been observed. Closer to the fault plane, the

fault breccia progressively changes its characteristics. It becomes

soft and is not coherent (Figure 3.8). This part of the fault rock is

designated as fault gouge (Hobbs, et al., 1976, p. 302).

As is shown in Figure 3.7, the fault plane of the Bezirgan Fault

is clearly observable along the eastern slope of the Bezirgan Dere.

However, it does not exhibit any slickensides in the map area. This

portion of the fault is steeply dipping to the NW (the orientation of

the fault plane at locality 2 in Plate 5 is N55E; 60 NW). The sense of

motion of the fault is determined as sinistral at locality 2 in Plate

5, based on structures in a strongly foliated high-strain zone (see

Figure 3.8 B).

At the transition zone between the fault gouge and the narrow

high-strain zone, some relatively unstrained marble lenses up to 30 cm

long are observed (Figure 3.8). The long axis of the marble lenses is

subparallel to the fault plane and the dip of the later foliation.
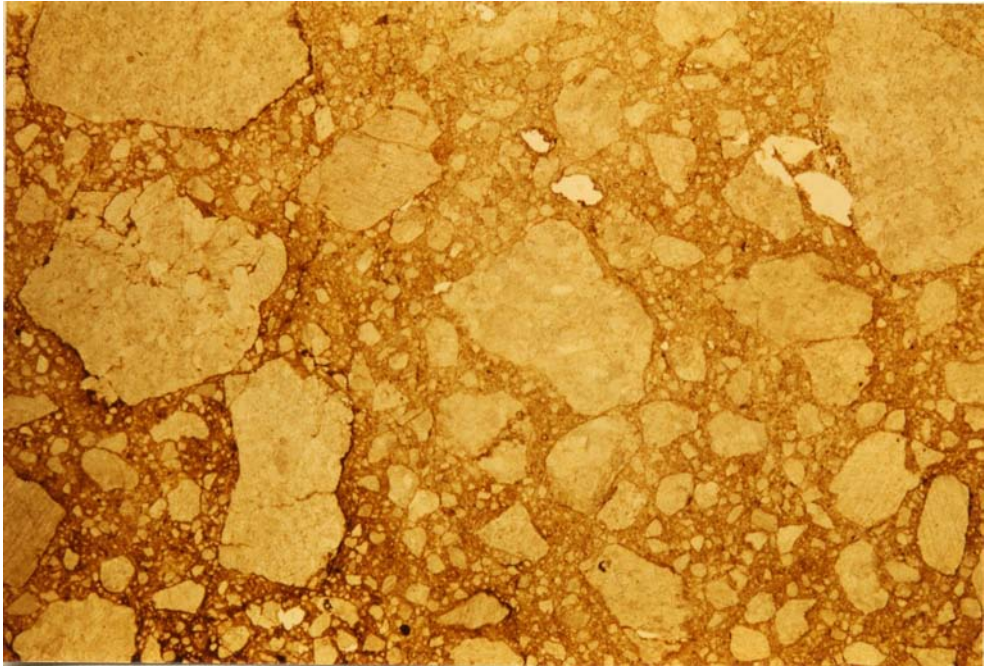
Figure 3.9 Fault breccia in the Kirklar Marble along the Bezirgan Fault. Photo is 3.3 cm across the horizontal dimension.
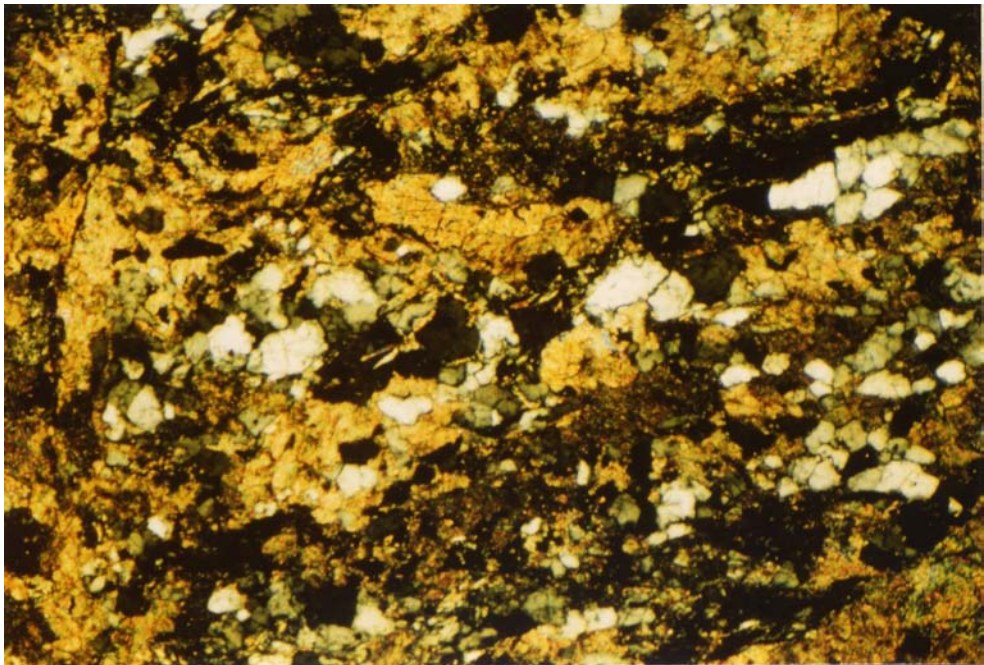
Figure 3.10 Optical micrograph of a fault rock, showing a weak mylonitic foliation (x40, crossed Nicols).

These lenses are composed of about 40-50% calcite, 40% quartz, 5% iron-oxide and up to 15% mica (muscovite) and some epidote. The preferred orientation of quartz, muscovite define a weak foliation (Figure 3.10). The mineralogy and microstructural features of highly strained rocks is discussed below in the section on the Hirsiz Fault.

In the map area, the orientation of the Bezirgan Fault varies from one place to another. For instance, it curves to the east near the northern end of the Bezirgan Dere (see Plate 5). At the southern end of the map area, the fault contact is isoclinally folded (Figure 3.11 and Figure 4 in Plate 3). The hinge line of these isoclinal folds plunges 70° to the SE (Plate 5). Other evidence for folding of the fault is a gently dipping patch of the Calik Formation overlying the Kirklar Formation (Figure 3.7, see Plates 2 and 5 for its location). From the discussion above, the Bezirgan Fault is designated as a thrust fault which was folded by a younger deformation phase (D_1). The sense of movement determined for the Bezirgan Fault shows that the Kirklar and Calik Formations represent footwall and hangingwall of the fault respectively (Figure 3.8 B).

C. Hirsiz Fault

The type localities for the Hirsiz Fault are located on the Hirsiz Tepe (Locality 3 in Plate 5) and in the Kavak Dere (Locality 7 in Plate 5). The thrust fault was formed between the Calik and Koyunatlayan Formations. It cuts across almost the entire map area roughly in the north-south direction. The map pattern of the Hirsiz Fault (Plates 1 and 5) clearly suggests that this fault was tightly folded as we have seen for the Corik and Bezirgan Faults in the previous parts. At
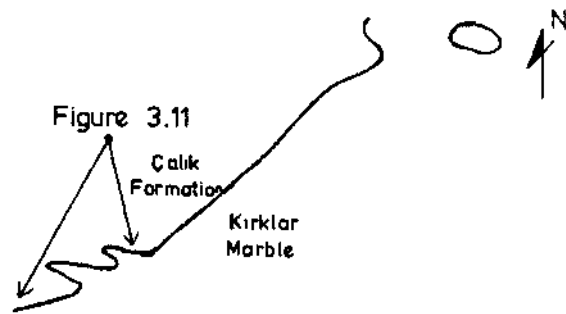
Figure 3.11 Isoclinally folded thrust contact of the southern end of the Bezirgan Fault in the map area. Its location is marked above on the map view.

Locality 7 in Plate 5, the fault plane can clearly be seen (Figure 3.12).
The orientation of the fault plane is determined as N15W; 35 NE in this
locality. As is shown in Figure 3.12, the Calik Formation is strongly
foliated under the thrust contact. The orientation of foliations is
subparallel to the fault orientation. The fault plane does not exhibit
any slickensides.

The best reference locality for the Hirsiz Fault is located on
the Hirsiz Tepe which is situated on the southern slope of the Hirsiz
Dere (Locality 3 in Plate 5). In this location, the fault zone is
characterized by fault rocks such as fault breccias in the Koyunatlayan
Limestones, show highly angular limestone fragments, and about 10 to
20 m thick mylonitic zone which was formed mainly in the Calik Formation.
A fault plane is partially exposed between the fault breccias and the
mylonitic zone. Some ductile deformation in the form of mylonitic and
shear band foliation is also observed (Figure 3.14) in the hangingwall
of the fault, in the Koyunatlayan Formation. Because these two different
mylonitic rocks formed in the Calik phyllitic psammite with calcschist
interlayers and in the Koyunatlayan Limestone units having different
physical properties, the rocks show different deformation mechanisms.
These are discussed below.

The geometry of the macrostructures of mylonitic rocks in the Calik
Formation are described first and then a detailed description of their
microstructure follows. The description of mylonites formed in the
Koyunatlayan Limestone follows this.

The mylonitic body formed in the Calik Formation shows a progres-
sive change in its texture within 15 m width from west to east across

Figure 3.12   An outcrop view of the Hirsiz Fault in the Kavak Dere; Locality 7 in Plate 5.

the zone. To the east, mylonitic rocks become much finer grained.
The stage in this development of the sequence is shown in Figure 3.13
A1, B1 and B2. The mylonitic rocks found in the west are composed of
40-50% quartz, 25-30% calcite (mostly in the form of pod shaped aggre-
gates up to 1.5 cm) and 20% muscovite-sercite-chlorite. The average
preferred orientation of grain shape of quartz and mineral elongation
of muscovite-sercite-chlorite crystals define the mylonitic foliation
(Sm). Long axes of relatively unsheared calcite pods up to 1.5 cm
long within the ductile matrix shown in Figure 3.13 A1 are subparallel
to the mylonitic foliation. Between the pods themselves smaller
scale ductile shear zones often occur at a low angle (30-35°) to the
larger shear zone defined by mylonitic foliation which surrounds the
calcite pods (Figure 3.13 A2).

To the east, the mylonitic rocks become much finer and do not
show any calcite pods in them. The mineralogy of these rocks are also
different. They are composed of 75 to 85% quartz, 10 to 15% muscovite-
sericite-chlorite, 1 to 5% iron oxide and about 1% epidote and virtually
no calcite. In these strongly foliated mylonites, the preferred orienta-
tion of grain shape of quartz-feldspar and mineral elongation of muscovite-
sercite-chlorite-epidote beautifully define mylonitic foliation (Sm)
(Figure 3.13 B1). As is shown in Figure 3.13 B1, these rocks also show
shear band foliations (Ss) which were formed oblique to the mylonitic
foliations at a low angle (30°). Generally, shear band foliation (Ss)
is defined by mineral elongation of micas. Where affected by a shear
band, the mylonitic foliation trends into parallelism with the shear
band boundary (Figure 3.13 B1). This is the best example of shear bands

Figure 3.13. Progressive change in the texture of fault rocks in the Hirsiz Fault;-Locality 3 in Plate 5.

(A1): Optical micrograph of relatively unsheared calcite pods within the ductile matrix (crossed Nicols). The location of A2 is marked on the micrograph;

(A2): Smaller scale ductile shear zone occurred between the calcite pods (x 40, crossed Nicols);

(B1): Optical micrograph of mylonite structure (mylonitic foliation: Sm and shear band foliation: Ss) within the Hirsiz Fault. The mylonite was formed in the Calik Formation (x 40, polarized light; section is perpendicular to the Sm). Shear band foliation is defined by the upper right-to-lower left dark zones. Within these zones mylonitic foliation has been reoriented. White grains are mostly quartz. Dark material is mostly fine-grained mica and chlorite. The average acute angle between Sm and Ss is 30° and the spacing between bands is up to 0.6 mm (see also text for detail). The direction of shearing is marked on the micrograph.

(B2): Mylonitic rock showing an anostomosing pattern with quartz pods surrounded by mica films (x 40, polarized light).

Figure 3.13 A1 Caption on p.94. Photo is 4 cm across the horizontal dimension. Apparent shear sense is left-lateral in this view
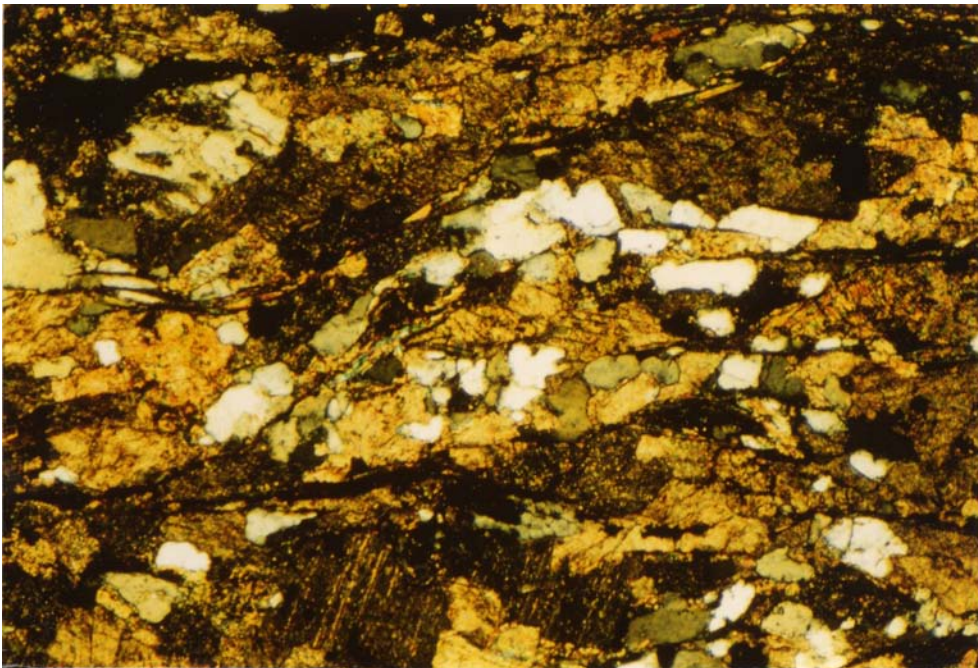
Figure 3.13 A2 Caption on p.94.
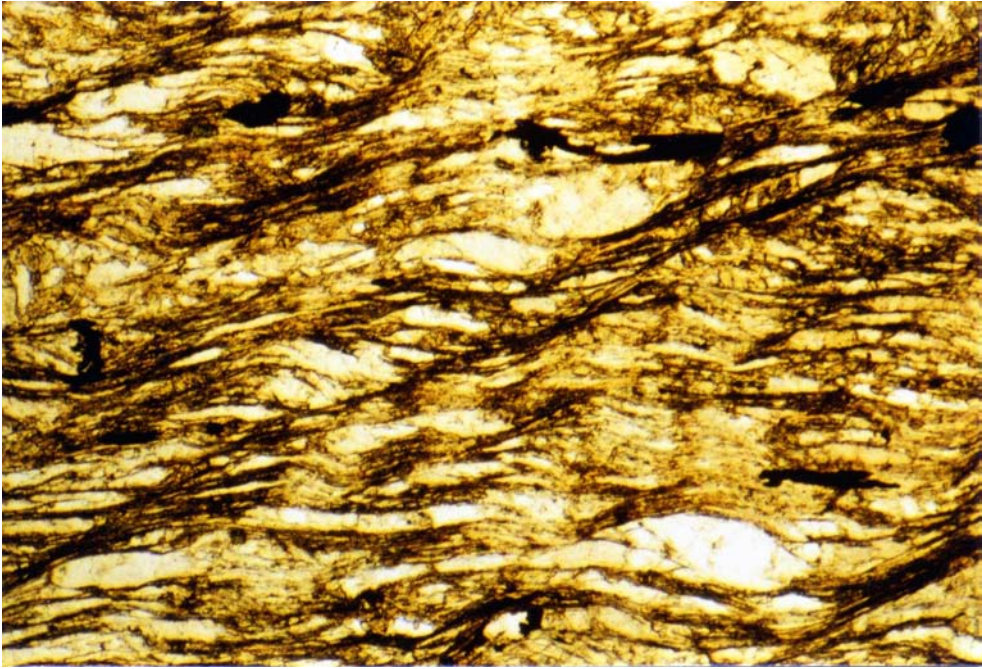
Figure 3.13 B1 Caption on p.94. In this view, apparent shear sense is left-lateral, Sm oriented approximately horizontal; Ss dipping to left.
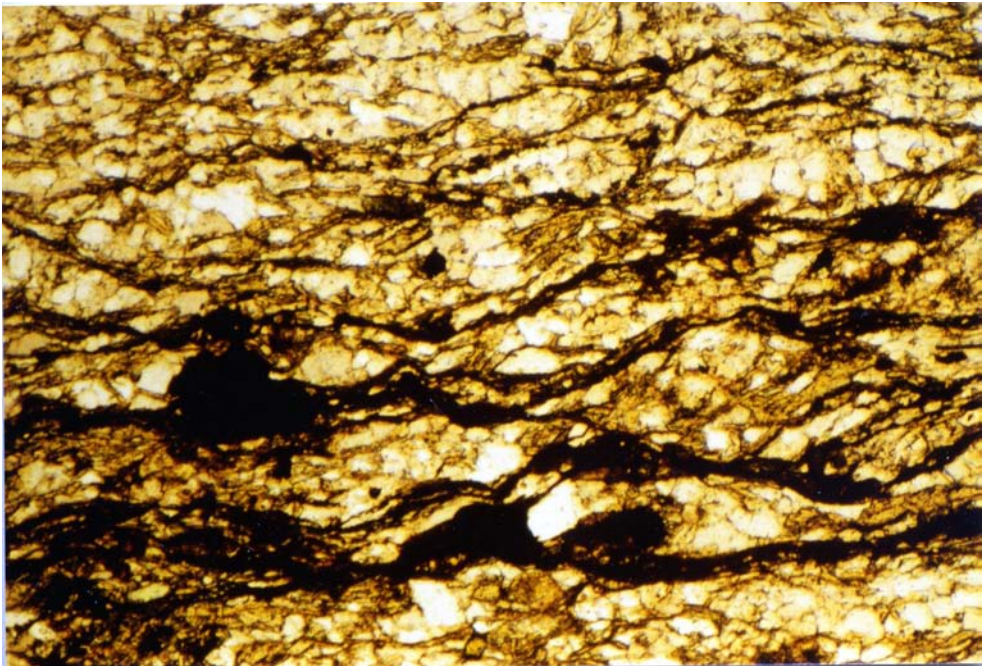
Figure 3.13 B2 Caption on p.94.

observed in the mylonitic zones in Keban area. The spacing between
bands varies between 0.1 mm and 0.78 mm. The width of the bands is
usually 0.01 to 0.17 mm. According to Gapais, 1979; Platt and Vissers,
1980; White et al., 1980; Gapais and White, 1982, "the acute angle
between shear band foliation (Ss) and mylonitic foliation (Sm) always
points in the shear direction" (Figures 3.5h and 3.19). Using this
criterion, the direction of shearing in this sheared rock is determined
as sinistral (Figure 3.13 B1), which indicates that the Koyunatlayan
Formation represents the hangingwall whereas the Calik Formation repre-
sents the footwall of the Hirsiz Thrust Fault. This microscopic obser-
vation based on the position of shear bands with respect to mylontic
foliation (see Figure 3.13 B1) corroborates the sense of shear observation
shown in Figure 3.13 A1 and the field observation for the same fault
zone. This result is consistent with the shear band interpretation of
White et al. (1980, p. 178, 186). A short review on general macro and
microstructural features and origin of shear bands is given below at
page 105 . The eastern mylonitic rocks also show an anastomosing
pattern with quartz pods surrounded by mica films (Figure 3.13 B2).
Quartz content of this type of mylonitic rock is relatively high (85%).

A different form of ductile deformation is observed in the
Koyunatlayan Formation at the Hirsiz Fault. In this part of the this
mylonitic zone, which is about one meter thick is characterized by
limestone lenses and quartz-mica rich calcschist layers between the
limestone lenses. At an outcrop scale, mylonitic foliation is
defined by long axes of relatively unsheared limestone lenses which
are up to 20 cm long, 2 cm wide, by grain shapes of calcite, quartz and
feldspar, and by elongation of mica (muscovite) crystals which were

formed between the limestone lenses in 1 to 4 cm thick zones (Figure
3.14). The thin mylonitic zones are composed of 35% quartz, 25-35%
calcite, 5-7% feldspar, and 20% muscovite-sericite-chlorite. In these
thin strongly foliated zones, there are some small scale open crenula-
tion cleavages occuring at a low angle to the mylonitic foliation
(Figure 3.14 B). Where affected by these open crenulation cleavages,
the mylonitic foliation trends into parallelism with these crenulation
boundaries. They are interpreted as shear band foliation due to the
resemblance to shear band foliation described by Platt and Vissers
(1980), White et al. (1980), and Gapais and White (1982). The sense of
movement determined, based on the position of these shear bands with
respect to mylonitic foliation (see Figure 3.19), indicates that the
Koyunatlayan Formation is situated in the hangingwall of this thrust
zone. This result is consistent with the result given above for the
same zone in Figure 3.13. Moreover, where affected by shear bands,
tips of the limestone lenses curve and trend into parallelism with shear
band boundaries (see Figure 3.14). In the main portion (body) of
the limestone lenses, there are some microfaults at a high angle
(usually greater than 45°) to the long axis of the lenses and to the
mylonitic foliation, so that the microfaults formed only in the lime-
stone lenses, and are oblique to the mylonitic foliation. The sense
of displacement for microfaults formed in the limestone lenses, is
in the same sense as the shear band foliations developed between the
limestone lenses (Figure 3.14 B). I interpret the shear band struc-
tures described above, in the same way as Gapais and White (1982) in
that at the same high strain-rate, the deformation mechanism was rather

Figure 3.14A

Figure 3.14   A shear zone, Locality 3 in Plate 5, showing brittle deformation in the limestone lenses, ductile deformation in the quartz-mica rich, strongly foliated (Sm, Ss: see B, next page) thin zones formed between the limestone lenses (A).

15 Cm.

Ss

Sm

S

Sm

Ss

c : calcite
f : feldspar
q : quartz

Limestone lens

Ss

Sm

microfaults
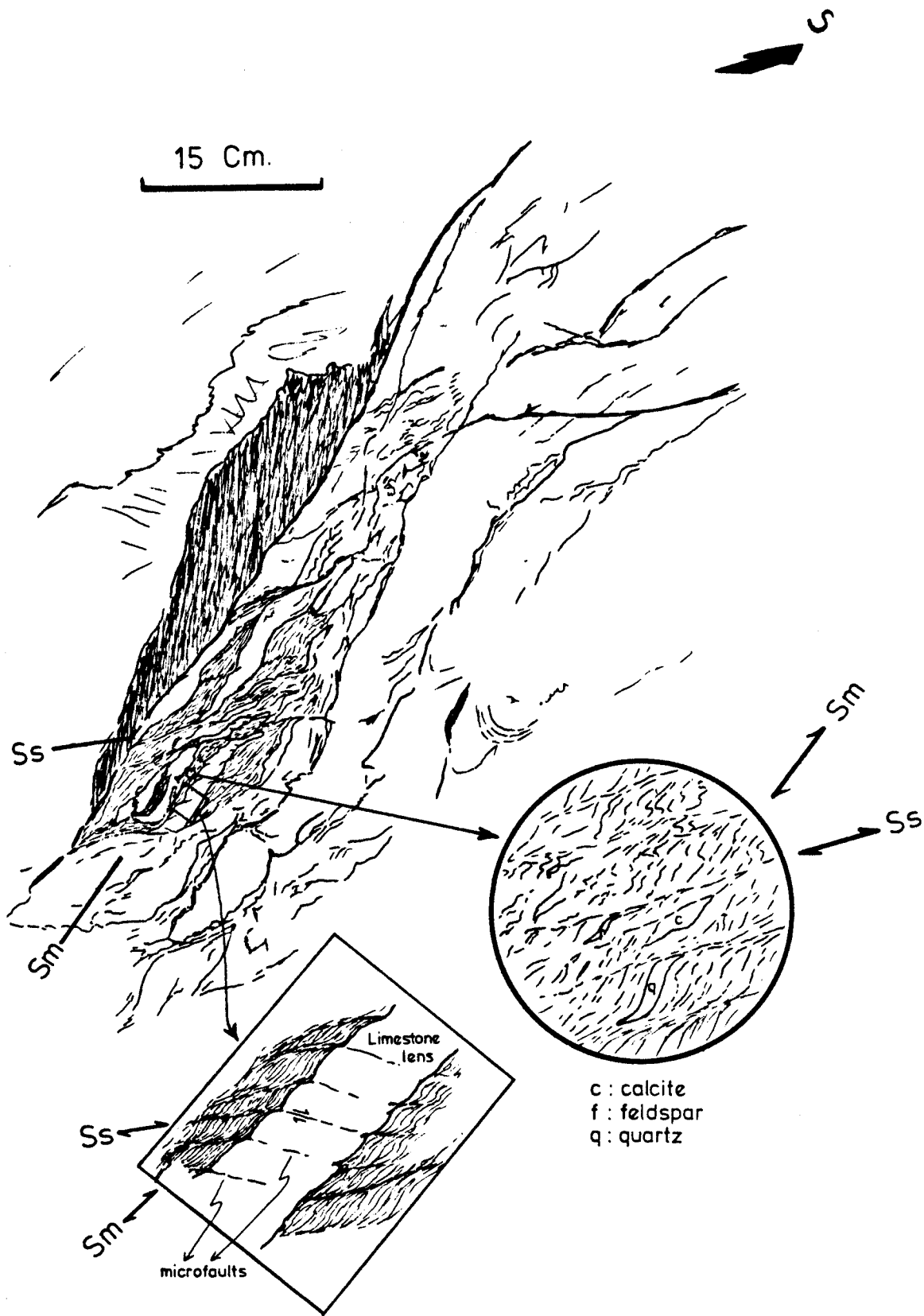
Figure 3.14 B

brittle in the limestone lenses compared with quartz-mica rich,
strongly foliated thin ductile shear zones which are between these
limestone lenses. In other words, if there are two rock types which
show different physical properties from each other (such as brittle
limestone lenses and quartz-mica rich more ductile calcschist),
a brittle and ductile deformation may occur at different places
within the shear zone at the same time. It is concluded that, in this
shear zone, when the bulk deformation cannot be accommodated by the
dominant deformation process at the imposed strain rate, it is accom-
modated by deformation in the form of ductile shear bands in the quartz-
mica rich calcschist and by deformation in the form of brittle micro-
faults in the limestone lenses.

D. Gelintaş Fault

The type localites for the Gelintas Fault are around Gelintaş
Magrasi (Locality 5 in Plate 5) and south of Kartaltasi (Locality 8 in
Plate 5). This fault cuts across the map area roughly in a north-
south direction (see Plates 1 and 5). As is shown in Plates 1 and 5,
the fault shows imbricate structure (=schuppen structure: AGI Glossary,
1972) in the south of Kartaltasi (Figure 3.15). Along the schuppen
structure, the evidence for the imbricated thrust fault are the
presence of fault rocks such as fault breccia and mylonite, and trees
which are preferentially located along the fault (see Figure 3.15),
because of its effect on groundwater.

At Locality 5 in Plate 5, the fault is recognized by a 3 to 5 m
thick fault breccia, 3 to 5 m thick mylonite zone (Figure 3.16) and
fault gouge (see Figure 2.4). The estimated structural thickness of

the fault gouge is about 20 to 35 meters. The structural and micro-
scopic features of the same kind of fault breccia formed here in the
Kirklar Marble are discussed in the previous section, on the Bezirgan
Fault. The mylonites formed in the Kirklar Marble, on the other hand,
are characterized by compositional layering showing different colors
(Figure 3.16). These different color layers (from few mm to 25 cm
thick) are determined as strongly deformed lepidoblastic calcite which
shows a high degree of twinning, and they cannot be distinguished
from each other under the microscope. In between the lepidoblastic
calcite crystals some muscovite (1-2%), epidote (1-2%) and some opaque
minerals (2%) can also be seen. These minerals define the mylonitic
foliation. The color change may be due to the difference in chemical
composition of the marble which gives rise to this mylonitic rock.
This could be verified by chemical analysis on each different layer.
For future work, a structural analysis will be done on the calcite
twins in order to determine the orientation of principal stress axes
in this deformed rock. For this, the technique for dynamic analysis
of calcite twins employed by Turner (1948, 1953) and Carter and Raleigh
(1969) will be used.

Figure 3.17 shows a representative microscopic view of the fault
gouge from Locality 5 in Plate 5. They are poorly exposed and are
not coherent. Therefore, they do not show any significant structural
features in larger exposure. Under the microscope (Figure 3.17), they
are deformed rocks composed of 35% calcite, 25-30% plagioclase, 5%
quartz, 25-30% mica (muscovite) and chlorite.

The Gelintas Fault was formed between the Kirklar and Koyunatlayan
Formations. The orientation of fault varies between N30E; 65 to 85SE

Figure 3.15 Schuppen structure along the Gelintas Fault, looking east toward south of Kartaltasi from the Elazig-Keban highway (K=Kirklar Marble, Ko=Koyunatlayan Limestone).
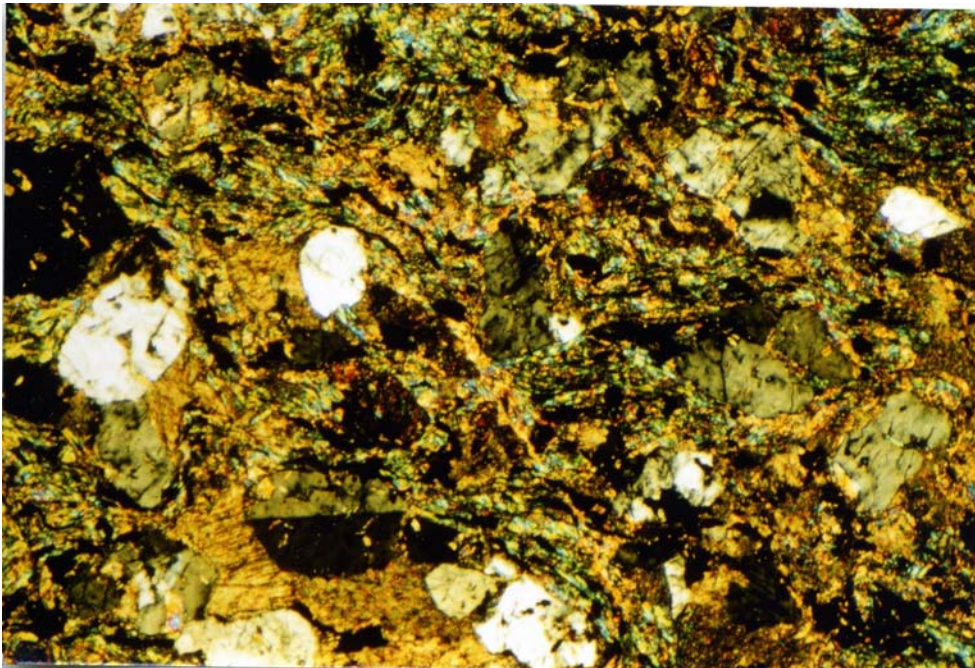
Figure 3.17   Optical micrograph of fault gouge, Locality 5 in Plate 5 (x40, crossed Nicols).

Figure 3.16   Compositional layering in the mylonite formed in the Kirklar Marble, south of Gelintas Magrasi, Locality 5 in Plate 5.

(in the Locality 5 in Plate 5) and N5E; 50 to 60SE (in the north).
In accordance with the data for a folding event after the thrusting,
which is given above in the previous sections, and also with conformity
to the map pattern of the study area, the Gelintas Fault is interpreted
as a folded thrust fault dipping generally about 45° to 60° toward the
east (see Plate 2).

Other evidence of deformation in the crystalline rock series has
been observed, such as small scale ductile shear zones formed in the
Koyunatlayan Limestone (Locality 9 in Plate 5 and see Figure 3.18), and
small local thrust faults (see Plates 1 and 5), joints have also been
observed, but not analysed in detail.

Review of Literature on "Shear Band Foliation"

Shear band foliation is a microstructure commonly found in mylonites
(Platt, 1979; Gapais, 1979; White, 1979; Platt and Vissers, 1980;
White et al, 1980; Gapais and White, 1982; Passchier, 1982). It is a
small scale open crenulation cleavage and occurs at a low angle (typically
less than 45°) to the enveloping surface of the older foliation (mylonitic
foliation) defined by the average grain shape fabric (Figure 3.19).
Shear band foliation has been intensively studied in pelitic mylonites
(phyllonites) (Sibson, 1977; White, 1979; White et al, 1980), in
phyllites (Platt and Vissers, 1980), in quartz mylonite (Gapais and
White, 1982), and in quartzofeldspathic mylonite (Gapais, 1979), within
the past few years. White (1979) morphologically discusses his field
and microstructural observations in the light of experimental studies on
high strain deformation of metals and concludes that the foliation
resembles shear bands which form during the high strain deformation of
metals particularly during rolling.

Figure 3.18 (A): A 10 meter thick mylonite zone formed within the Koyunatlayan Formation, Locality 9 in Plate 5; (B): closer view of A. (Mylonitic foliation is defined by compositional layering).
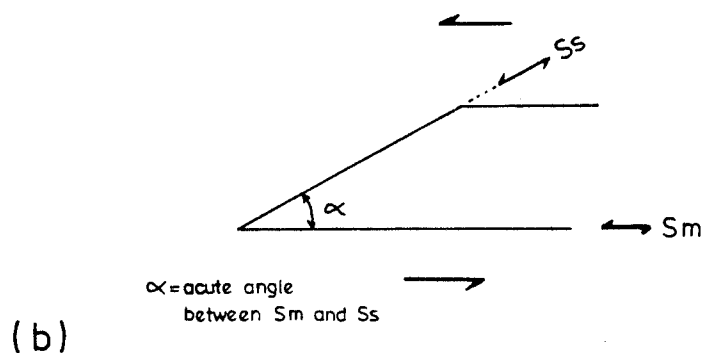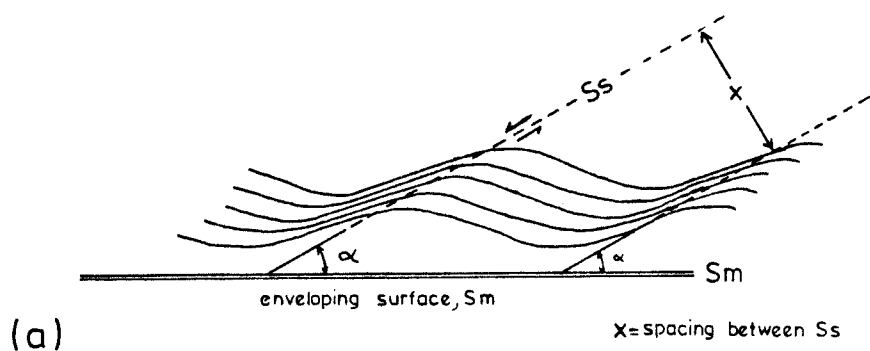
Figure 3.19. (a) Geometry of shear band foliation (modified
after Platt and Vissers, 1980, figure 9); (b) the acute
angle between shear band foliation (Ss) and mylonitic folia-
tion (Sm) always points in the shear direction (data compiled
from White et al., 1980).

These reserarchers mentioned above defind "shear band foliation" as narrow planar zones of intense deformation which formed oblique to the mylonitic foliation at a low angle (less than 45°). The spacing between bands is described as about 300 μm by Gapais and White (1982) for quartz mylonite. They determined the width of the bands as about 60 μm. Usually two sets of bands may develop both at a low angle (less than 45°) to the mylonitic foliation but the main one is always approximately parallel to the complementary shear plane to the active shear zone. If only one is formed, it can be used to deduce the shear direction. The acute angle between shear band foliation (Ss) and mylonitic foliation (Sm) always points in the shear direction (White et al., 1980, p. 178 and 186). According to Berthe et al. (1979 a, b), White (1979), Platt and Vissers (1980), White et al. (1980), and Gapais and White (1982), shear bands develop during the same deformation that produced the mylonitic foliation but at a late stage in the history of the zone. They further note that the shear band development is associated with a low temperature during deformation. Gapais and White (1982) suggest that shear bands are the result of inhomogeneous deformation. They develop after a critical amount of strain beyond which the rock is incapable of accommodating (homogeneously) the bulk deformation. From the foregoing, they conclude that ductile shear bands develop because bulk deformation cannot accomodate the imposed strain rate, so that it is accommodated by deformation in the shear bands (Gapais and White, 1982, p. 13), an explanation similar to that given by other researchers (Berthe et al., 1979a, b; Platt, 1979; Gapais, 1979; White, 1979; Platt and Vissers, 1980; White et al., 1980; Passchier, 1982).

Platt (1979), Platt and Vissers (1980), and Passchier (1982) named this microstructure found in mylonites as "extensional crenulation cleavage." Platt and Vissers (1980) describe this as follows (p. 397): "Extensional crenulation cleavage is defined by sets of small scale ductile shear bands along the limbs of very open microfolds in the foliation. The sense of movement on the shear bands is such as to cause a component of extension along the older foliation."

The above review focuses mostly on the macro and micro-structural features of shear band foliation. For more detailed discussion on their origin, see Cobbold (1977), Berthe et al. (1979 a, b), Gapais (1979), Platt (1979), White (1979), Platt and Vissers (1980), White et al. (1980), Gapais and White (1982).

3.2.2. Fold Generations

In this part of the thesis, fold generations are identified and then their styles are described and compared in detail. There is also a short description of the foliations that are related to the fold generations and a discussion on layering-foliation relationship. The technique is based on overprinting relationships, employed, for example, by Weiss and McIntyre (1957); Turner and Weiss (1963); Williams (1970), used in order to identify the fold generations. The fold descriptions used are on the basis of interlimb angle (Figure 3.20) (Hobbs et al., 1976, p. 170-175).

Structures in each of the fourteen outcrops shown in Plate 3 and other illustrations in Figures 2.8, 3.27, have been analysed in order to date the fold structures relative to one another on the basis of overprinting relationships, and similar features emerge in each. Two
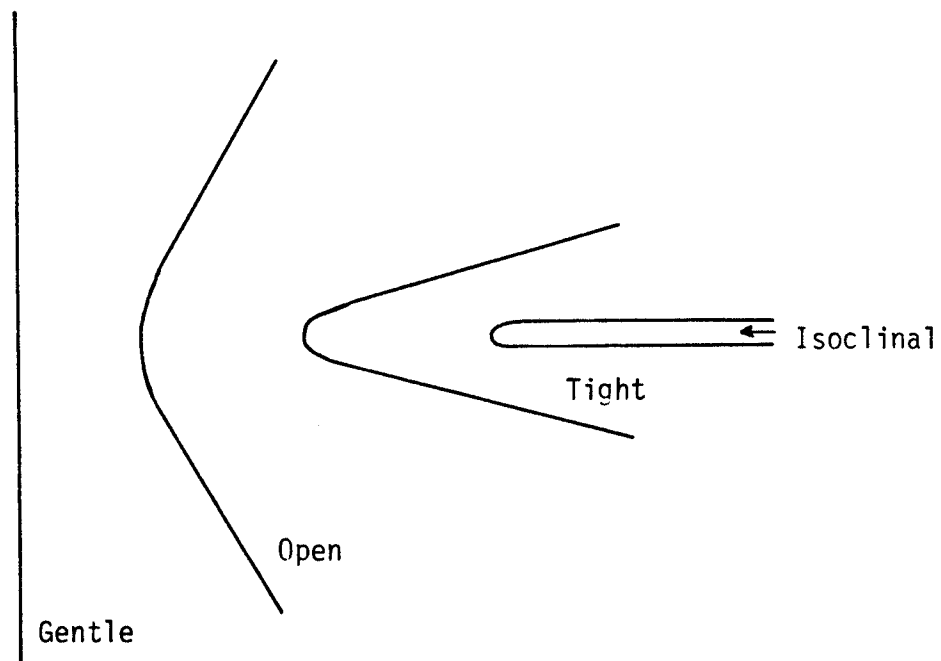
Figure 3.20. Terms used to describe folds on the basis of interlimb angle (after Hobbs et al., 1976, p. 171).

generations of folds are well defined. As is mentioned in the previous chapter, since no younging criteria have been found, they are named synforms or antiforms on the basis of their geographic orientation.

Earlier folds (F_1) are usually tight (Figure 3.21, 3.23 and folds 3, 9, 12, 14 in Plate 3) to isoclinal structures (Figures 3.22, 3.24 and folds 2, 4, 5, 7, 8, 11 in Plate 3). They have steeply dipping axial planes in most places. Transposition of layering (Hobbs et al., 1976, p. 252) is also common both in the Calik Formation (Figure 3.25 and folds 1, 6 in Plate 3) and in the Koyunatlayan Formation (Figure 3.26 and folds 13 in Plate 3) in some places. The earlier folds, F_1, do not fold any earlier folds but do fold earlier tectonic structures (T_{oo}; faulting) that juxtaposed the metamorphic rock units. They are refolded by later folds (F_2) (Figure 3.22, 3.24 and folds 2, 7, 8, 10, 11, 12 in Plate 3). These later folds (F_2) are generally open (Figures 3.22, 2.24 and folds 2, 8, 10, 11 in Plate 3). They have variably dipping axial surfaces (moderately dipping to the N and/or SE).

F_1 and F_2 folds are separated from each other on the basis of overprinting criteria (refolding of one fold by another); overprinting of foliations has also been used. F_1 and F_2 are groups of folds of different ages. The difference in age may be great or extremely small, but where they found in the same outcrop, F_2 folds postdate F_1 folds (Figures 3.22, 3.24 and folds 2, 7, 8, 10, 11 in Plate 3).

I have also observed two generations of foliations (Figures 3.27, 3,28, 3.29) related to the folds described above, and defined two related lineations (Figure 3.29). Earlier foliations (S_1) are parallel to axial surfaces of F_1 folds, and later foliations (S_2) are parallel to axial surface of F_2 folds. These are considered below.

Figure 3.21.   Tight F_1 folds in the Calik Formation (phyllitic psammite with calcschist interlayers) (Fold 9, in Plate 3). The interlimb angle is 32°.

Figure 3.22.   An open F_2 fold overprinting an isoclinal F_1 fold in the Calik Formation (Fold 2 in Plate 3).
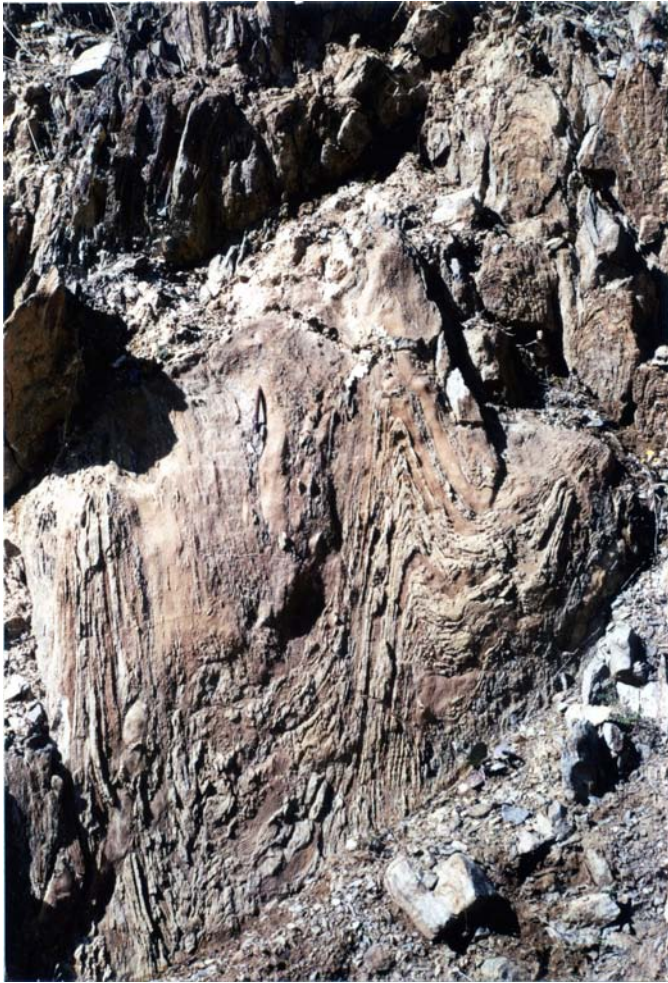
Figure 3.21; caption on previous page

Figure 3.22; caption on previous page

Figure 3.23. A tight F_1 fold in the limestone layers of the Koyunatlayan Formation (Fold 14 in Plate 3) showing a convergent folaition fan. The fan angle is 85° to 95° and interlimb angle 55°. Foliation is oblique to the axial plane of the fold by 50° in the limb area.

Figure 3.24. Isoclinal F_1 folds overprinted by later open folds (F_2) in limestone layers of the Koyunatlayan Formation (Fold 10 in Plate 3). Interlimb angle of F_2 fold is 120° to 140°.

Figure 3.23; caption on previous page.
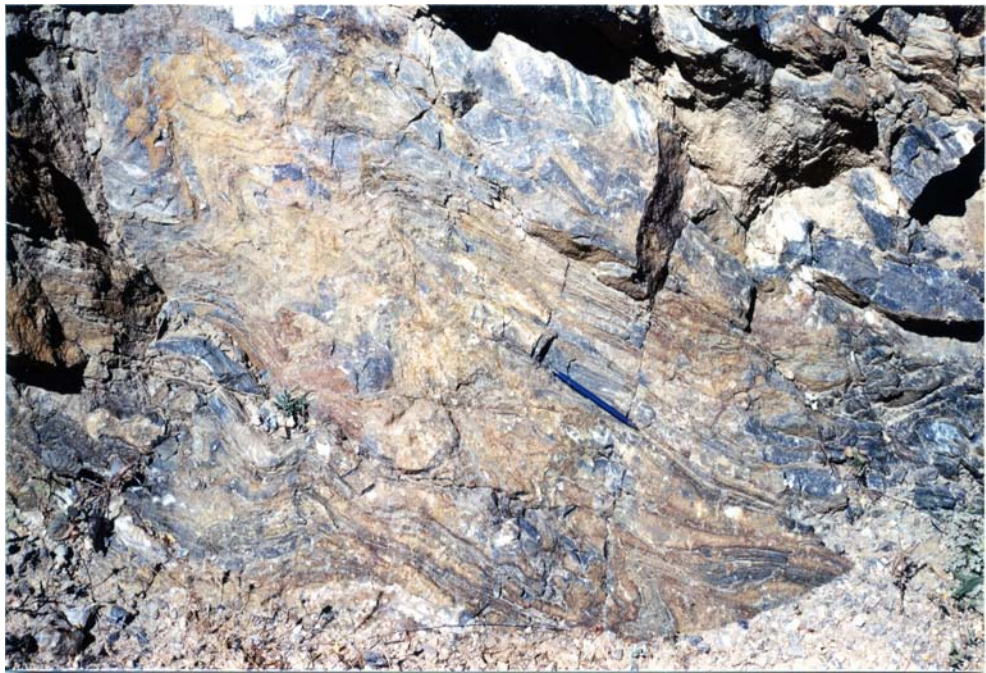
Figure 3.24; caption on previous page.

Figure 3.25   Very tight to isoclinal folds in the Calik Formation (Fold 1 in Plate 3), showing weak transpositional layering.

Figure 3.26   Transposed layers (Figure 13 in Plate 3) in the Koyunatlayan Formation.

Style of F_1 Folds

F_1 folds show considerable variations in their style and size
from one outcrop to another (see Plate 3). They are generally tight
(Figures 3.21, 3.23 and folds 3, 9, 14 in Plate 3) and in outcrops when
they are overprinted by later folds (F_2) they are remarkably isoclinal
(Figures 3.22, 3.24 and folds 2, 7, 8, 10, 11 in Plate 3). All these
F_1 folds show an axial plane foliation (S_1). S_1 is parallel to the
surface plane of F_1 folds in the hinge region, but fans considerably
in limb areas (see Figure 3.30). In phyllitic psammite layers of the
Calik Formation (fold 8 in Plate 3) it forms a divergent fan (Ramsay,
1967, p. 403; Hobbs et al., 1976, p. 215), whereas in calcschist layers
of Calik Formation and in limestone layers of Koyunatlayan Formation
(Figure 2.23 and folds 11, 14 in Plate 3) it forms a convergent fan.
Folds 8, 11, 14 in Plate 3 illustrate foliation-fold relationships
in profile views of folds. The fold 8 is an isoclinal synform in
phyllitic psammite layers of the Calik Formation (see also Figure 2.8)
showing a divergent folaition fan. The fan angle is 5 to 10°. The
fold 11 is an isoclinal antiform in limestone layers of the Koyunatlayan
Formation showing a convergent foliation fan. The fan angle is 60 to
65°. Foliation is oblique to the axial plane by 20° in the limb area.
The fold 14 (see also Figure 3.23) is a tight fold in limestone layers
of the Koyunatlayan Formation illustrating a convergent foliation fan.
The fan angle is 85 to 95° and interlimb angle 55°. Foliation is
oblique to the axial plane of the fold by 50° in the limb area. The
above data shows that with decreasing interlimb angle of folds, folia-
tions become almost parallel to axial surfaces of fold in limb areas.

Gray (1981) suggests that the variation in these angles (foliation fan angle, layering-foliation angle etc.) are influenced by fold tightness, and by fold flattening strain.

Some small parasitic folds are also observed on the limbs of the F_1 folds (Figure 3.23 and fold 14 in Plate 3). These folds are in most instances tight.

In general, the size of the F_1 folds in outcrop scale is related to the thickness of folded layers. For instance, thick-layered Kirklar Formation usually shows relatively large-size folds (fold 4, 12 in Plate 3), while thin-layered phyllitic psammite Calik Formation shows very small isoclinal folds (fold 8 in Plate 3).

In some folds, there is some minor faulting associated with F_1 folds (fold 5 in Plate 3). These types of minor faulting was probably contemporaneous with folding.

Transposition layering (Hobbs et al., 1976, p. 252) (Figure 3.25, 3.26 and folds 1, 6 in Plate 3) observed in the metamorphics is considered below in the next section (3.2.3).

Style of F_2 Folds

Later folds, F_2, are usually represented by open folds and in all the outcrop observations they postdate the earlier F_1 folds (Figure 3.22, 3.24 and folds 2, 7, 8, 10, 11 in Plate 3). S_2 foliation, defined below, is parallel to the axial surface of F_2 folds and therefore they are identified as the second generation foliation. It is a crenulation cleavage whereas the axial surface foliation formed in the F_1 folds is a slaty cleavage or schistosity. These are discussed below. Generally F_2 folds are smaller than F_1 folds. They have variable axial plane

orientations. The interlimb angle of F_2 folds is typically 130° to 155°.
Figure 3.27 shows an isoclinally folded quartz vein within the phyllitic
psammite of the Calik Formation. The vein is also affected by a later
deformation phase (D_2: F_2 folding). In this outcrop, orientation of
crenulation cleavage is parallel to the axial surface of the F_2 fold formed
in the quartz vein.

3.2.3. Foliations and Lineations

In the metamorphics, two generations of foliations are well
defined on the basis of overprinting relationships. Earlier foliations
(S_1) are parallel to the axial surfaces of the F_1 folds in the hinge
regions but fans considerably in limb areas. These were discussed in
detail above in layering-foliation relationships. In addition to these,
Figure 3.30 is a representative microscopic view of layering-foliation
relationships in limb area of an F_1 fold which was formed in the Calik
Formation composed of phyllitic psammite (dark colour layers in the
figure) with calcschist interlayers (white colour layers in the figure;
see Chapter 2 for their mineral compsition) (see figure caption of Figure
3.30 for more explanation).

The metamorphic rocks, in the study area, vary greatly in physical
and mechanical properties so that the earlier foliation (S_1) has a differ-
ent form in one rock type compared to another. These are two main types
of S_1 foliations defined, in the form of slaty cleavage in fine-grained
phyllitic psammite layers of the Calik Formation (Figure 2.10, 3,28, 3.29,
3.31), and in the form of schistosity in relatively coarse grain calc-
schist interlayers of the Calik Formation and in limestone layers of
the Koyunatlayan Formation. In the Kirklar Marble, a very weak schistosity

Figure 3.27   An isoclinally folded quartz vein within the phyllitic psammite of the Calik Formation.

Figure 3.28   Slaty cleavage (S$_1$) and crenulation cleavage (S$_2$) in the phyllitic psammite layers of the Calik Formation.

Figure 3.29   An outcrop of the phyllitic psammite of the Calik Formation, showing S_1 (slaty cleavage, marked by white rock pen in the picture), S_2 (crenulation cleavage, marked by red pen), L_1 (mineral elongation lineation, marked by brown mechanical pencil) and L_2 (intersection of foliations lineation).

Figure 3.30   A representative microscopic view of layering-foliation relationships in limb area of an F_1 fold which was formed in the Calik Formation composed of phyllitic psammite (dark colour layers) with calc-schist interlayers (white colour layers). It shows a divergent foliation fanning (polarized light).

defined by elongation of muscovite and of lepidoblastic calcite crystals is observed under the microscope, but this foliation is not obviously visible in hand specimen or outcrop.

In phyllitic psammite layers of the Calik Formation, slaty cleavage is defined by preferred orientation of elongate quartz grains and mica (muscovite-sericite) films that anastomose around the quartz grains (Figures 2.10, 3.30, 3.31). The preferred orientation of opaque minerals, chlorite, epidote crystals which represent other mineral constituents of phyllitic psammite layers of the Calik Formation, are also subparallel to the slaty cleavage. In calcschist interlayers of the Calik Formation, the preferred orientation of muscovite, chlorite crystals and elongate calcite, quartz grains define schistosity (Figure 2.9, 3.32). In the limestone layers of the Koyunatlayan Formation, very weak schistosity is defined by elongate lepsidoblastic calcite crystals and very rarely by preferred orientation of mica, quartz and opaque minerals (2.13).

Later foliation (S_2) which is parallel to the axial surface of F_2 folds (folds 2, 8 in Plate 3), is designated as crenulation cleavage (Hobbs et al., 1976). Crenulation cleavage is well developed in the Calik Formation, both in phyllitic psammite layers and in calcschist interlayers (Figures 3.31, 3.32). As is shown in Figure 3.32, earlier foliation (S_1) formed in the Calik Formation, is crenulated on a microscale. These microfolds (crenulations) are asymmetrical. The foliation (S_2) is defined both by the parallel limb of the microfolds and by microfaults developed parallel to the microfold limbs (Figure 3.32).

Two lineations related to folds and foliations are also observed in the metamorphics. Both in the Calik Formation and in the Koyunatlayan Formation, some muscovite rods up to several mm in length often exist on
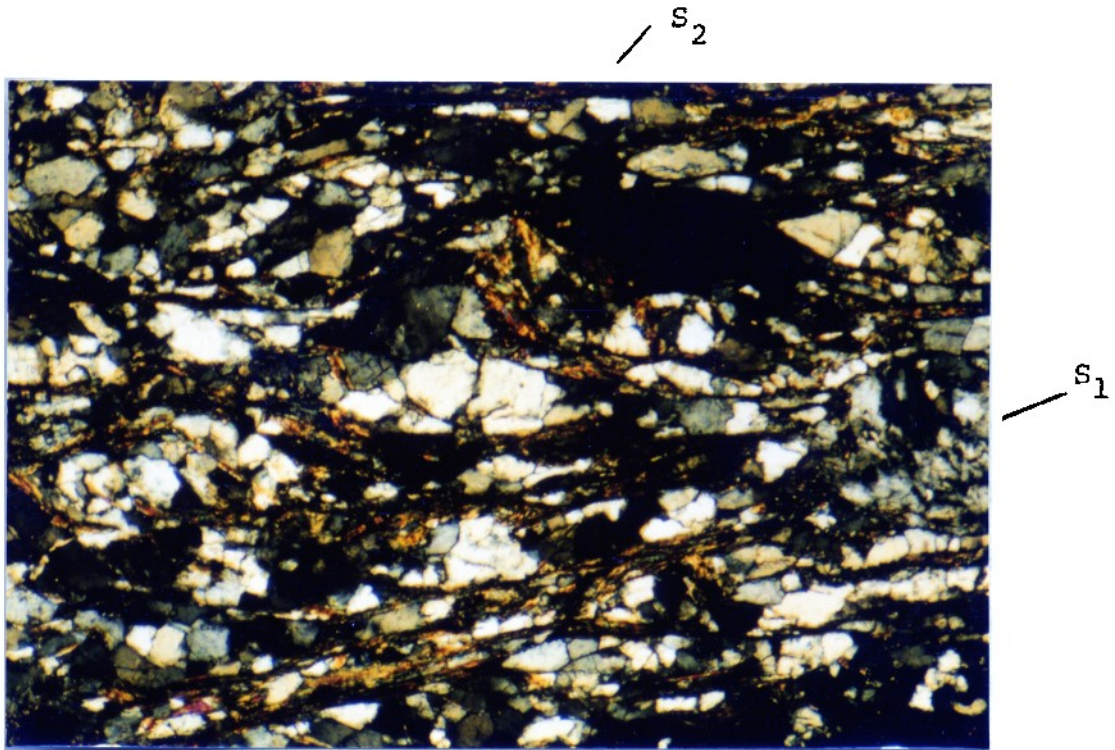
Figure 3.31
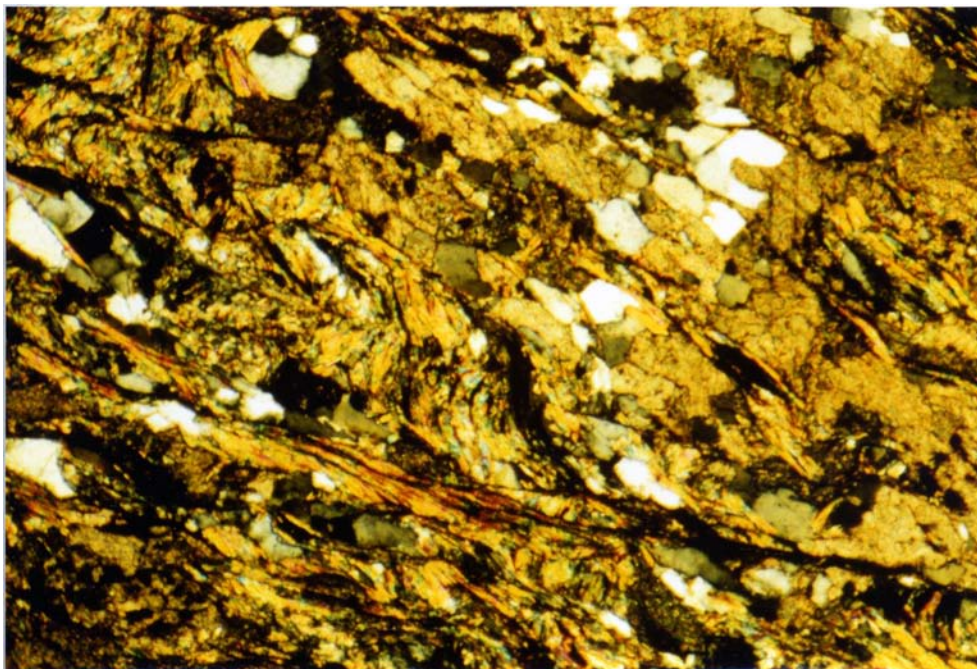
Figure 3.32

layer surfaces and define L_1 (=mineral elongation lineation) (Figure 3.29).

Where they are observed together, mineral elongation lineation (L_1) is

parallel with hinge lines of F_1 folds (fold 14 in Plate 3). In the

phyllitic psammite of the Calik Formation, L_2 is well developed at the

intersection of the S_1 and S_2 (Figure 3.29). They are designated as

"intersection of foliations lineation."

Figures 3.25, 3.26 and folds 1, 6, 13 in Plate 3 are representation

of transposition layering (Hobbs et al., 1976, p. 252) in the Calik Forma-

tion (Figure 3.25, folds 1, 6 in Plate 3) and in the Koyunatlayan Formation

(Figure 3.26 and fold 13 in Plate 3). This is another type of foliation,

parallel with the axial surface of isoclinal F_1 folds. In other words,

the original S_0 surfaces (layering) are coincident with S_1, except at

the closures of these isoclinal folds (see Figures 3.25, 3.26).

3.2.4. Orientation Data for F_1 and F_2 Folds

Orientation data for the metamorphics in the study area are presented

in Figures 3.34, 3.35, 3.36, 3.37. Although a small number of data points

are used here, the 229 data points are divided into four domains as has

been done in classic terrains within the Scottish Highlands, for example

Weiss and McIntyre (1957). The distribution of the domains are shown in

Figure 3.33. Figure 3.34 A shows the equal-area projection of 79 poles

to layering (So), 18 poles to axial surfaces of the F_1 folds (S_1), and

5 hinge line orientation of F_1 folds for Daomin I. Figure 3.34 B is the

contoured equal-area projection of 79 poles to layering (So) illustrated

in Figure 3.34 A. Although in Figure 3.34 A the scatter of the poles to

S1 is concentrated in the west quadrant, a representative girdle can not

be distinguished because it is observed (see Figure 3.34 A) that the Domain
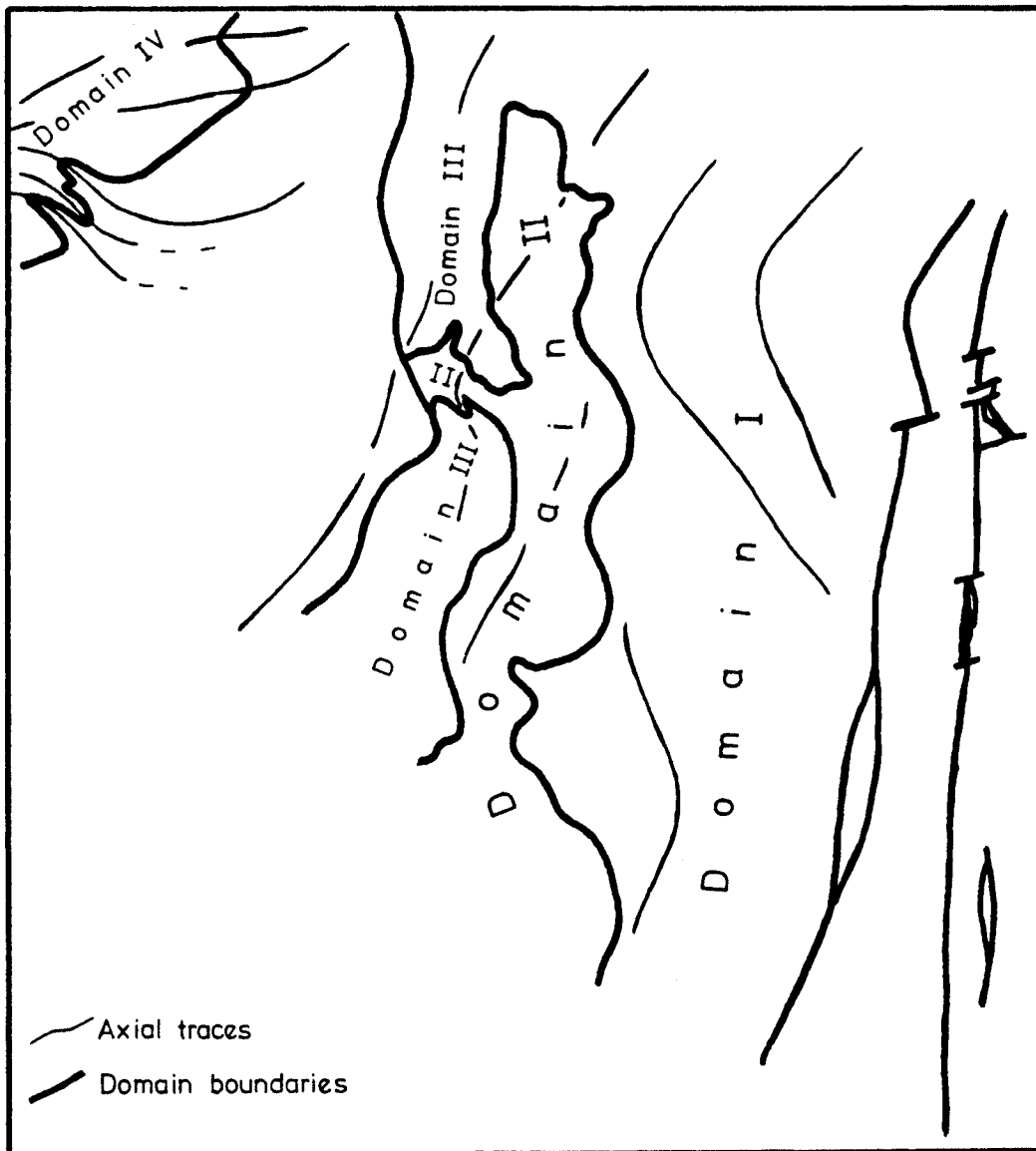
Figure 3.33. Structural Domain and axial traces in the map area. For geological signature see Plate 1. For detailed orientation data for each Domain, see Figures 3.34, 3.35, 3.36, and 3.37.
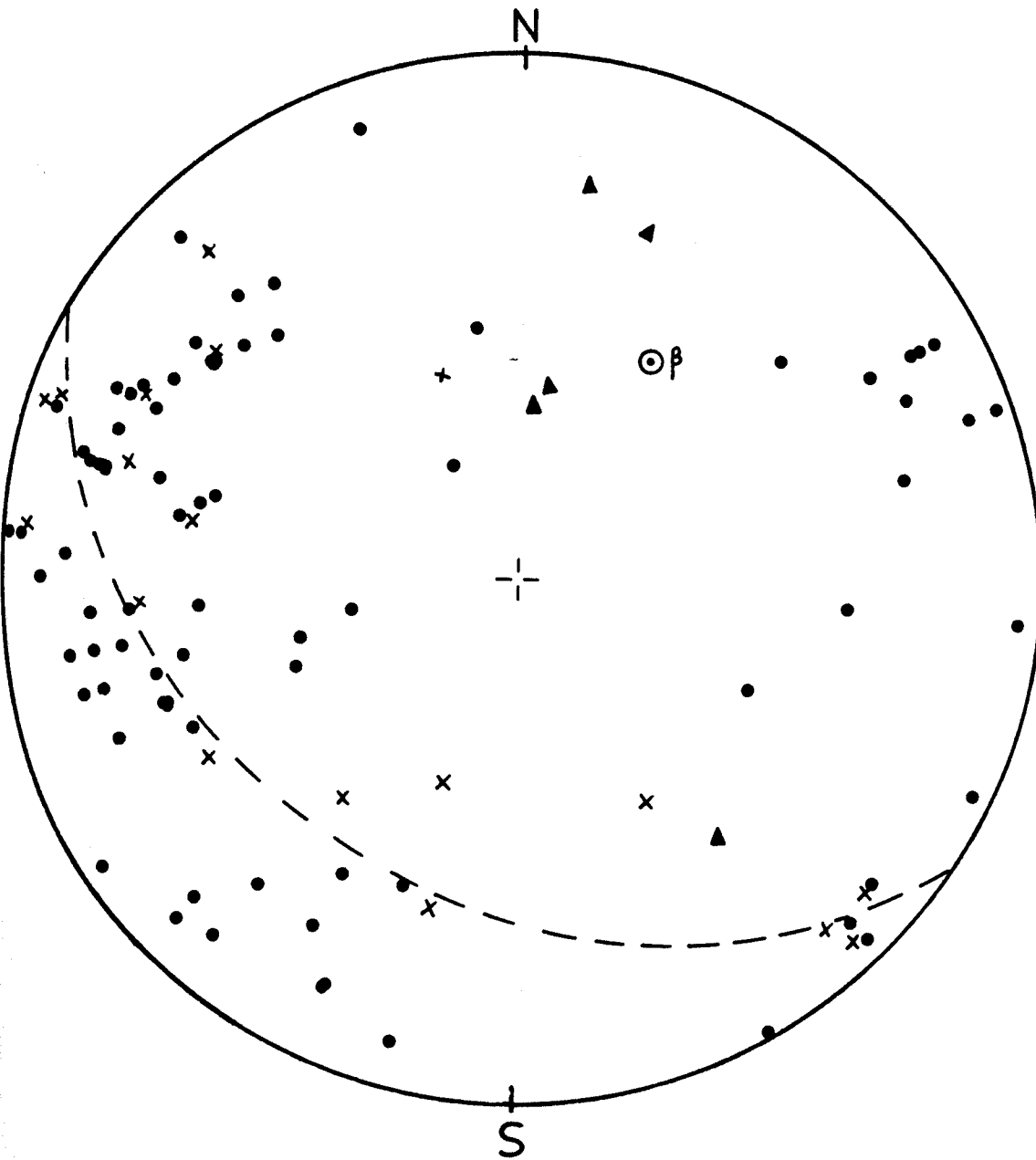
- • Poles to S₀   N=79
- × Poles to S₁   N=18
- ▲ Hinge line orientation of F₁   N=5

Figure 3.34 A.   Orientation data for Domain I (see text for more explanation).
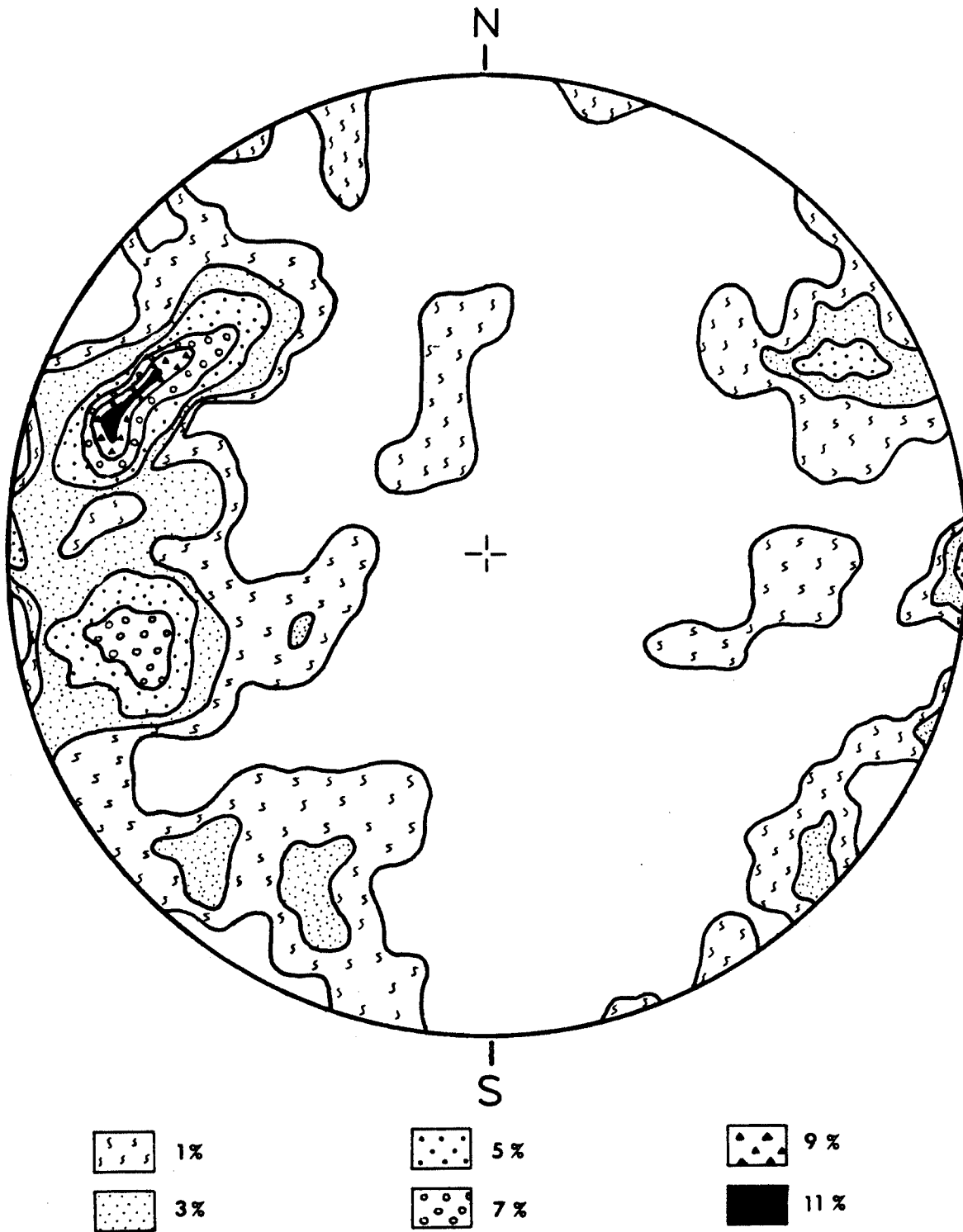
Figure 3.34B. Contoured equal-area projection of 79 poles to layering (S_o) for Domain I.

I is too hetrogeneous to plot on one diagram. This alignment is likely to have been caused by the first (D_1) and second (D_2) generation of deformation combined. This result concurs with the map pattern of this domain shown in Plate 5. In the equal-area projection of poles to axial plane of F_1 folds (S_1) (Figure 3.34 A), a girdle can be distinguished which trends northwest-southeast. Its poles plunges 50° toward 31°. This indicates that S_1 was refolded about a northeast-southwest axis that plunged to the northeast.

Another equal-area projection is a projection of 74 poles to the axial surfaces of F_1 folds (S_1), 3 poles to the axial plane of F_2 folds and 1 hinge line orientation of F_2 folds for Domain II (Figure 3.35 A). Figure 3.35 B is the contoured equal-area projection of 74 poles to S_1 illustrated in Figure 3.35 A. In Figure 3.35 A, the scatter of the poles to S_1 is considerable but there are empty area near the perimeter in the north, south and southwest quardrants and in the centre. The greatest concentration of poles is in the north-west and some in the southeast. The hetrogeneous distribution in the scatter implies no representative consistency or pattern of orientation. Since the orientation data for the axial plane of F_2 folds are quantitatively very small, no concentration or pattern is apparent but as is mentioned, the data is not abundant enough to be very significant.

Other projection of 25 poles to layering (So) for Domain III show a concentration in the northwest (Figure 3.36). The broad scatter in the projection of 24 poles to the axial surfaces of F_1 folds (S_1) for Domain IV may suggest a broad girdle which trends NNE-SSE and plunges to the SW (Figure 3.37).
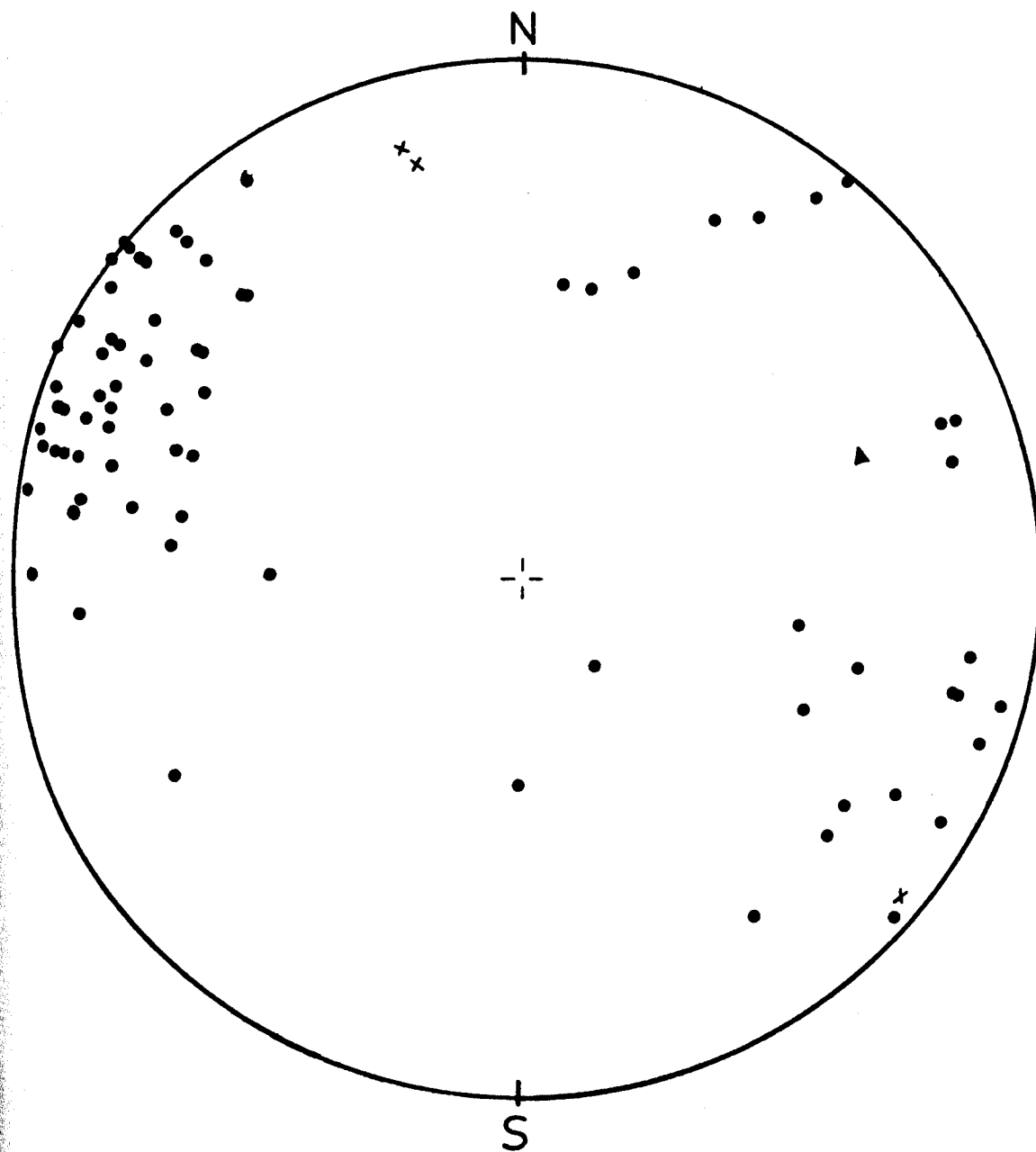
- • Poles to S_1 N = 74
- × Poles to S_2 N = 3
- ▲ Hinge line orientation of F_2 N = 1

Figure 3.35 A.   Orientation data for Domain II (see text for more explanation).
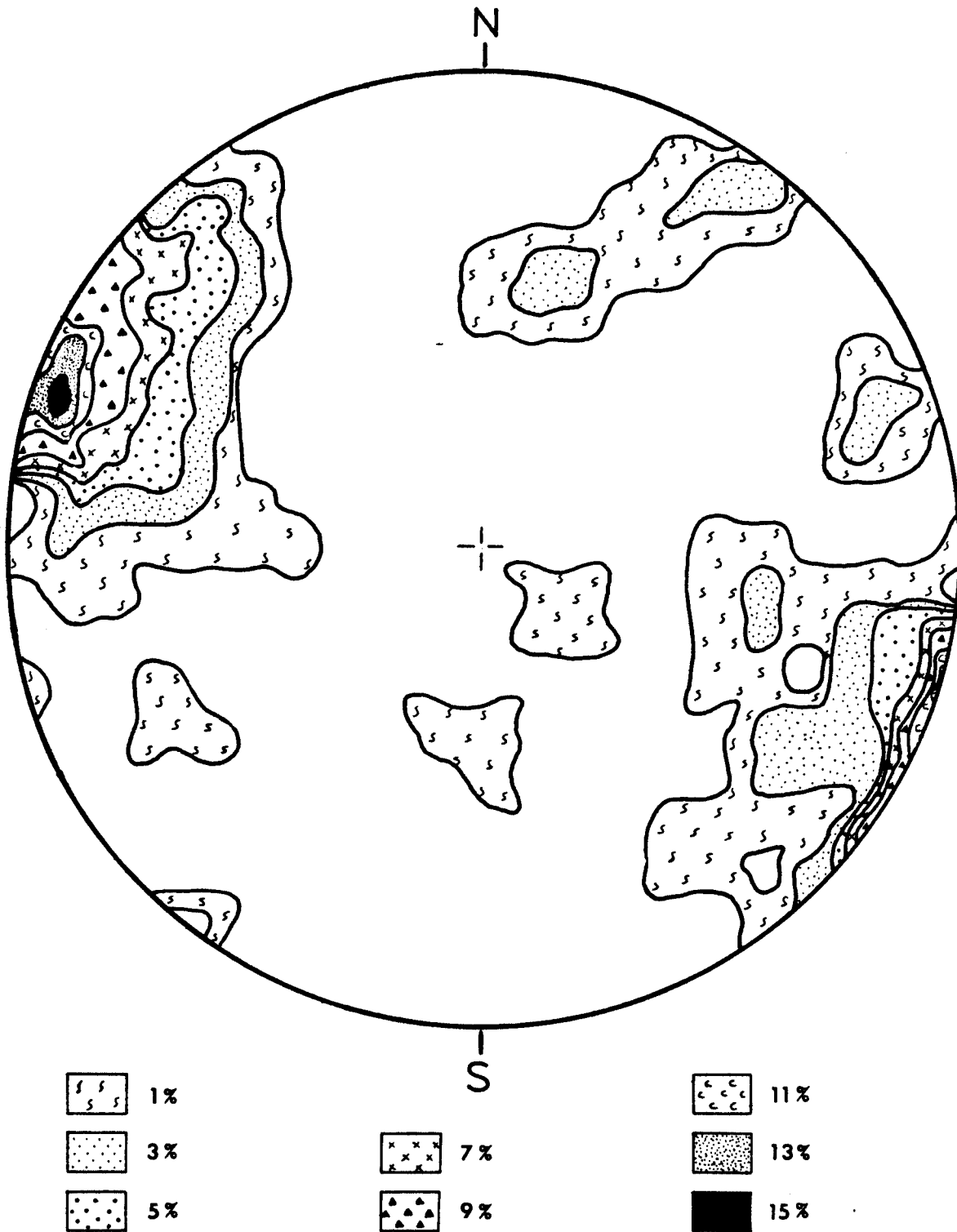
Figure 3.35 B. Contoured equal-area projection of 74 poles to S_1 for Domain II.
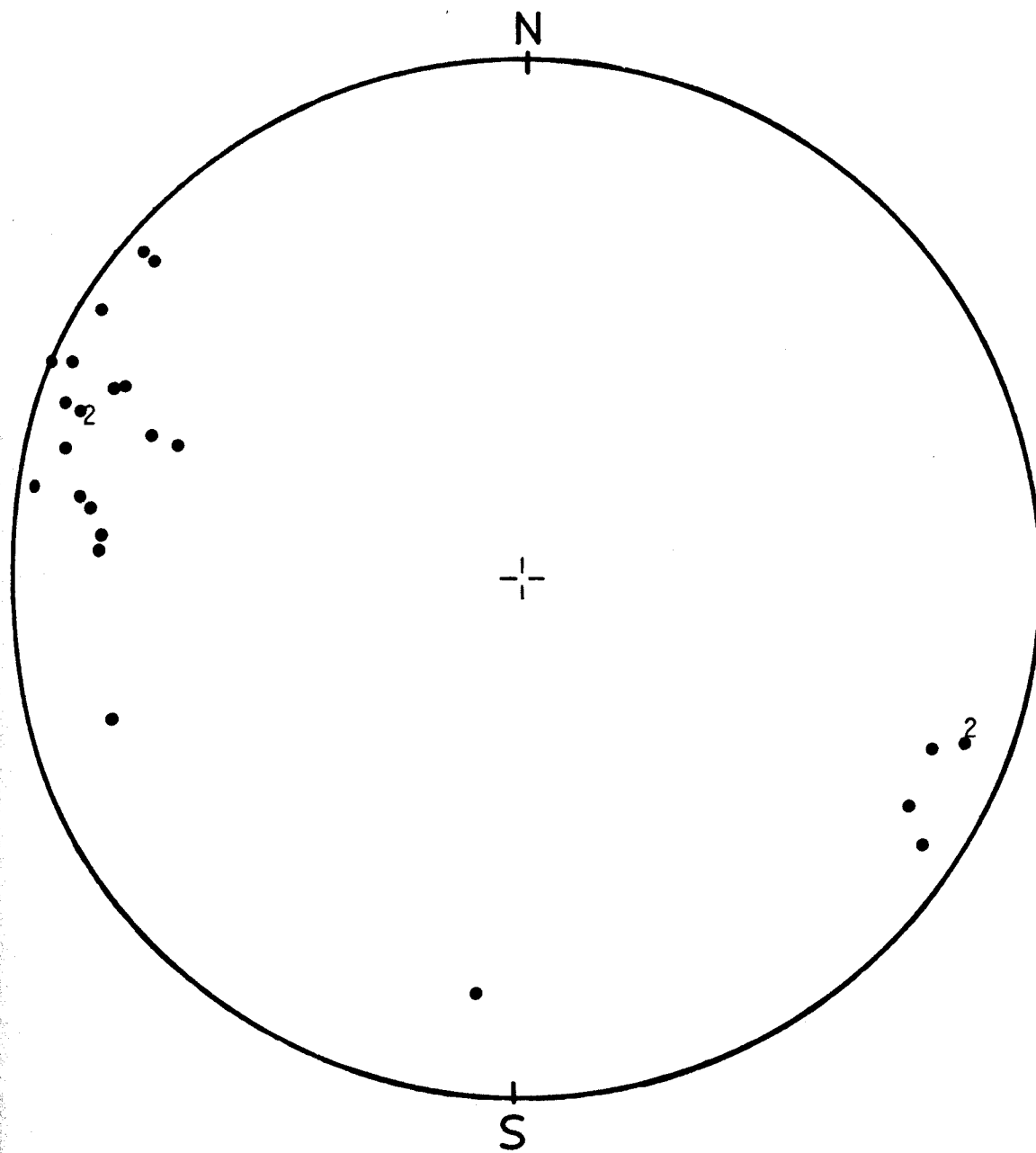
25 points

Figure 3.36 A. Equal-area projection of 25 poles to layering
(S_o) for Domain III.
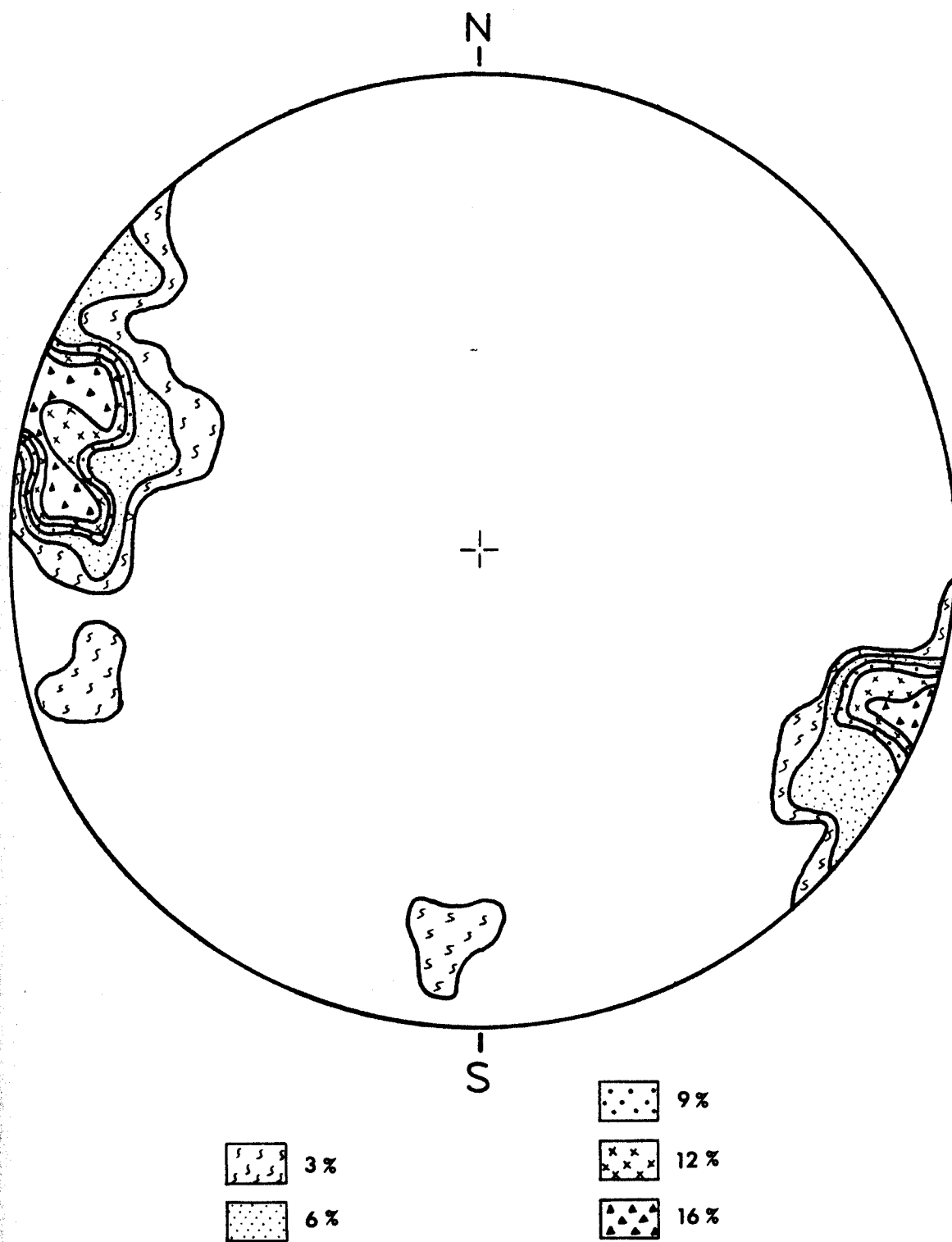
Figure 3.36 B. Contoured equal-area projection of 25 poles to layering (S_o) for Domain III.
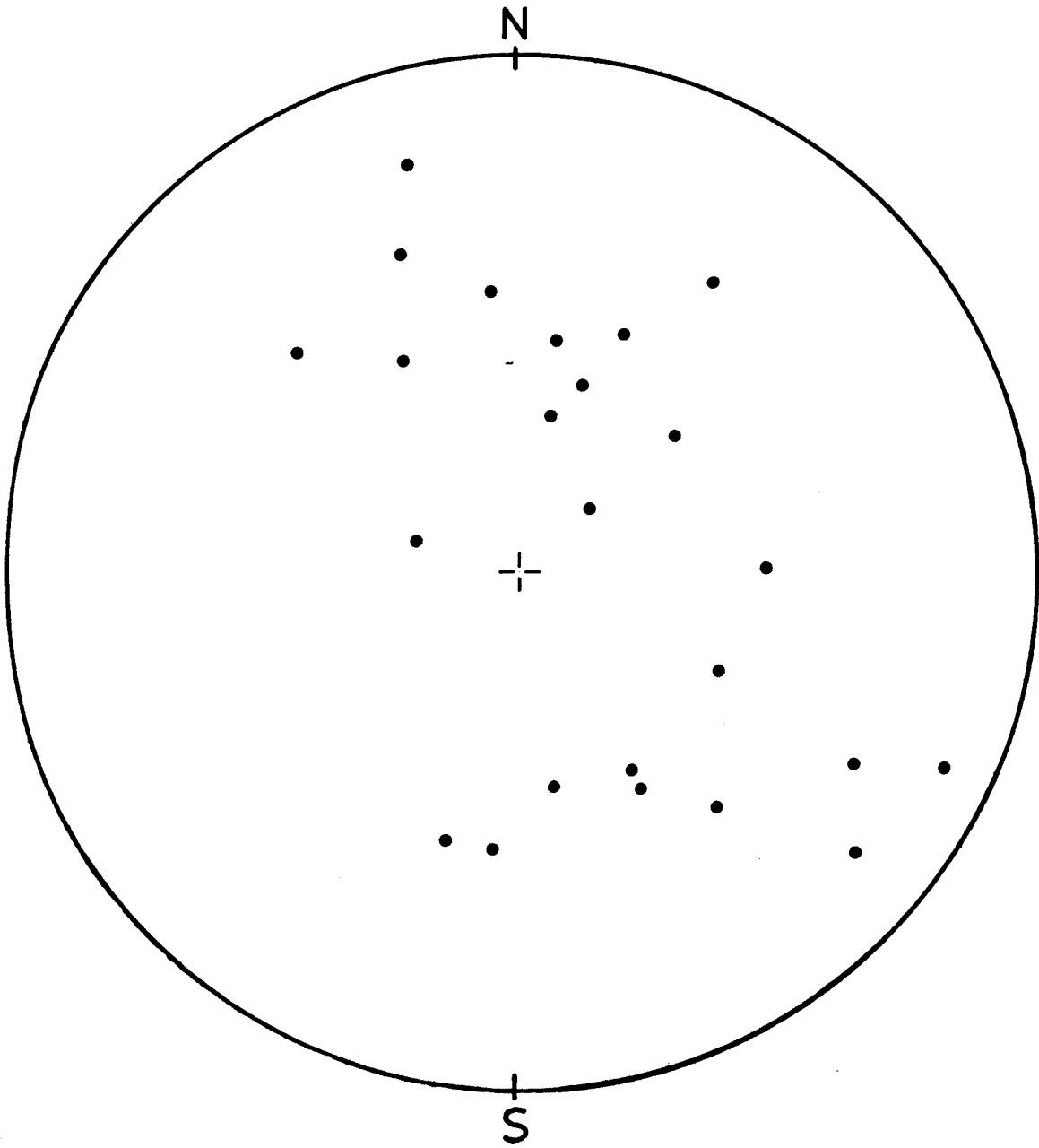
24 points

Figure 3.37A. Equal-area projection of 24 poles to S_1 for Domain IV.
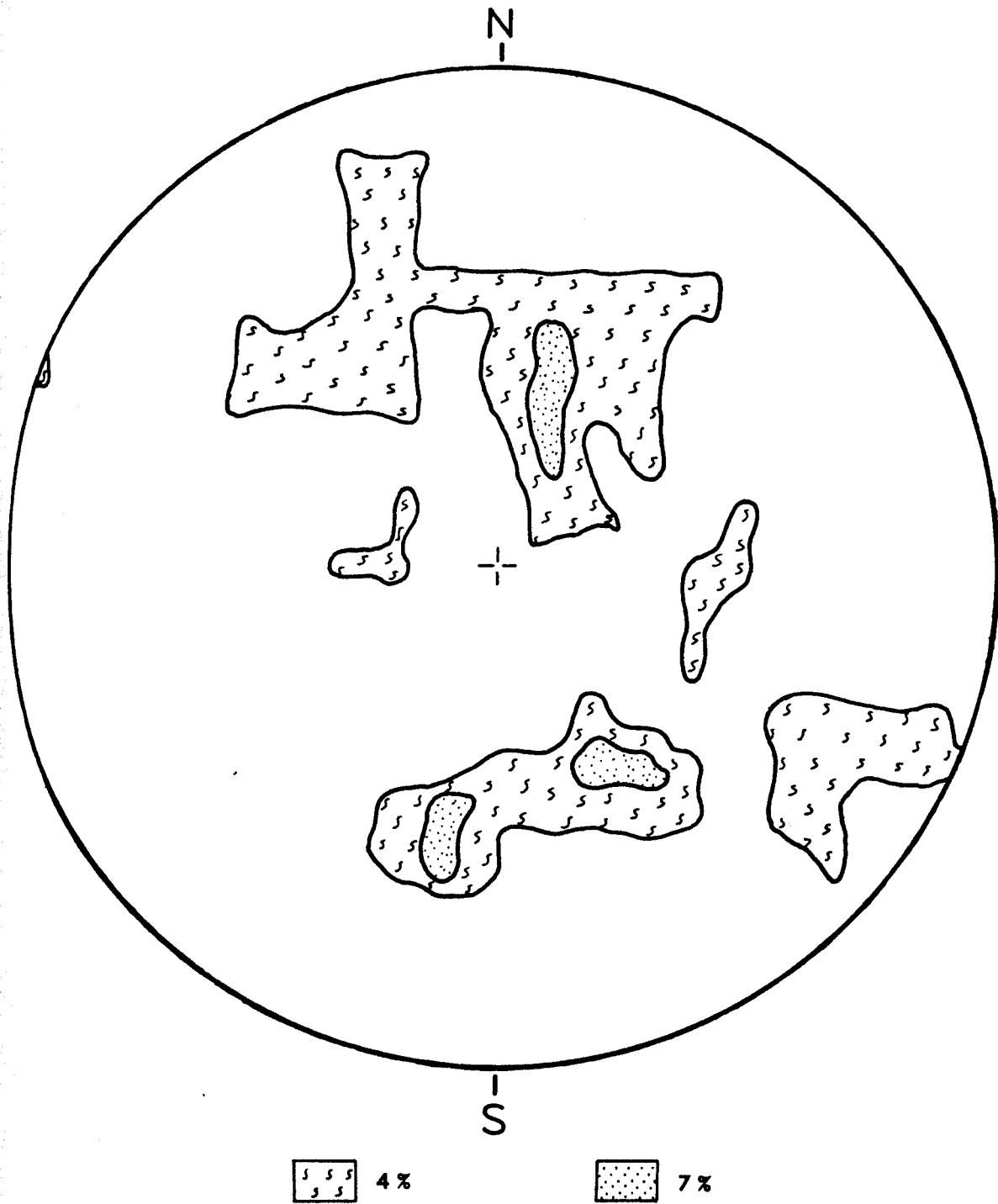
Figure 3.37 B.   Contoured equal-area projection of 24 poles
to S_1 for Domain IV.

3.2.5. Keban Fault

In the map area, the north-south directed Keban Fault was formed between the Yuksekova Volcanics of the Bitlis-Puturge Complex and the Keban Metamorphics of the Keban-Malatya Complex. It extends for about 25 km from the Lake Keban in the north to about 10 km north of Baskil in the south (see Figure 1.4). Detailed mapping and structural analysis were conducted on the Keban Fault.

Within the study area, the best reference localities of the Keban Fault are in the Keban stream (Locality 6 in Plate 5) and about 150 meters west of the Kirklar Koyu (Locality 11 in Plate 5). In the map area this fault extends for about 6 km in a north-south direction (Plate 1). An approximately 50 meter long portion of the fault (Locality 11 in Plate 5; see Plate 4A) was mapped in detail at a scale of 1:80 and 1:2 (Plate 4) in order to elucidate contact relationships between the Keban Metamorphics and the Yuksekova Volcanics.

The fault zone is characterized by the fault plane which is clearly observable between Sino Mahallesi and Kirklar Koyu (Figures 3.38 and 3.39). Other characteristics of the fault zone are brittle structural features such as fracture cleavage well-developed in the Yuksekova Volcanics along the fault zone, joints (usually two sets) and small faults developed both in the Keban Metamorphics (Kirklar Marble) and the Yuksekova Volcanics (Plate 4). Along the fault zone, I also observed some ductile structural features such as mylonite showing compositional layering developed in the Kirklar Marble (Locality 6 in Plate 5; see Figures 2.5 and 3.41) (This mylonite zone was first recognized by John F. Dewey and was shown to me by him in a field trip organized by T.P.A.O. to the above mentioned area in June 1981).

Figure 3.38   The dip of the N-S directed Keban Fault varies between 85E to ESE and 80W to WNW (see also Plate 4). The fault is characterized mainly by fault breccia (yellowish portion of the picture) and strongly foliated volcanics (gray coloured portion). The orientation of foliations is parallel to the orientation of the fault plane. View to N.

From 1 mm to 6 cm long relatively unstrained marble lenses surrounded by high strained and foliated Yuksekova Volcanic rocks (see Plate 4) also indicate a ductile deformation in the fault zone. Structural relationships between brittle and ductile deformations developed along the Keban Fault are discussed below. Along the fault zone, another characteristic of the Keban Fault is up to 500 m long volcanic and marble slivers within the fault zone (see Plates 1, 2 and 5).

Along the fault zone, the surface of Kirklar Marble outcrops and the fault surface are partially plastered with iron-oxide. The orientation of fault is generally NS, steeply dipping to the west. However, the strike of the fault plane usually fans between N-S and N10E directions in short distances. The dip of the fault mostly varies between 65 to 89 W to WNW. Where the dip of fault plane is very steep, it changes between 85 E to ESE and 80 W to WNW (Figure 3.38 and Plates 1 and 4). Along the fault zone, another diagnostic feature of the fault plane, slickensides, is observed (Figure 3.39). The orientation of slickenside striations are 50-55° N plunge. No characteristic steps have been observed on the polished surfaces of the fault plane. If the Keban Fault is not a folded Pertek Fault (discussed below, see also Figure 3.42), the orientation data for slickenside striations suggest that the direction of relative movement along the NS to N10E directed Keban Fault, is in the N-S direction. This evidence and the characteristics of the Keban Fault rocks (such as mylonites) mentioned above imply the existence of considerable amount of relative strike-slip movement with a large thrust component or imply that the fault is a folded thrust fault between the Keban-Malatya Complex and the Bitlis-Puturge Complex, along the Keban Fault. These are discussed below.

Figure 3.39   Slickensides on the Keban Fault plane.

Figure 3.40   A high strain zone along the Keban Fault, showing both ductile and brittle structural features (for more explanation, see text).

Figure 3.41   Mylonite showing compositional layering developed in the Kirklar Marble along the Keban Fault. Horizontal dimension of the picture is 1.25 cm.

Structural mapping at a scale of 1:80 and 1:2 (Plate 4) was

conducted on a 50 meter long portion of the Keban Fault (Locality 11 in

Plate 5). The structural positions of the relatively unstrained marble

lenses surrounded by the strained and foliated Yuksekova Volcanics

(see Plate 4A), and the orientation of the foliations developed in the

volcanics as a consequence of faulting (see Plate 4A and Plate 4B;

Localities 1 and 2) suggest that the relative strike-slip movement along

the Keban Fault is sinistral (see Plate 4) or if it is a folded thrust

that the Keban rocks are overthrust. As is shown in Figure 3.44, the

Keban Fault postdates the foldings (F_1 and F_2) in the map area. It is

also clearly seen on the landsat image of this region that the Keban

Fault is characterized by a N-S directed straight line and do not show

any folding evidence (see Figure 3.43). Moreover, the Keban Fault can

be traced to the north up into the Keban Lake (Figures 3.42 and 3.43).

These show that the Keban Fault is younger than the Pertek Fault. This,

of course, suggests that the Keban Fault is either a strike-slip fault

with a large thrust component or a strike-slip fault which was initiated

along the N-S directed folded thrust (Pertek Fault). In the map area,

since there is not any clear evidence for folded Pertek thrust fault for

now, the Keban Fault is named as a sinistral strike-slip fault with a

large thrust component. A future field work has planned on all along

the Keban and Pertek Faults, in the Keban Metamorphics and the Yuksekova

Volcanic Complex in order to better understand their relationships.

Along the Keban fault zone, besides brittle fault breccia (in the

Kirklar Marble), fracture cleavages, joints, and some small faults

(usually subparallel to the main fault break; see Plate 4 B), there are

ductile structural features such as mylonite (Locality 6 in Plate 5;
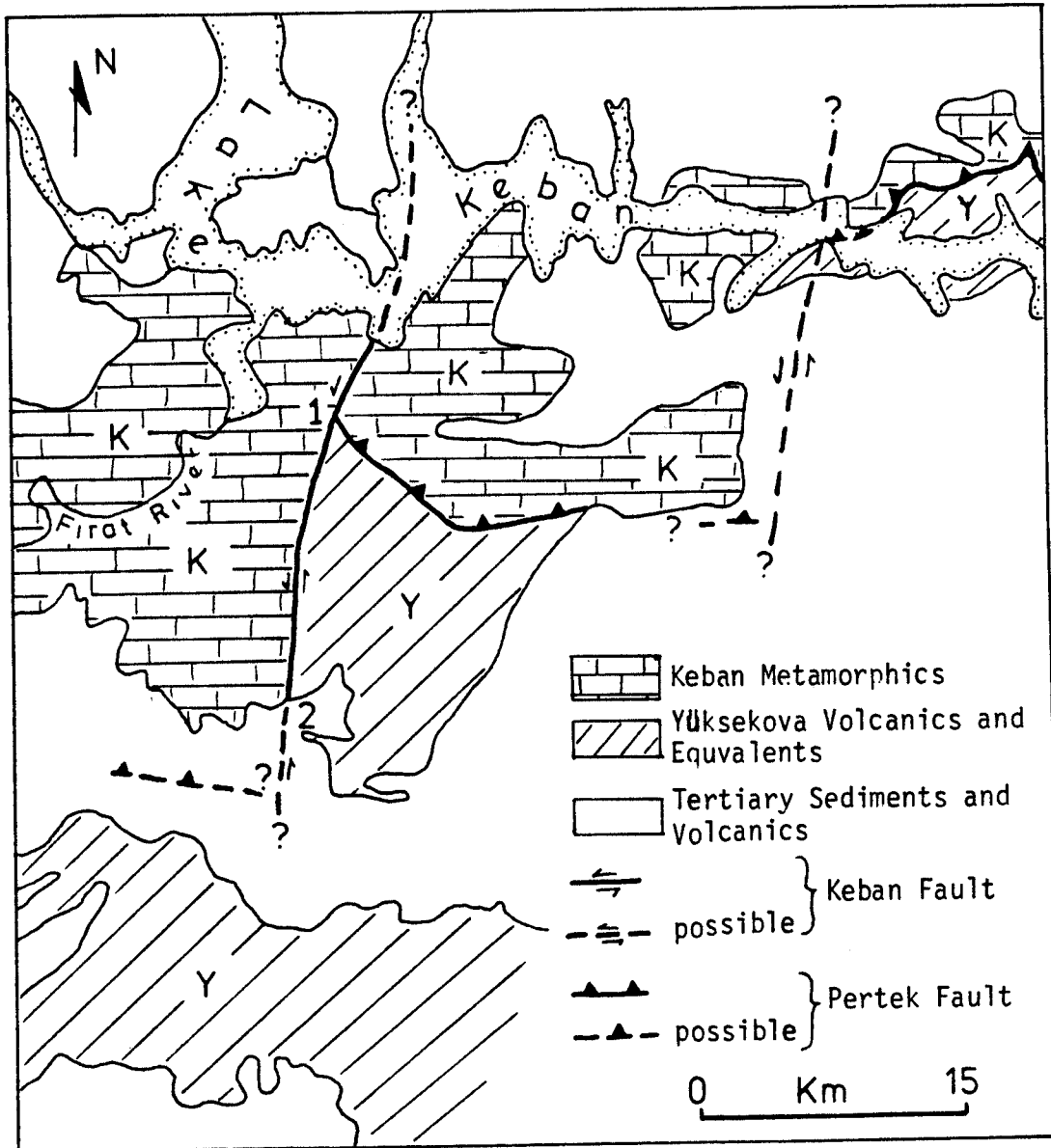
Figure 3.42. Schematic map illustrates possible strike-slip offset of the Keban Fault.
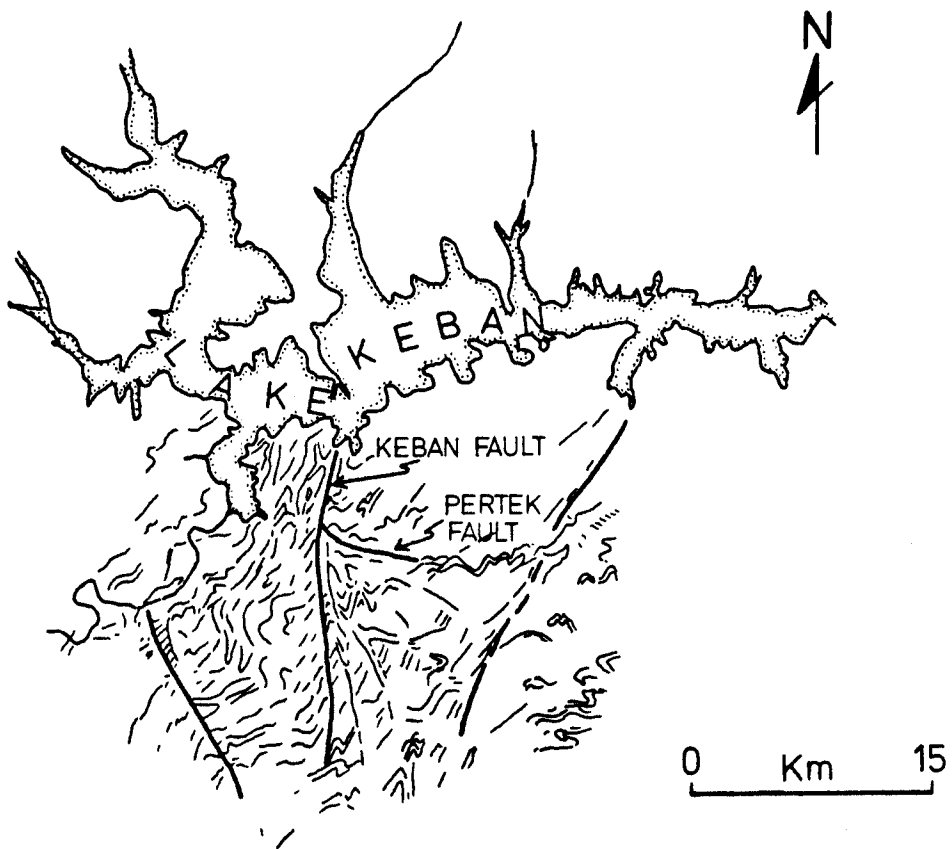
Figure 3.43. Map of the area shown in Figure 3.42 illustrates major structural features of the area.(compiled from the landsat image of the area). See text for more explanation.
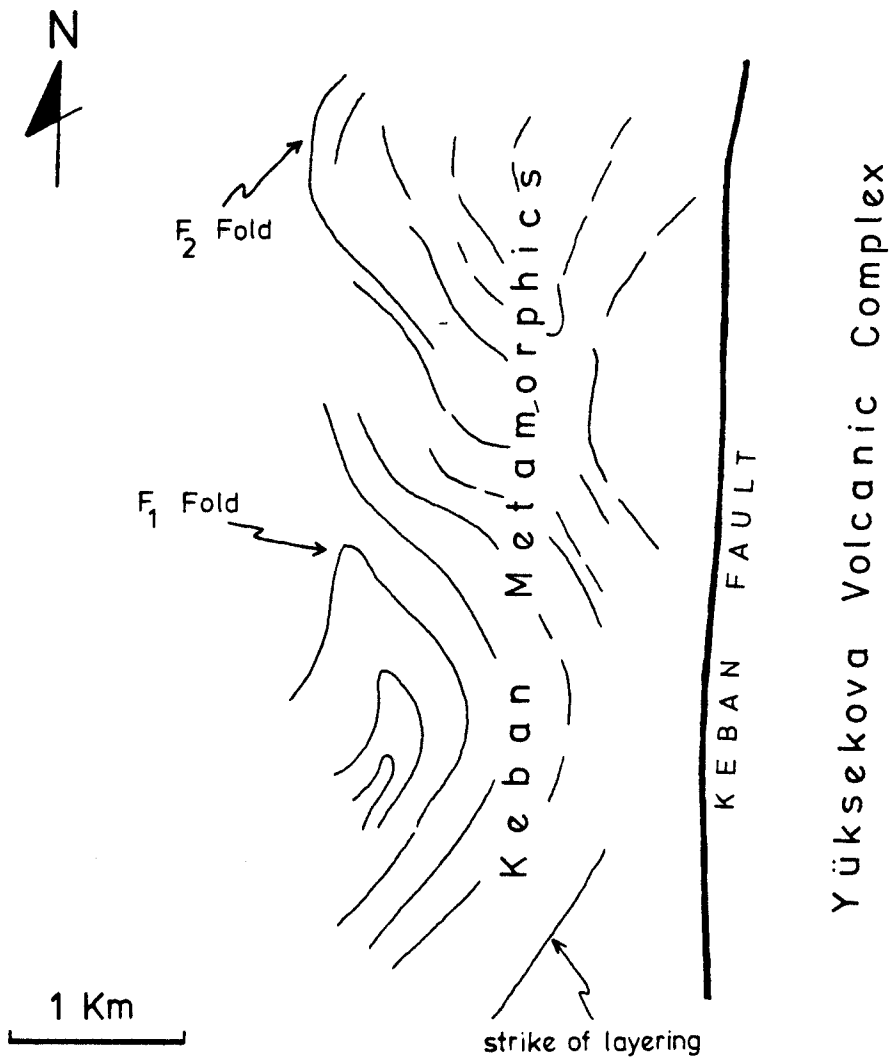
Figure 3.44. Simplified form surface map of the Keban Metamorphics in the map area, shows that the Keban Fault postdates the folding.

Figures 2.5 and 3.41) and relatively unstrained marble pods and/or lenses surrounded by strained and foliated volcanics (Locality 11; Plate 4, and Locality 12). The mylonites are characterized by compositional layering which shows different colours (Figures 2.5 and 3.41). These different colour layers (from 1 cm to 10 cm thick) are determined as deformed lepidoblastic calcite which shows a high degree of twinning. The colour change may be due to differences in chemical composition of the marble which give rise to this mylonitic rock. The relatively darker layers of the mylonite are rich in iron-oxide (about 5-7%), whereas the lighter colour layers are poor in iron-oxide (about 1%) (Figure 3.41). Figure 3.40 illustrates an about 30 cm long, 15 cm wide marble pod surrounded by strained and foliated volcanics in the fault zone (Locality 12 in Plate 5). In addition to these ductile structural features, brittle structural features (=generally two sets of conjugate micro-faults cutting across the relatively unstrained marble lenses and/or pods and strained and strongly foliated volcanics) have been observed (Figure 3.40). The relative age relationships between the ductile and brittle features show that the brittle structural features postdate the ductile structural features (see Figure 3.40). The difference in relative age might be great or extremely small. The presence of these ductile and brittle structural features in the same zone might be due to the variation in strain-rate (from relatively low strain-rate: ductile deformation -to- relatively high strain-rate: brittle deformation) during the faulting process (Sibson, 1977; J.F. Dewey, personal communication, 1982).

Another common diagnostic feature of the fault zone along the Keban Fault is crenulation cleavages developed in the Kirklar Marble. As is

shown in Plate 4B (Locality 3), earlier foliations are folded (crenulated).
The folds are generally asymmetrical. The crenulation cleavages are
defined by microfaults usually developed parallel to the fold limbs.
The spacing between crenulation cleavages is between mm scale to 3-4 cm.
According to their experimental and structural analysis in the Loch Leven
schists in Scotland, Turner and Weiss (1963) state that from incipient
stage to final stage of crenulation cleavage development all active
glide surfaces as well as the passive domain boundaries become progre-
sively rotated toward the normal to the principal compressive stress, σ_1
(see Figure 12.8 of Turner and Weiss, 1963, p. 465). So the orientation
of crenulation cleavage should be approximately normal to σ_1 in the
final stage (Turner and Weiss, 1963, p. 464-466). Based on this, the
direction of the principal compressive stress σ_1 for the crenulations
associated with the Keban Fualt seems N50W-S50E (see Plate 4B; Locality
3).

All these structural features mentioned above suggest that the
Keban Fault is a strike-slip fault with a large thrust component. As
is discussed above, the thrust component of the fault may have been
either an earlier tectonic structural feature (Pertek Thrusting) which
might have been folded in NW-SE axis direction or a latter tectonic
structural feature related with a strike-slip faulting. As is discussed
in Chapter 2 (see p. 19), the age of the fault is determined as post-
early Paleocene to medial Eocene. This age is determined on the assump-
tion that the Keban Fault is a strike slip fault with a large thrust
component. Based on the assumption that the Keban Fault is a strike-slip
fault developed along the folded Pertek Fault, the age of the Keban Fault
is automatically be much younger than early Paleocene.

In the map area, the absence of any structural criteria does not allow determination of the strike-slip offset of the fault. However, in its eastern part the Keban Fault cuts the east-west directed early Paleocene Pertek thrust to the north of the map area (Figures 3.42 and 3.43). Since the Keban Fault is determined as having sinistral displacement, the western portion of the Pertek Fault must be located to the south. However, the southern end of the Keban Fault is covered by young sediments and volcanics and there is not trace of the western portion of the Pertek Fault (see Figure 3.42). This suggests that the western portion of the Pertek Fault is covered by the young sediments and volcanics. Since these two points, point 1 in the north and point 2 in the south shown in Figure 3.42, are separated by approximately 15 km from each other along the Keban Fault, a minimum strike-slip offset of at least 15 km is assumed for the sinistral strike-slip with a large thrust component Keban Fault. No evidence has been found to determine the thrust component of the fault. Again, if the Keban Fault was a strike-slip fault initiated along the folded Pertek Fault, then the strike-slip offset of the Keban Fault will be less than 15 km.

3.3. Conclusions

The results of outcrop mapping in the Keban area are displayed on Plate 1. In the map area, the field observations and structural analysis indicate five faults, four of which are thrust faults developed between the metamorphic rock units while the fifth one is located between the Keban Metamorphics and the Yuksekova Volcanic Complex (strike slip fault with a large thrust component: Keban Fault). Fortunately, outcrops are reasonably abundant in the study area, so that the faults are definitely identified.

Both field observations and the map pattern of the study area show that the thrust faults were formed between the metamorphic units and folded by later deformation phases (D_1 and D_2) (see Figures 3, 6, 7, 11 and Plate 5). Therefore, they are the folded thrust faults. The Keban Fault displays more or less a straight line in its map pattern. It trends approximately N-S. The regional map pattern (see Figure 3.42) and structural analysis show that this is a strike-slip fault with a large thrust component or a strike-slip fault initiated along the folded Pertek thrust (see 3.2.5). Along the fault zone, volcanic and marble slivers within the fault zone trend in the same direction as the Keban Fault, except one example (Plate 1). This one irregularity may be due to the neotectonic effect, but there are no specific data to prove this.

In the map (Plate 5) and outcrop scale, F_1 folds show variable orientations (see Figures 3.34, 3.35, 3.36 and 3.37). In the outcrop, the open F_2 folds are seen to postdate the earlier tight F_1 folds (see Plate 3), and similar features emerge in the map pattern (see Plate 5: Form Surface Map).

The cross section (Plate 2) shows the folding of the faults and the very tight to isoclinal folds which produce moderately steep southeastward dipping layers. Only across the second generation of folds (F_2) are layers vertical or steeply dipping to the NW. The second generation of folds are also displayed on the cross section because their distribution and overprinting relationships between F_1 and F_2 folds are well understood in the map area (see also Plate 5). On the cross section the faults are marked with their relative sense of movement observed by field observations and structural analysis (see Figure 3.5).

3.4. Discussion: Deformation History

3.4.1. Introduction

The metamorphic units in the study area have the structural charac-
teristics of polyphase deformation. Structural data indicate at least
two phases of penetrative strain (D_1 and D_2). The first phase is mani-
fested as tight to isoclinal folds (F_1), schistosity and/or slaty
cleavage (S_1) and mineral elongation lineation (L_1). The second generation
of deformation is indicated by overprinting mesoscopic open folds (F_2),
a second foliation (S_2: crenulation cleavage), and a lineation from
the intersection of foliations (L_2). The fold interference pattern
shown in Plate 5 also indicates the overprinting relationships between
F_1 and F_2. There is also an evidence for two other major tectonic
deformations (T_{OO} and T_3) which did not produce folds. These are
discussed below.

3.4.2. Deformation History of the Keban Metamorphics
(Figure 3.45)

Deposition of the Keban Group (D_0)
_____

The Keban Metamorphic rocks are formed between Palaeozoic to
Triassic (Kipman, 1981; Perincek and Ozkaya, 1982), and are interpreted
as a deformed ancient continental margin sequence (see 2.2.6). These
sediments dominantly in carbonate facies could have once formed part of
the Cimmerian Continent before the disintegration of the Cimmerian
Continent began in early Jurassic (Sengor and Yilmaz, 1981)(See Chapter 4).
In the study area no evidence for early Jurassic rifting was found.

Metamorphism of the Keban Group
_____

This part is discussed in detail in Chapter 2.2.5. As is mentioned
there, the continental margin sediments of the Keban Group experienced a

154
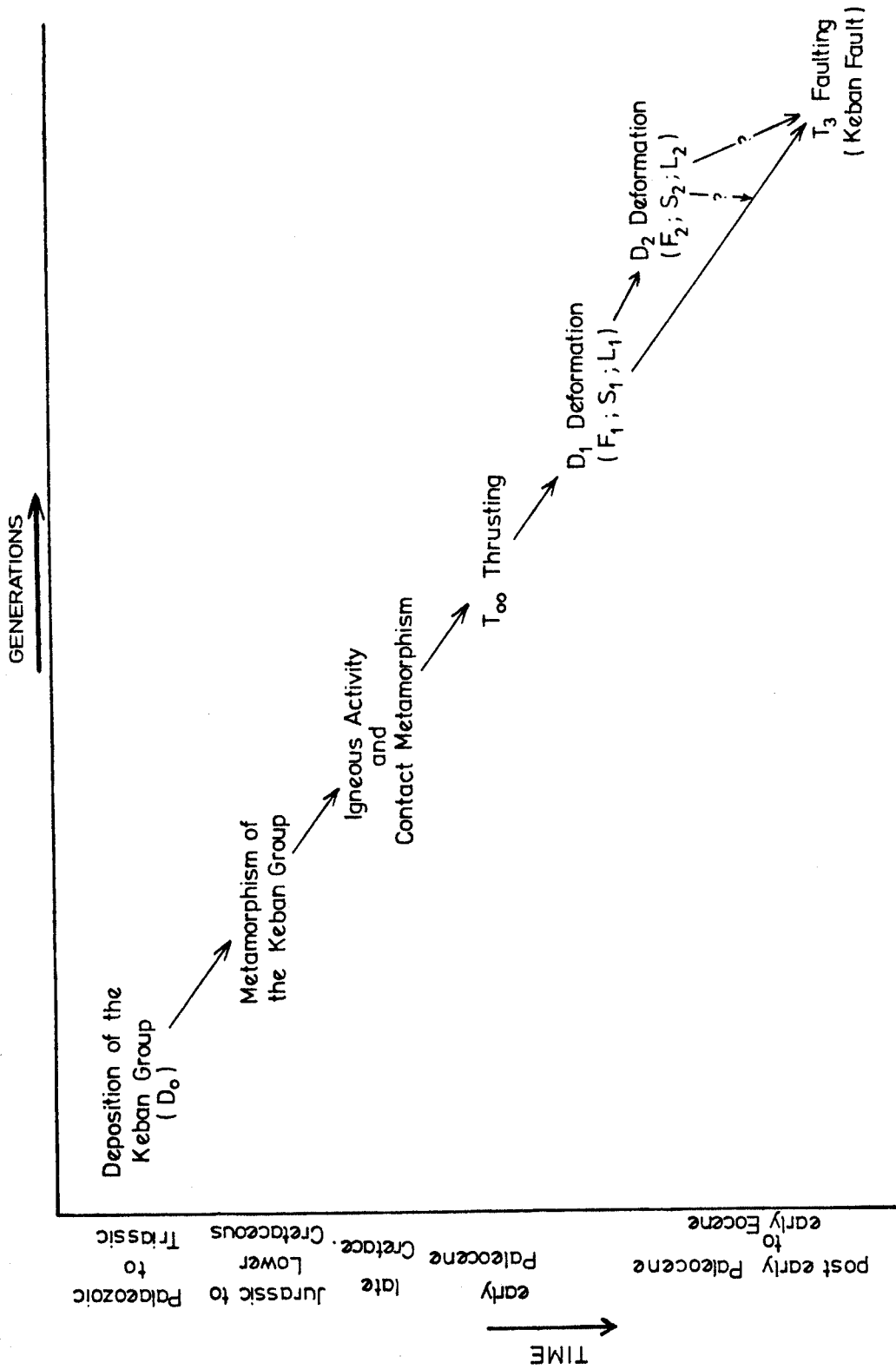
Figure 3.45. Deformation History of the Keban Area (on the assumption of that the Keban Fault is a strike-slip fault with a large thrust component; see Chapter 3.2.5).

low grade greenschist metamorphism sometime in Jurassic to early Cretaceous times.

Igneous Activity and Contact Metamorphism

A group of hypabyssal igneous rocks (syenite porphyry) which cut across the Keban Group rocks are discussed in Chapter 2.2.3. They caused contact metamorphism of the surrounding crystalline rocks. As is pointed out in 2.2.3., the age of the intrusion and, of course, the age of the contact metamorphism are determined as late Cretaceous. Assuming that an extensional regime (rifting) was the cause of syenite porphyry magmatism (Burke and Dewey, 1973) (see Chapter 4), the time of late Cretaceous indicates an extensional regime (rifting) in the Keban Continental fragment. The tectonic implications of this igneous activity for the northern margin of the Bitlis Suture Zone are discussed in Chapter 4.

T_{oo} Thrusting

As is described in Chapter 2 and Chapter 3.2.1, the metamorphic rock units of Keban Group define a tectonostratigraphy with the Kirklar Formation at the base and the Koyunatlayan Formation at the top (Plate 2). The contacts between the metamorphic rock units are folded thrust faults marked by fault rocks (Figure 3.2): no associated folding has been seen, but the faults are folded by the D_1 deformation phase (see 3.2.1). In the east, the fault zones are characterized both by brittle fault gouge, fault breccia, and by a ductile foliated mylonite zone (Gelintas Fault: see 3.2.1. D). This type of shear zone is defined as "brittle-ductile shear zone" (Ramsay, 1980). In the west, they represent a structurally higher level of the T_{oo} faulting (Plate 2). There, the faults are characterized generally by fault gouge, fault breccia and

foliated high-strain zone, showing some brittle minor faults parallel
to the main fault (Bezirgan Fault: see 3.2.1. B). This type of shear
zone is defined as "brittle shear zone" (Ramsay, 1980). This shows that
in the map area, from east to west, the fault zones change from brittle-
ductile shear zone into a brittle zone with the western side of the zone
showing less ductile features (Corik Fault: 3.2.1. A and Bezirgan Fault
3.2.1.B) than the eastern side (Hirsiz Fault: 3.2.1. C and Gelintas
Fault: 3.2.1. D). From these observations, it is inferred that the
Gelintas Fault in the east represents a relatively lower structural level
of the shear zone whereas the Bezirgan Fault in the west represents a
relatively higher level of the zone (see Figure 3.1 for the relationship
between deep level ductile shear zones and high level brittle shear zones
in the regional development of shear zones: Ramsay, 1980).

These thrust faults cut the Upper Cretaceous igneous rocks (syenite
porphyry). The age of the later tectonic structural event (T_3: Keban
Fault) is determined as post-early Paleocene to medial Eocene (see p.
19). This suggests that the age of the T_{oo} thrusting is same as major
early Paleocene thrusting (Pertek Fault) of Keban-Malatya Complex over
the Bitlis-Puturge Complex.

D_1 Deformation

The D_1 deformation phase is marked by tight to isoclinal folds (F_1);
associated foliation (S_1: slaty cleavage and/or schistosity) and
lineation (L_1). They do not overprint any earlier deformation phase,
but they do overprint the earlier tectonic structures (early Paleocene
T_{oo} thrusting) that juxtaposed the metamorphic rock units. They are
overprinted by later D_2 deformation phase. This is observed from meso-

scopic fold interference patterns in the field (see Plate 3) and

structural analysis (see Chapter 3.2.4).

Although the exact age of the D_1 deformation is not clear, based

on the overprinting relationships, it is assumed to be younger than early

Paleocene T_{oo} thrusting and older than D_2 deformation.

D_2 Deformation

The latest deformation phase (D_2) is marked by open folds (F_2), a

crenulation cleavage (S_2: parallel to axial surfaces of the F_2), and a

lineation (L_2). They overprint both the earlier tectonic structures

(T_{oo}) and the earlier deformation phase (D_1) (see Plate 3 and Chapter

3.2.2, 3.2.4). Because the data for D_2 is very limited, the relation-

ship between the D_2 and the latest tectonic structures (T_3) is not well-

understood. According to form surface map (Plate 5), the Keban Fault

postdates the D_2 deformation phase (see also Figure 3.44).

T_3 Faulting

The latest tectonic structures in the Keban area, Keban Fault, is

marked by brittle fault rocks and slickensides and also by mylonite and

foliated high-strained rocks (ductile). These are discussed in Chapter

3.2.5. No folds associated with this tectonic structure have been seen.

As is mentioned above, because of limited data on D_2 deformation, the

relationship between the F_2 folds and the Keban Fault is not understood.

D_2 might be associated with the Keban Faulting, but there is not any

evidence to support this (see Plate 5), so that the Keban Faulting is

defined as T_3 instead of T_2. The displacement is inferred to be sinistral

strike-slip with a large thrust component. The age of the Keban Fault

is determined as post-early Paleocene to medial Eocene (see Chapter

3.2.5 for more explanation).

CHAPTER 4

TECTONICS

4.1 Introduction

After the 1965-75 revolution in geology (Wilson, 1965; Dewey and
Spall, 1975), southeastern Turkey became a main focus for geologists
in order to better understand plate tectonics. Before the plate tecto-
nic revolution in geology, some contemporary studies have been published
by Ketin (1959, 1966) and by Rigo de Righi and Cortesini (1964) concern-
ing the tectonic setting of southeastern Anatolia. But, the first compre-
hensive discussion for this region in terms of plate tectonics was
published by Dewey et al. (1973). They first described the Bitlis-Zagros
Zone as a late Tertiary Suture between the Arabian and Eurasian plates.
Since Dewey et al. (1973), plate tectonic models have evolved for south-
eastern Turkey mainly by Albany-Turkish group and French group. The
Albany-Turkish group (Sengor, 1979a; Sengor et al., 1980; Sengor and
Yilmaz, 1981) basically describe a Bitlis Ocean (Neo-Tethys) which
opened sometime between the Permian and Medial Triassic and extended
from the eastern Mediterranean to the east between the Arabian Platform
and the Anatolian Block. The French group (Ricou et al., 1974, 1975,
1979; Brunn, 1979; Bergougnan and Fourguin, 1982) objects to the existence
of the Bitlis Ocean in Permo-Triassic. These problems are discussed
later in this Chapter.

The Purpose of this chapter is to give a brief summary of the
geological history of southeastern Turkey, and to review the proposed
models for the tectonic evolution of the Bitlis Suture Zone, and
finally to build a new plate tectonic model of the Bitlis Suture Zone

and implication of the Keban Metamorphics for the evolution of Neo-Tethys, based on the data obtained, and the comparison of the structural and regional findings fo the study with that of the findings of data from the larger region.

4.2. Regional Tectonic Setting of Southeastern Turkey

As is well known, the area of southeastern Turkey lies within the Alpine-Himalayan orogenic belt which was developed from the Tethys Ocean through the long geological history. In southeastern Turkey, three main geological provinces can be recognized (Rigo de Righi and Cortesini, 1964; Ilhan, 1974; Hall, 1976; Sungurlu, 1974; Perincek, 1979b; Sengor et al., 1979; Sengor and Yilmaz, 1981). They are shown on figure 4.1 and are discussed next, from south to north.

4.2.1. Arabian Shelf Platform

The northern margin of the Arabian continent is mainly formed by carbonate and clastic sediments in two separate periods separated by a pre-late Campanian to early Maastrichtian thrusting episode (Figure 4.2). The first sedimentary sequences are named "Autochthonous Units," and the second one as "Neo-autochthonous Units."

A. Autochthonous Arabian Platform

This is mainly composed of a thick sequence of carbonate and clastic continental margin sediments. Mostly clastic sediments with minor carbonates (Bedinan Formation: Ordovician-Silurian, and Koprulu Formation: Devonian) represent the base of continental margin sequence. Carboniferous sediments are completely absent in the section and the Permian Tanin Group (Hazro and Gomaniibrik Formations), which lies disconformably on the Devonian, lies below a Lower Triassic (Cigli
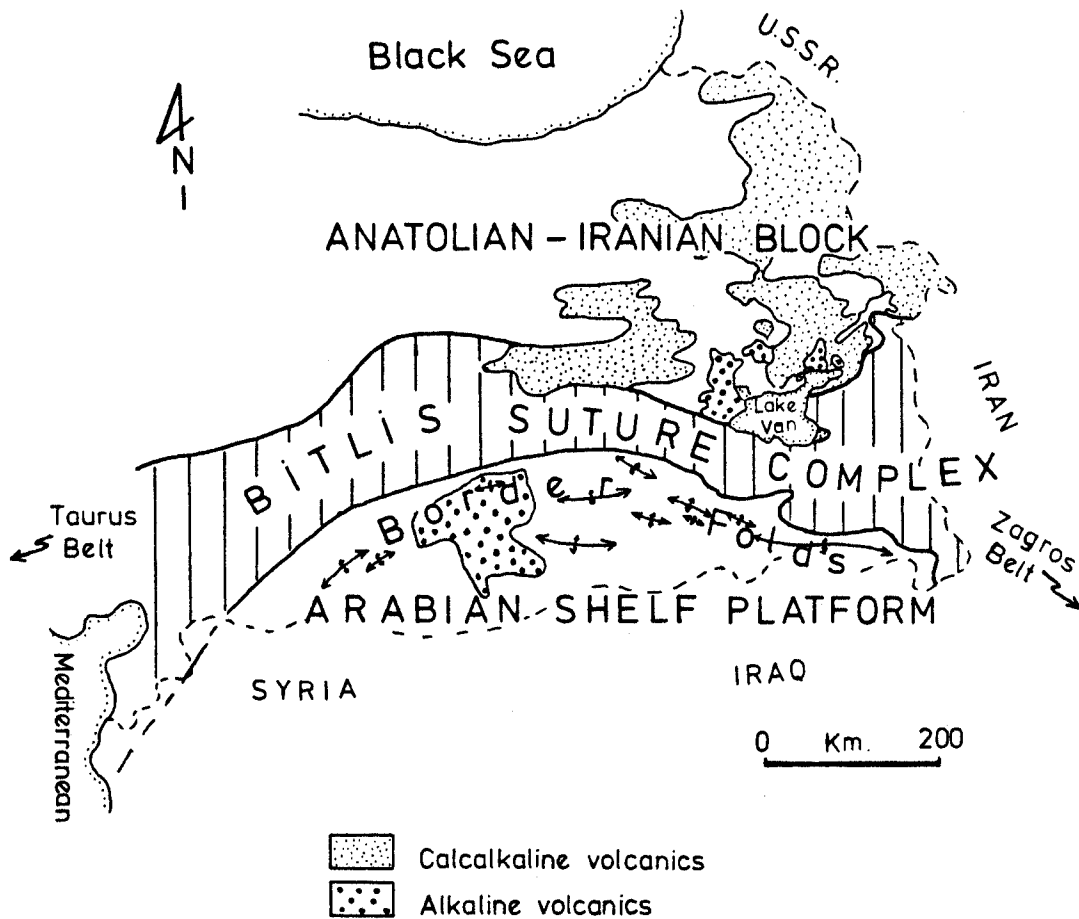
Figure 4.1.   Map illustrates the distribution of the main geological provinces of Southeastern Turkey and the distribution of the volcanic rocks of Eastern Turkey (simplified after Savci, 1980; figure 1).
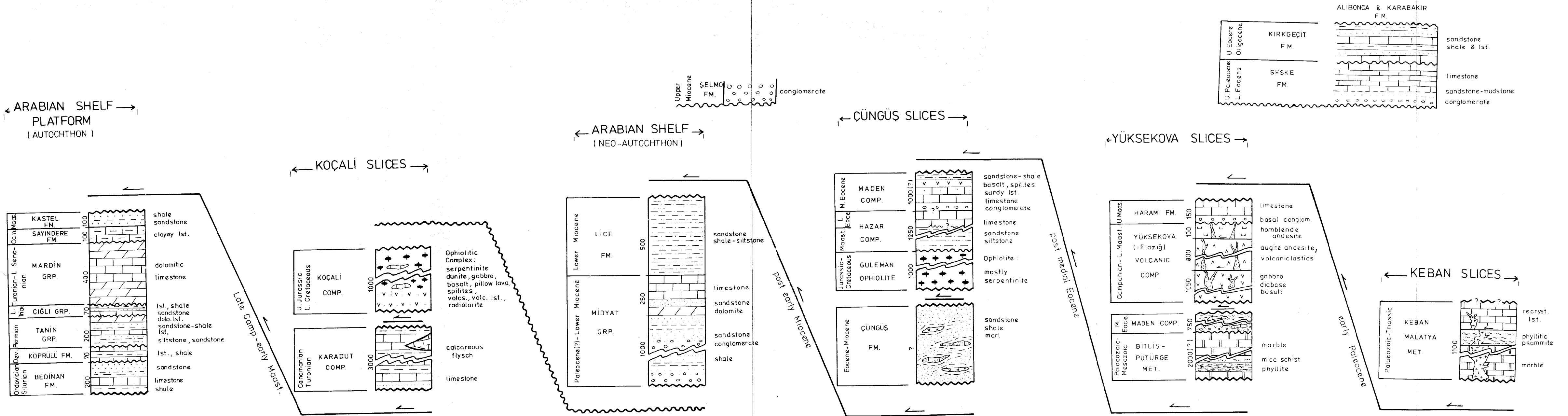
Figure 4.2. Schematic tectonostratigraphic column sections illustrating the tectonic setting of the Bitlis Suture Zone

Group) disconformity. The carbonate Mardin Group (Turonian-Albian in age) represents the major petroleum reservoir. Fine-grained, flysch type deep-water sediments of the Campanian-Lower Maastrichtian Sayindere and Kastel Formations lie disconformably on the Mardin Group. They represent the last stage of the sedimentation of the Autochthonous Arabian Platform. The sedimentation stopped during the late Campanian-early Maastrichtian ophiolite obduction (Kocali Slices in Figure 4.2) which were emplaced from the north. For more detail on the Autochthonous Arabian Platform, see Sungurlu (1974), Horstink (1971), and Perincek (1979b).

Another characteristic of this domain is Pleistocene through Quaternary alkalic volcanism (Karacadag basalts: M.T.A., 1962) (Figure 4.1). This alkalic volcanic activity is supposedly related to the splitting of the Arabian continental crust as a consequence of the post-early Miocene continental collision between the Eurasian and Arabian Continents (Sengor and Burke, 1978).

B. Neo-Autochthonous Arabian Platform

After the ophiolite obduction which is inferred to have occurred from the southern branch of the Neo-Tethys (Sengor and Yilmaz, 1981) in late Maastrichtian-early Paleocene, shelf sedimentation resumed on these allochthons (Kocali Slices) and on the autochthonous Arabian Platform, and continued until the post-early Miocene continental collision (Sungurlu, 1979a, 1979b). The Neo-autochthonous Arabian Shelf sediments occur in a narrow zone along the southearn margin of the Bitlis Suture Zone, unconformably overlying the late Campanian-early Maastrichtian Kocali Slices (Upper Jurassic-Lower Cretaceous Kocali Ophiolites and Cenomanian-Turonian Karadut Complex) and/or the Maastrichtian Kastel

Formation of the Autochthonous Arabian Platform (Figure 4.2).

The Neo-autochthonous Arabian Platform is represented by a shallow-water sequence, mostly carbonates and some clastic sediments of the Midyat Group (Paleocene-Lower Miocene), and by the flysch of the Lower Miocene Lice Formation. The Lice Formation overlies the Midyat Group with partially conformable and partially unconformable contact. This unit is tectonically overlain by the north dipping, post-early Miocene Cungus thrust Slices. The Upper Miocene-Lower Pliocene coarse grained molasse Selmo Formation unconformably over-lies the post-early Miocene Cungus Slices and/or the Lower Miocene Lice Formation. This implies that a major episode of the continental collision between the Eurasian and Arabian Continents along the Bitlis Suture Zone had been initiated between the post-early Miocene and pre-late Miocene. For more detail on the Neo-autochthon rock units of Arabian Platform, see Rigo de Righi and Cortesini (1964), and Perincek (1979 b).

4.2.2. Bitlis Suture Zone

The Bitlis Suture Zone is an Alpine-Himalayan orogenic belt that connects the Taurus belt in the west and Zagros belt in the east, and forms the northern boundary of the Arabian Continent (Figure 4.1). This Himalayan type orogenic setting (Mitchell and Reading, 1969), a consequence of continental collision between the Eurasian Continent in the north and Arabian Continent in the south, in post-early Miocene time (Sengor, 1980; Sengor and Kidd, 1979; Sengor and Yilmaz, 1981), caused an increase in crustal thickness of the Eastern Anatolian region to an estimated 45 km (Canitez and Toksoz, 1980).

The Bitlis Suture Zone was developed from the Neo-Tethys ocean through a long geological history, and is interpreted to have formed as a consequence of multiple opening and closing of portions of this ocean between Liassic and early Miocene time (Sengor, 1979 a; Sengor et al., 1980; Sengor and Yilmaz, 1981). The suture zone consists structurally of four main slices (Sungurlu, 1974; Perincek, 1979a, 1980; Sengor and Yilmaz, 1981). They are named as follows (see Figures 1.2 and 4.2): Late Camapanian-early Maastrichtian Kocali Slices; early Paleocene Keban Slices; post-medial Eocene Yuksekova Slices; and post early Miocene Cungus Slices. Major tectonostratigraphic units within the each tectonic slice are described below. The emplacement age of each slice is determined by younger key sediments (see page 170) which subsequently covered each tectonic slice after thrusting (Figure 4.2).

A. Late Campanian-early Maastrichtian Kocali Slices

The Kocali Slices are a consequence of the development of the southern branch of the Neo-Tethys (see Figure 6A of Sengor and Yilmaz, 1981, page 207). These are comprised mainly of an ophiolitic complex (Kocali Complex) composed of serpentinite, peridotite, dunite, gabbro, basalt, pillow lavas, spilites, volcanics, volcanic-limestone-radiolarite intercalations, and locally of calcareous flysch, dominantly micritic cherty limestone, and limestone blocks (Kardadut Complex) (Sungurlu, 1974; Perincek, 1979b) (Figure 4.2). Perincek (1979b) showed that the ophiolitic Kocali Complex (Upper Jurassic-Lower Cretaceous) occurs as the upper tectonic slice above the Karadut calcareous flysch (Cenomanian-Lower Turonian) including limestone blocks of early Jurassic-early Cretaceous age. Perincek states that the limestone blocks were plucked

from the Arabian Shelf. These slices were thrust over the northern

marginal shelf of the Arabian Continent.

After the late Maastrichtian, the shelf sedimentation (carbonate

and flysch: Paleocene-Lower Miocene Midyat Group and Lower Miocene

Lice Formation; see Figure 4.2) was reinstated again on these allochthons

and on the Arabian Shelf, and continued until the post early Miocene

thrusting (Sungurlu, 1979a, 1979b).

The next three slices described below are a consequence of the

development of the northern branches of the Neo-Tethys.

B. Early Paleocene Keban Slices

The Keban Slices are a consequence of the development of the first

northern branch of the Neo-Tethys: Inner Yuksekova Ocean (see Chapters

4.3 and 4.4). The major tectonostratigraphic units of Palaeozoic-

Triassic contintnetal margin sequences of the Keban Group are discussed

in detail in Chapter 2.2. Compared with the Bitlis-Puturge continental

margin sequences, the Keban-Malatya continental margin sequences are

mostly carbonate (over 85%) and internally imbricated (see Chapter 3).

Their lithological and structural features and structural position show

that the Keban-Malatya Complex does not resemble to the Bitlis-Puturge

Complex. Moreover, the ensimatic Yuksekova island arc volcanics (Hempton

and Savci, 1982) always occupies an intermediate position between these

two complexes and no Yuksekova Volcanic rocks outcrop on or north of the

Keban-Malatya Complex. This suggests that an Oceanic basin (Yuksekova

Ocean; Figure 4.3 B) was present between the Keban-Malatya Complex in

the north and the Bitlis-Puturge Complex in the south, and that the

island arc volcanism occurred on a portion of this oceanic crust

(probably Guleman ophiolite: Hempton, 1982; Perincek and Ozkaya, 1982).
The closing episode of the Yuksekova Ocean is of early Paleocene age.
This is discussed later in this Chapter. For the lithological and
structural features of the Keban Slices, the reader is referred to
Chapters 2 and 3 of this thesis, Perincek 1979a, and Perincek and Ozkaya,
1982.

C. Post Medial Eocene Yuksekova Slices

The major tectonostratigraphic units of the Yuksekova Slices are
the Btilis-Puturge metamorphic rock units, the Hazar Complex, the Maden
Complex, the Yuksekova Volcanic Complex and the Harami Formation. The
general relationships between the units are shown in Figure 4.2.

Bitlis and Puturge Metamorphics: These low grade metamorphic
complexes consist of metapelite and marble units. All the post-
early Miocene Cungus Slices (see Figure 4.2) are covered in places by
the thrust sheet of Bitlis-Puturge Metamorphics. The Bitlis-Puturge
Metamorphics are covered unconformably by Maastrichtian-Lower Eocene
Hazar and Middle Eocene Maden Complexes and tectonically by the Yuksekova
Volcanic Complex. Boray (1975), Bastug (1976) and Hempton (1982)
contain more detail on these rocks and their relations.

Hazar Complex: This unit is composed of a Maastrichtian-Paleocene
age sandstone-siltstone-marl-shale assemblage (Simaki Formation) and an
early-Eocene massive limestone with marl and shale interbeds (Gehroz
Formation). In the Yuksekova Slices, this complex lies unconformably
on both the Bitlis-Puturge Metamorphics and the Yuksekova Volcanic
Complex (see Figure 2 of Perincek 1979b, page 4). For more detail about
Hazar Complex, see Rigo de Righi and Cortesini (1964), Sungurlu (1974),

Erdogan (1977), Ozkaya (1978) and Perincek (1979b).

Maden Complex: Although the Middle Miocene Maden Complex generally shows melange characteristics, it consists in the Baykan area of the following stratigraphic sequence: siltstone-sandstone(Ceffan Formation); limestone (Arbo Formation); limestone-marl-shale sandstone-siltstone-sandy limestone (Melafan Formation); basalt-spilite (Karadere Formation); and sandstone-shale (Narlidere Formation) (Perincek, 1979b). The Maden Complex is one of the key pieces of data which indicate the completion of the thrusting episode of the Yuksekova slices over the Cungus Slices (see page 170). For more detail about the Maden Complex, see Ozkaya (1974), Sungurlu (1974), Perincek (1979b), Aktas (1982), and Hempton (1982).

Yuksekova Volcanic Complex: This Campanian-Lower Maastrichtian unit in the western Yuksekova terrain (see Figure 2.17) is discussed in detail in Chapter 2.3. As is mentioned there, the eastern Yuksekova terrain is represented by large thrust slices of ophiolitic rocks, whereas in the western Yuksekova terrain the rocks have island-arc affinities (Yuksekova Volcanic Complex). The latter terrain has been renamed the Elazig Volcanic Complex by Hampton and Savci (1982). Both the ophiolitic rocks in the eastern terrain and the volcanics in the western terrain of the Yuksekova Complex structurally overlie the Middle Eocene Maden Complex. For more detail, see Chapter 2.3 of this thesis, Perincek (1978, 1979b), Hempton (1982), and Hempton and Savci (1982).

The Yuksekova Volcanic Complex is covered by the Upper Maastrichtian Harami Formation with an angular unconformity. For more information about the Harami Formation, the reader refers to page 67 of this thesis and Perincek (1979b).

D. Post Early Miocene Cungus Slices

These represent the lowest tectonic slice in the Bitlis Suture Zone.
The major tectonostratigraphic units of the Cungus Slices are Cungus
Formation, Guleman Ophiolite, Hazar Complex and Maden Complex. The
last two complexes are described above.

Guleman Ophiolites: The Jurassic to Cretaceous Guleman Ophiolites
are composed mostly of serpentinites and some pyroxenite, dunite, harz-
burgite and minor gabbro, diabase and basalt. It is overlain unconfor-
mably by the Hazar and Maden Complexes. See Erdogan (1977) and Perincek
(1979b) for more detail.

Cungus Formation: The Eocene-Miocene Cungus Formation represents
the lowest tectonic slice in the Cungus Slices. It consists of
repetitions of sandstone-shale-marl, which possibly were deposited in
shallow water. This unit is overlain structurally by both the Maden
Complex and the Guleman Ophiolites.

The Cungus Slices were thrust over the para-autochthonous Arabian
Shelf Sediments. Both the top of the para-autochthonous Arabian Shelf
Sediments (Paleocene-Lower Miocene Midyat Group, Lower Miocene Lice
Formations) and the Cungus Slices are overlain unconformably by the
coarse-grained molasse of Selmo Formation (Upper Miocene-Lower Pliocene).
See Sungurlu (1974) and Perincek (1979b) for more detail about Cungus
Formation and Selmo Formation.

Tertiary Key Sediments in the Northern Domain of the Suture Zone

In this volume, the term key is used to define a formation or complex
that covers and blankets a thrust sliver and/or to describe the youngest
formation or complex beneath a thrust sliver, and thus it indicates the
completion of the thrusting episode over one another. Those sediments

and complexes, such as the Upper Paleocene-Lower Eocene Seske Formation and Upper Eocene-Oligocene Kirkgecit Formation which lie over the early Paleocene Keban thrust slices, the Middle Eocene Maden Complex underneath the post medial Eocene Yuksekova Slices, and the Upper Miocene Selmo Formation and Lower Miocene Lice Formation over and underneath the post early Miocene Cungus Slices, respectively, are used here in this meaning (Figure 4.2). Some of these formations mentioned above have been termed "paraalochthonous" and "shut-in formation" by Perincek (1979b) and Perincek (1980), respectively.

In the northern domain of the Bitlis Suture Zone which this study is converned with, the Seske and Kirkgecit key sediments discontinuously overlie the Keban Metamorphics, the Yuksekova Volcanic Complex and Harami Formation and the thrust contact between the Keban and Yuksekova-Harami in many places. Based on Perincek's (1979a, b) observations, the Upper Paleocene-Lower Eocene Seske Formation is composed of conglomerate, sandstone-mudstone and mostly neritic limestone. The Upper Eocene-Oligocene Kirkgecit Formation is represented by flysch type sediments consisting of sandstone-shale-limestone. The lower Miocene sandstone-shale-limestone Alibonca and Upper Miocene basaltic-tuffaceous agglo-merate, conglomerate and sandstone Karabakir Formations unconformably overlay the Seske Formation, the Kirkgecit Formation, and the Keban Metamorphics. For more details about the Northern Sedimentary Domain of the Bitlis Suture Zone, see Perincek (1979a, b).

4.2.3. Anatolian-Iranian Block

In this thesis, the term "Anatolian-Iranian Block" (Savci, 1980) is used for the Turkish Van and Iran plates that Dewey et al. (1973)

defined and the Turkish-Iranian Plateau that Sengor and Kidd (1979)
described. Characteristics of this domain are Mesozoic and Tertiary
sedimentary formations such as Munzur Limestone (Upper Triassic-Senomanian
thick neritic carbonates and Turonian-Upper Campanian pelagic micrites:
see Ozgul et al., 1982), and Neogene to Quaternary volcanic sequences.
Two coexisting petrological types of Late Miocene-Recent volcanics are
recognized in the region. These are: calcalkalic and alkalic (Ozpeker,
1973; Lambert et al., 1974; Ota and Dincel, 1975; Innocenti et al.,
1976) (Figure 4.1). The East Anatolian volcanic activity is related to
the convergent motion, a consequence of the continental collision
between the Eurasian and Arabian Continents along the Bitlis Suture Zone
after the early Miocene (Savci, 1980). Sengor and Kidd (1979) suggest
that the volcanism of the Anatolian-Iranian Block is due to partial
melting of the continental crust and a consequence of the splitting of
the continental crust along the extension fractures.

4.3. Review on Proposed Models for the Tectonic Evolution

The general tectonic frame of Turkey began to be established
between late 1950's and late 1960's (M.T.A., 1963,1966; Ketin, 1959,
1966; Rigo de Righi and Cortesini, 1964; and many others). Because the
Bitlis Suture Zone is situated in a tectonic position that is a critical
region in the evolution of the Alpine-Himalayan orogenic belt, south-
eastern Turkey became in early 1970's an area of special interest from
the point of view of plate tectonics. Dewey et al. (1973) published the
first plate tectonic model for this region. After Dewey et al. (1973),
plate tectonic models for Turkey have been proliferating (Ricoue et al.,
1974, 1975, 1979; Brinkmann, 1976; Hall, 1976; Sengor, 1979a, 1979b,

1980; Sengor and Burke, 1978; Sengor and Kidd, 1979; Sengor and Yilmaz, 1981; Sengor et al., 1979; Sengor et al., 1980; Dewey and Sengor, 1979; Gutnic et al., 1979).

The first complete geological map of Turkey was accomplished by M.T.A. (Geological Survey of Turkey) in early 1960's (M.T.A., 1963-1966).

Ketin (1959, 1966) describes four main tectonic units in Anatolia. From north to south they are: Pontides, Anatolides, Taurides, and Border Folds (Foreland-type folding) zone. He proposed that the tectonic evolution of Anatolia proceeded gradually from north to south.

Rigo de Righi and Cortesini's (1964) classic paper deals with the geology of the foothills structure belt of the Taurus Mountains in southeastern Turkey. They subdivided southeastern Anatolia into the following three main geological provinces from south northward: the foreland area, the foothills structure belts which grades into the Taurus-Zagros orogenic ridge. For southeastern Turkey, their paper was the first reliable study which clearly defines the tectonostratigraphic units and relationships among these units. Their detailed cross-sections from the orogen show numerous north-dipping thrusts. They evoke gravity sliding origin for the nappe-like terrain of the foothills region of southeastern Turkey.

Hall (1976) proposed that the Bitlis Massif is a composite structural entity consisting of a northern area of pre-Permian metamorphic rocks and a southern zone of Alpine rocks that have undergone high pressure-low temperature metamorphism. He describes an internally imbricated ophiolitic melange within the Bitlis Massif. Hall (1976) recognized two episodes of ophiolite emplacement in late Cretaceous and in Miocene. The first ophiolite emplacement involved with a north-dipping subduction,

and the second one emplaced during the final phase (Miocene) of contintnetal collision.

Dewey et al. (1973) describe the Bitlis-Zagros Suture Zone as a late Tertiary suture between the Arabian and Eurasian Continents. They were the first to note a north-dipping subduction underneath the Taurides and subsequent ophiolite obduction onto the northern margin of the Arabian Platform. They also recognized convergent regime in the late Cretaceous. Based on the young sediments and volcanics in eastern and south-eastern Turkey, they claimed that the time of the suturing was Pliocene. Later detailed mapping in southeastern Anatolia showed that the suturing had been completed by post early Miocene (Sengor, 1980; Sengor and Kidd, 1979; Sengor and Yilmaz, 1981; Sengor et al., 1980).

With conformity to the geotectonic interpretation of Dewey et al. (1973), Innocenti et al. (1975, 1976) claim that the Tertiary volcanism of Eastern Turkey is a consequence of subduction of the Arabian Continent beneath the Eurasian Continent. However, present mapping in this region provides no evidence of subduction after post-early Miocene collision (Sengor, 1979b; Sengor, 1980; Sengor and Kidd, 1979). Sengor and Kidd (1979) and Savci (1980) suggest that the young volcanism of Eastern Anatolia is associated with collisional tectonics.

Recently, contemporary plate tectonic models for Turkey have been evolved by the Albany-Turkish group (Dewey and Sengor, 1979; Sengor, 1979a, 1979b; Sengor, 19800 Sengor and Burke, 1978; Sengor and Kidd, 1979; Sengor and Yilmaz, 1981; Sengor et al., 1979, 1980; Hempton and Savci, 1982). The palaeotectonic evolution model for Turkey in general, and southeastern Turkey in particular, have proposed by Sengor et al. (1980) and Sengor and Yilmaz (1981). Based on data collected mainly

from T.P.A.O. and their own observations, they show that the age of emplacement of ophiolites in south-eastern Turkey and northwest Syria is older (Campanian) than the mainly late Senonian nappes of the Anatolide-Tauride Platform. Using this criterion and the comparison of the geotectonic data from the larger region of the eastern Mediterranean, they proposed a Ladinian-Norian rifting event throughout southern and southeastern Turkey (opening of southern branch of Neo-Tethys; Bitlis Ocean: Sengor and Yilmaz, 1981) (Figure 4.3 A). They pointed out that in southeastern Turkey, evidence of Carnian-Norian rifting and subsidence of the carbonate platform is found a number of places within the lowest tectonic slice of the Bitlis Massif.

A group of French geologists (Ricou et al., 1974, 1975, 1979; Delaune-Mayere et al., 1977; Gutnic et al., 1979; Brunn, 1979; Bergougnan and Fourquin, 1982) object to Sengor et al.'s (1980) and Sengor and Yilmaz's (1981) Triassic rifting event throughout the eastern Mediterranean. They developed a concept that all the ophiolites in the eastern Mediterranean have their roots in the Izmir-Ankara-Ilgaz-Erzincan-Zagros ophiolitic suture (see Figure 1 of Sengor et al., 1982, p. 933) and that they have been thrust over the Anatolide-Tauride Platform during the late Senonian. This view suggests that the Neo-Tethyan evolution of the eastern Mediterranean ranges has been the result of the closure of a single Neo-Tethyan ocean. As is mentioned above, Sengor et al. (1982), Sengor and Yilmaz (1981) and Sengor et al. (1982) clearly show that the roots of the eastern Mediterranean ophiolites are to the south of the Anatolide-Tauride Platform. Their view, of course, suggests that the Neo-Tethyan evolution has been the result of multiple opening and

closing of parts of the Neo-Tethyan ocean (Figure 4.3 B). Sengor and Yilmaz (1981; p. 210) state that "this is an ocean that began opening during the late Triassic and partially closed along the Bitlis Suture (Sengor et al., 1979) during the middle Miocene."

For the tectonic evolution of Turkey, Sengor et al. (1980) and Sengor and Yilmaz (1981) present seven and nine evolutionary stages, respectively, from the Permo-Triassic to present. Although their model (particularly Sengor and Yilmaz, 1981) contains some aspects that can be disputed (such as the implications of the Keban-Malatya Metamorphics and Maden Basin, discussed in the next section), it is the most compre-hensive model so far proposed for the tectonic evolution of Turkey.

4.4. A Plate Tectonic Approach in the Neo-Tethyan Evolution: SE Turkey.

4.4.1. Implications of the Data from This Study

The lithological and structural features of the Keban Metamorphics and the Yuksekova Volcanic Complex near Keban has been described and briefly interpreted in the previous chapters. The purpose of this section is to integrate the new data obtained from the study area with the information from other parts of the suture zone in an attempt to refine the plate tectonic model, emphasizing the implication of the Keban Metamorphics.

Keban Metamorphics

The detailed lithological description of the Keban Metamorphic rock assemblages suggest that they represent a deformed continental margin sedimentary sequence. They were probably formed mainly on the continental shelf and perhaps on the continental slope (see Chapter 2.2.6). Because

Figure 4.3. Schematic sequential block diagrams showing the successive steps in the palaeotectonic evolution of the southeastern Turkey from Permo-Triassic to medial Miocene. In conjuction with author's own observations, the evolutionary stages are compiled and somewhat reinterpreted from Sungurlu (1974), Perincek (1979b), Sengor et al. (1980), Sengor and Yilmaz (1981), Aktas (1982), Hempton (1982), Hempton and Savci (1982), and Ozgul et al. (1982). For more detailed explanation, please refer to Sengor and Yilmaz (1981).

A

LAURASIA
(scythian platform)

PALAEO-TETHYS

andesitic volcanism
(Sengör et al. 1980)

CIMMERIAN
CONTINENT

Southern Branch of
NEO-TETHYS

ARABIAN
PLATFORM

PERMO-TRIASSIC

179
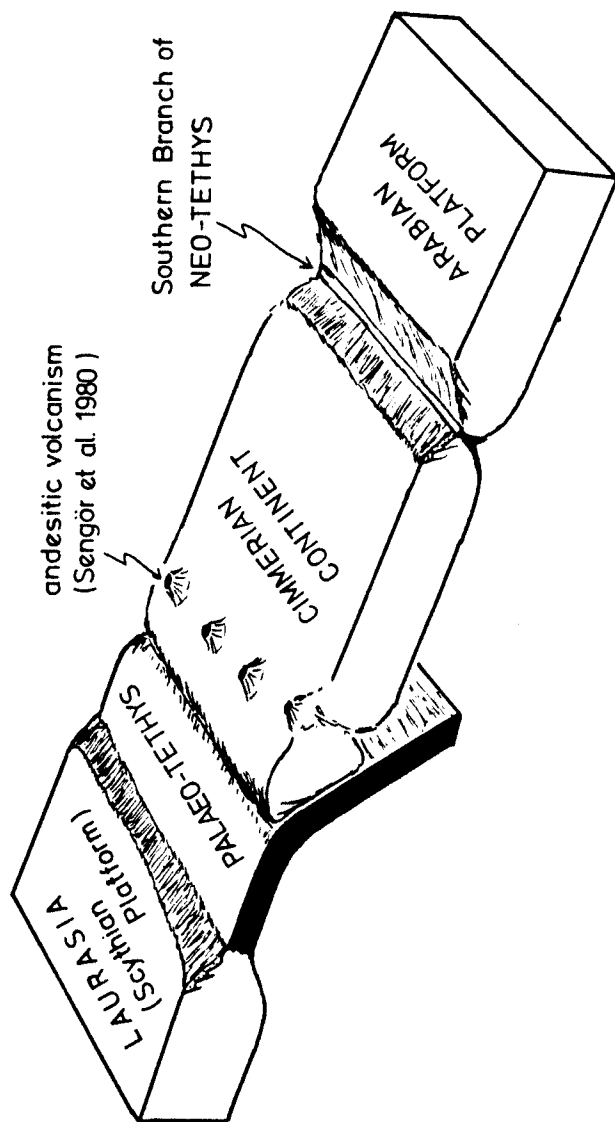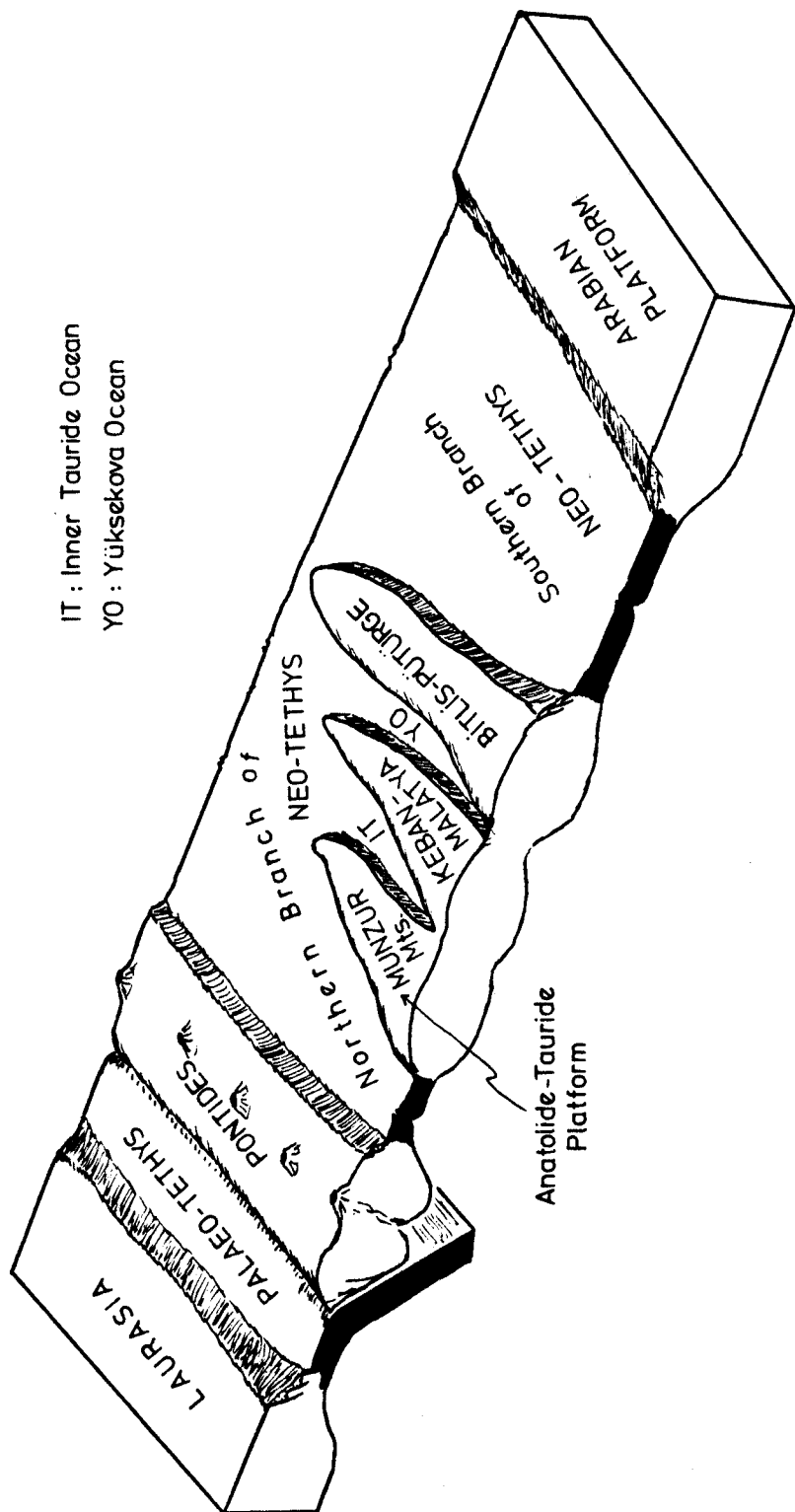
EARLY JURASSIC

IT : Inner Tauride Ocean
YO : Yüksekova Ocean

B

C

Palaeo Tethyan Suture

Tibetan-tye volcanism (Sengör & Yılmaz 1981)

LAURASIA

PONTIDES

Northern Branch of NEO-TETHYS

MUNZUR

IT

KEBAN-MALİ-YO

BITLİS-PÜTÜRGE

Southern Branch of NEO-TETHYS

ARABIAN PLATFORM

MEDIAL JURASSIC

181

D

Palaeo-Tethyan Suture

BLACK SEA Marginal Sea

PONTIDES

mélange wedge (Şengör & Yılmaz 1981)

Northern Branch of NEO-TETHYS

MUNZUR Mts.

KEBAN-MAL.

syenite porphyry intrusion

ophiolite obduction: Ovacık Ophi. (Özgül et al. 1982)

YUKSEKOVA OCEAN

YA

ophiolite obduction: Kocali Oph. (Sungurlu 1974)

BITLIS-PUTURGE

Kastel-Ditch

ARABIAN PLATFORM

MB: Midyat Shelf Basin (Perincek 1979 b)
YA : Yüksekova Island Arc
(Hempton 1982 ; Hempton & Savcı 1982)

LATE CRETACEOUS
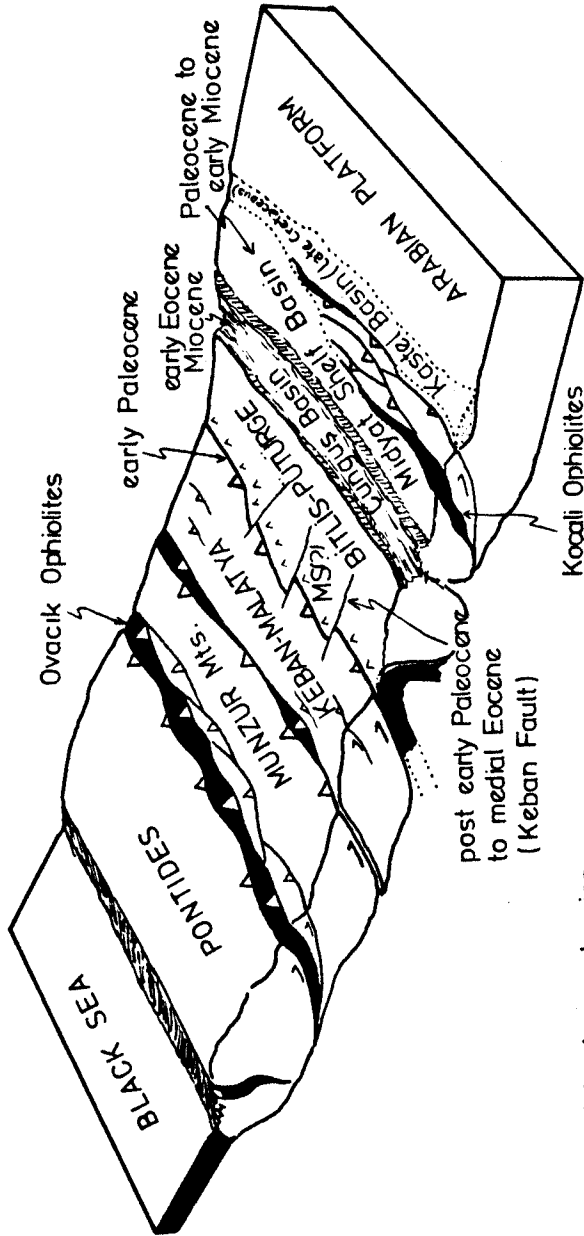
∧∧ Yüksekova Island arc volcanics
(Hempton,1982; Hempton¢Savcı,1982)

MS(?): Maden Strike-slip Basin (?) and/or Marginal Basin (?)
(Aktaş,1982)   (Şengör¢Yılmaz,1981)

PALEOCE - EARLY EOCENE

F
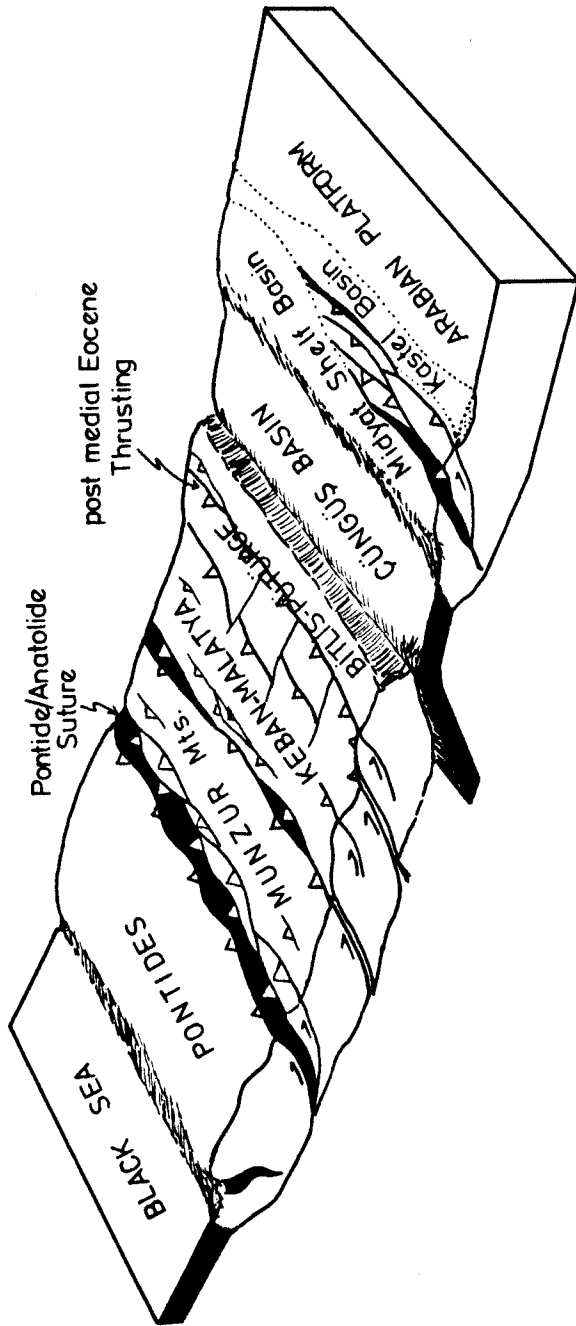
LATE EOCENE

G

MEDIAL MIOCENE

Northern Branch of Neo-Tethyan Sutures

early Paleocene Thrusting

post medial Eocene Thrusting

post early Miocene Thrusting

Pontide/Anatolide Suture

BLACK SEA

PONTIDES

MUNZUR Mts.

KEBAN SLICES

YÜKSEKOVA SLICES

CUNGUŞ SLICES

Lice Molasse

ARABIAN PLATFORM

Southern Branch of Neo-Tethyan Suture
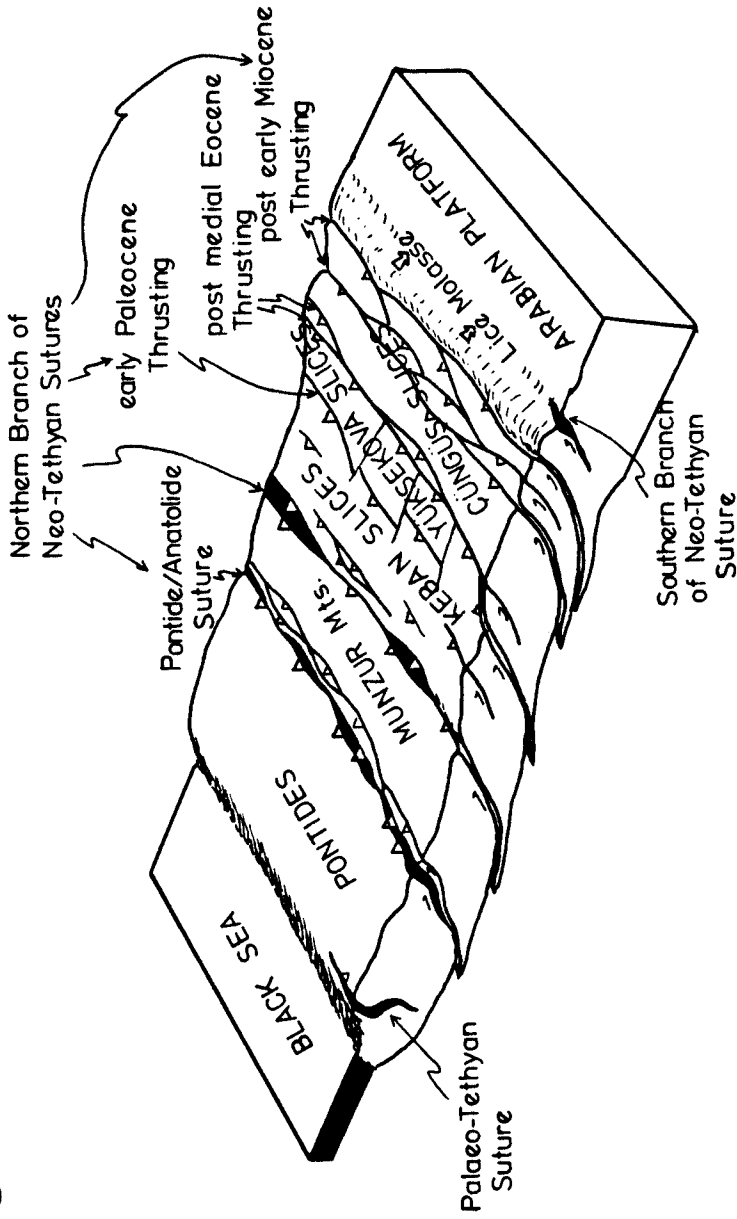
Palaeo-Tethyan Suture

of the absence of data on the Keban-Malatya Metamorphics, in all the
proposed tectonic models (see above section, 4.3), almost all the
researchers thought of the Keban-Malatya Metamorphics as a part of the
Bitlis-Puturge Metamorphics. As is mentioned in Chapter 2.2., the Keban
Metamorphics (over 80% carbonate, and amphibolite interlayers) are a
different lithological assemblage than the Bitlis-Puturge Metamorphics
to the south (over 80% meta-pelite; Hempton, 1982). Moreover, in the
late Cretaceous, the Keban Metamorphics were cut by a distinctive group
of hypabyssal syenites, which may be interpreted to indicate a rifting
event (Burke and Dewey, 1973) (Figure 4.3 D). It is observed that the
Bitlis-Puturge Metamorphics do not show the same lithological and tectonic
features that the Keban Metamorphics show. For example, no sedimentary
deposition has occured on the Keban continental margin sequences during
the whole of Jurassic and Cretaceous times, whereas sedimentary deposition
(such as Simaki flysch: Perincek, 1979b) has occured on the Bitlis-
Puturge continental margin sequences. In other words, after Jurassic-
medial Cretaceous, these two metamorphic masses experienced different
tectonic histories (see Figure 4.3). In addition to these, the ensimatic
Yuksekova island arc complex (Hempton and Savci, 1982) always occupies
an intermediate position between the Keban-Malatya and Bitlis-Puturge
Metamorphics. This implies an existence of an oceanic basin (Yuksekova
Ocean: Figure 4.3 B) between the Keban-Malatya and Bitlis-Puturge micro-
continents. Sengor and Yilmaz (1981) consider that the Keban-Malatya
and the Bitlis-Puturge Metamorphics are segments of the same continental
margin sequences. However, the above results are not consistent with
their tectonic model, Here, I propose that the Keban-Malatya micro-

continent is an independent fragment of the Cimmerian Continent, which

disintegrated in the early Jurassic (Figure 4.3 B), such as the Alanya

Massif and the Bitlis-Puturge Massifs (excluding the Keban-Malatya micro-

continent) described by Sengor and Yilmaz (1981). The inner Yuksekova

Ocean (see Figure 4.3 B) separates the Keban-Malatya micro-continent

in the north from the Bitlis-Puturge micro-continent in the south. This

proposal automatically puts Sengor and Yilmaz's (1981) "Inner Tauride

Ocean" to the north between the Munzur and Keban-Malatya micro-continents

(Figure 4.3 B). The late Cretaceous extensional regime (Figure 4.3 D)

(rifting event: syenite porphyry intrusion; see Chapter 2.2.3) might be

the reason for the south-dipping subduction which created the Yuksekova

Volcanic Complex in late Cretaceous (Sengor and Yilmaz, 1981) (See Figure

4.3 B).

The destruction of the Inner Tauride Ocean occurred in Campanian-

Maastrichtian time between the Munzur and Keban-Malatya micro-continents,

while the Ovacik ophiolite nappes began to climb onto the Anatolide-

Tauride Platform (Munzur). The obduction of the Ovacik nappe occurred

all along the northern margin of the Anatolide-Tauride Platform and

partially on the northern margin of the Keban-Malatya micro-continent

(Ozgul, 1976; Ozgul et al., 1982; Sengor and Yilmaz, 1981) (Figure 4.3 B).

In early Paleocene to Eocene, the Yuksekova ocean closed (Sengor and

Yilmaz, 1981: these authors suggest the Eocene age) and the Keban-

Malatya Complex collided with the Bitlis-Puturge Complex (see Chapter 1

for the description of these complexes) (Figure 4.3 E). Evidence for

strike-slip faulting (Keban Fault) has also been observed in this study

(see Chapter 3.2.5 and 3.42). As is mentioned in previous chapters, the

age of the strike-slip faulting is determined as post early-Paleocene to medial Eocene. Sengor and Yilmaz (1981, p. 221 and 223) state that "the opening of the Maden Basin (they interpret this basin as marginal sea) probably began during the latest Maastrichtian. . . . Maden basin in southeastern Anatolia was about to reach its maximum development in early to middle Eocene-" Here, I would like to emphasize that the age of the strike-slip faulting (Keban Fault) dovetails nicely with the age of the Maden Basin sediments and volcanics. The Maden Complex is interpreted as "marginal sea basin" by Sengor and Yilmaz (1981), and as "near-arc basin" by Hempton (1982). Aktas' (1982) Ph.D work mainly deals with the geochemistry of the Maden Complex. Based on his geochemical result, he suggests that the sediments and volcanics of the Maden Complex were formed in a strike-slip basin. O. Sungurlu (personal communication, 1982) has noticed some parallel palaeo-strike slip faults along the Bitlis Suture Zone. He has also noticed that the volcanics of the Maden Complex are usually located between these faults. He is planning to map these volcanics and faults in order to better understand their geotectonic implication. Although there is not yet any strong evidence to support the idea that the Maden Complex was formed within a strike-slip basin, from the foregoing discussion and the conformity of the age of the Keban strike-slip faulting, I suggest that the Maden Complex might have been formed within a strike-slip basin which might also have been a marginal basin (Figure 4.3 E). But I believe that the interpretation of the Maden Complex will only be possible after the completion of detailed mapping of southeastern Turkey.

Yuksekova Volcanic Complex

The mafic extrusives and volcaniclastics metamorphosed to lower greenschist facies represent the Yuksekova Volcanic Complex in the study area. This lithology resembles the "Unit 1" that Hempton and Savci (1982) defined and the "basalt unit" that Hempton (1982) described to the south of Elazig city. The Yuksekova Volcanic Complex is renamed as Elazig Volcanic Complex for the Elazig-Sivrice area by these authors. The structural and lithological criteria Hempton and Savci (1982) employed led them to suggest that the volcanic complex represented an ensimatic island arc such as the Tongo-Kermadec island arc complex described by Bryan et al. (1972). The immature type of island arc development have been discussed by many workers. Miyashiro (1974) shows that there are two main volcanic rock series in island arcs such as calc-alkalic (CA) and tholeiitic (TH), and very rare alkalic (A). The first two are called the non-alkalic series by the same author. The non-alkalic group was assigned various names such as subalkalic, calc-alkalic, and calcic by different workers. Miyashiro (1974) claims that the reaction series for the non-alkalic series (both CA and TH) is basalt→andesite→dacite→ rhyolite. The main rock types in primitive island arc series are usually basalt and basaltic andesite of the TH series, whereas those in well developed island arcs with a thick continental type crust are basalt, andesite, dacite and rhyolites of the TH and CA series (Miyashiro, 1974) (Table 4.1). In active island arcs and in mature state of their develop-ment such as northeast Japan and Kamchatka, petrographic provinces of the TH series and CA series are present successively in the above order from the oceanic to the continental side of the volcanic belt, though

Table 4.1. Characteristics of Immature and Well-developed (mature) Island Arcs.

AREA	PRIMITIVE ISLAND-ARC	WELL-DEVELOPED ISLAND-ARC
VOLCANIC ROCK SERIES	TH	TH + CA
MAIN ROCK TYPE	basalt, basaltic andesite, andesite	andesite, dacite, rhyodacite and rhyolite
PROVINCES AND REFERENCES	Tongo-Kermadec island arc (Bryan et al., 1972) Elazig (Yuksekova) Volcanic Complex (Hempton and Savci, 1982)	Japan Arc (Miyashiro, 1972)

there may be marked overlapping of provinces (Miyashiro, 1973). It is generally supposed that the earliest phases of island arc generation are characterized by massive outpourings of TH basalt which builds a foundation upon which more differentiated volcanics are later extruded. Kuno (1950) classified non-alkalic volcanic rocks of Japan into the hypersthenic (H series) and pigeonitic (P series) rock series. Kuno (1959, 1966, 1968) regarded his hypersthenic and pigeonitic series as representing volcanic suites of the CA and TH series respectively. Jakes and Gill (1970) proposed the term "island arc tholeiite series" for primitive volcanic regime in island arcs, whereas Donnelly and Rogers (1980) label it the "primitive island arc series." While the latter two studies are based on geochemical criteria, Miyashiro (1974) presented histograms showing relative proportions of island arc lithologies within selected well-known arcs. He shows that the immature arcs are characterized by greater proportions of more mafic rocks (basalt, basaltic andesite, and andesite) while older arcs possess greater proportions of more differentiated rocks (dacite, rhyodacite, and rhyolite) (Table 4.1).

The Yuksekova Volcanic rocks are represented mostly by dacite and rhyodacite around the Pertek-Palu area (F. Bingol, personal communication, 1981). Based on the above discussion, this level of the volcanic complex may represent the more differentiated mature-last phase of the island arc activity which developed upon Hempton and Savci's (1982) immature island arc.

This study shows that the Yuksekova Volcanic Complex always occupies an intermediate position between the Keban-Malatya and the Bitlis-Puturge Metamorphics. Hempton (1982) and Hempton and Savci (1982) proposed that

the Yuksekova Volcanics are an ensimatic island arc lithology. Based on these authors' data and with comparison with the Bolkardag region, Sengor and Yilmaz (1981) suggest a late Cretaceous south-dipping subduction zone beneath the ophiolite-laden Bitlis-Puturge micro-continent in order to produce the Yuksekova Volcanic Complex. As is mentioned above, the late Cretaceous extensional regime occurred in the Keban-Malatya continent might be the reason for the south-dipping subduction (Figure 4.3 D).

REFERENCES

Adamia, S., Bergougnan, H., Fourguin, C., Haghipour, A., Lordkipanidze, M., Ozgul, N., Ricou, L.E. and Zakariadze, G., 1980, The Alpine Middle East between the Aegean and the Oman Traverses: in Aubouin, J., Debelmas, J. and Latreille, M., eds., Geology of the Alpine Chains Born of the Tethys: Memoire du B.R.G.M., no. 115 p. 122-136.

AGI Glossary, 1972, Dictionary of Geological Terms, Anchor Press, NY, 545 pp.

Aktas, G., 1982, Significance of the Maden Complex (SE Turkey) for the Cretaceous and Tertiary development of the Eastern Tethys: The Geological Evolution of the Eastern Mediterranean Abstracts, Edinburgh, p. 8.

Altinli, E., 1963, Geological Map of Turkey, scale 1/500,000, Erzurum Sheet with Explanatory Text, MTA Ankara.

Bastug, M.C., 1976, Bitlis napinin stratigrafisi ve Guneydogu Anadolu sutur zonunun evrimi: Yeryuvari ve Insan, v. 1., p. 55-61.

_____, 1980, Sedimentation, deformation, and melange emplacement in the lice basin, Dicle-Karabegan area, Southeast Turkey; Ph.D dissertation, Middle East Technical University, Ankara, Turkey, 458 pp.

Baykal, F., 1966, Geological Map of Turkey, scale 1/500,000, Sivas Sheet with Explanatory Text, MTA Ankara.

Bell, A.M., 1981, Vergence: an evaluation: Jour. Structural Geology, v. 3, p. 197-202.

Bergougnan, H. and Fourguin, C., 1982, Remnants of a pre-Late Jurassic Ocean in northern Turkey: Fragments of Permian-Triassic Paleo-Tethys?: Discussion: Geol. Society of Am. Bull., v. 93, p. 929-932.

Berthe, D., Choukroune, P. and Jegouzo, 1979a, Orthogneiss, mylonite and non coaxial deformation of granites: the example of the South Armorican Shear Zone: Jour. Structural Geology, v. 1, p. 31-42.

Berthe, D., Choukroune, P. and Gapais, D., 1979b, Orientations preferentielles du quartz et orthogneissification progressive en regime cisaillant: l'exemple du cisaillement sudarmoricain: Bull. Mineral. v. 102, p. 265-272.

Boray, A., 1972, The Structure and Metamorphism of the Bitlis area, SE Turkey: Ph. D. Dissertation, London Univ., 233 pp.

_____, 1975, Bitlis dolayinin yapisi ve metamorfizmasi: Bull. Geol. Society of Turkey, v. 18, p. 81-84.

Borchert, H., 1952, Keban cevher yataklarinda yapilan tetkikata dair rapor: unpublished MTA report.

Brinkmann, R., 1976, Geology of Turkey, Enke. Stuttgart, 158 pp.

Brunn, J., 1979, Oceanisations of East Mediterranean crust, Tauric and Aegean inducted arc and ophiolites: Rapp. Comm. Int. Mer. Medit., v. 25/26, 2a, p. 99-101.

Bryan, W.B., Stice, G.D., and Ewart, A., 1972, Geology, petrography and geochemistry of the volcanics islands of Tonga: Am. Geophy. Union, v. 77, p. 1565-1585.

Burke, K. and Dewey, J.F., 1973, Plume generated triple junctions: key indicators in applying plate tectonics to old rocks: Jour. Geology, v. 81, p. 406-433.

Canitez, N., and Toksoz, M.N., 1980, Crustal structure beneath Turkey: EOS Transactions, Am. Geophy. Union, v. 61, no. 17, p. 290.

Carter, N.L. and Raleigh, C.B., 1969, Principal stress directions from plastic flow in crystals: Geol. Society of Am. Bull., v. 80, p. 1231-1264.

Cobbold, P.R., 1977, Description and origin of banded structures. II Rheology and the growth of banded perturbations: Canad. Jour. Earth Sci., v. 14, p. 2510-2523.

Cobbold, P.R. and Quinquis, H., 1980, Development of sheath folds in shear regimes: Jour. Structural Geology, v. 2, p. 119-126.

Delaune-Mayere, M., Marcoux, J., Parrot, J.F. and Poisson, A., 1977, Molele d'evolution Mesozoique de la paleo-marge tethysienne au niveau des nappes radiolaritiques et ophiolitiques du Taurus Lycien, d'Antalya et du Baer-Bassit: in; Biju-Duval, B. and Montadert, L. (eds.), Structural History of the Mediterranean Basins. Editions Technip, Paris, p. 79-94.

Dewey, J.F. and Bird, J.M., 1970, Mountain belts and the new global tectonics: Jour. Geophy. Res., v. 75, p. 2625-2647.

Dewey, J.F. and Spall, H., 1975, Pre-Mesozoic plate tectonics: How far back in earth history can the Wilson Cycle be extended?: Geology, v. 3, p. 422-424.

Dewey, J.F. and Sengor, A.M.C., 1979, Aegean and surrounding regions: complex multi-plate and continuum tectonics in a convergent zone: Geol. Society of Am. Bull., v. 90, p. 84-92.

Dewey, J.F., Pitman, W.C. III., Ryan, W.B.F. and Bonnin, J., 1973, Plate tectonics and the evolution of the Alpine system: Geol. Society of Am. Bull., v. 84, p. 3137-3180.

Donnelly, T.W. and Rogers, J.J.M., 1980, Igneous series in island
    arcs: the northeastern Caribbean compared with world wide island
    arc assemblages: Bull. Volcanol., v. 43/2, p. 347-382.

E.I.E.I., 1972, Keban projesi rezervuar sol sahili muhtemel su kacak
    yollarinin arastirilmasi: E.I.E.I. unpublished report no. 72, 19 pp.

Erdogan, B., 1977, Geology, geochemistry and genesis of the sulphide
    deposits of the Ergani-Maden region, SE Turkey: Ph.D. Thesis,
    University of New Brunswick, Canada, 288 pp.

Fischback, 1900, Keban gumus madeni hakkinda rapor: M.T.A. unpublished
    report no. 384.

Gapais, D., 1979, Deformation progressive d'un quartzite dans une zone
    plissee (segment Hercynien de Bretagne Centrale): Bull. Mineral.,
    v. 102, p. 249-264.

Gapais, D. and White, S.H., 1982, Ductile shear bands in a naturally
    deformed quartzite: Textures and Microstructures, v. 5, p. 1-17.

Gawlik, J., 1958, Keban (Elazig) prospeksiyon raporu: M.T.A. unpublished
    report no. 3096

Gosh, S.K. and Ramberg, H., 1976, Reorientation is inclusions by a
    combination of pure shear and simple shear: Tectonophysics, v.34,
    p. 1-70.

Gray, D.R., 1981, Cleavage-fold relationships and their implications
    for transected folds: an example from southwest Virginia, U.S.A.:
    Jour. Structural Geology, v. 3, p. 265-277.

Gutnic, M., Monod, O., Poisson, A. and Dumont, F.D., 1979, Geologie
    des Taurides occidentales (Turquie): Mem. Soc. Geol. Fr., N.S.,
    v. 58, 112 pp.

Hall, R., 1974, The structure and petrology of an ophiolitic melange
    near Mutki, Bitlis province, Turkey: Ph.D. Thesis, London Univer-
    sity, London, 351 pp.

_____, 1976, Ophiolite emplacement and the evolution of the Taurus
    Suture zone, southeastern Turkey: Geol. Society of Am. Bull.,
    v. 87, p. 1078-1088.

Hempton, M.R., 1982, Structure of the Northern Margin of the Bitlis
    Suture Zone near Sivrice, Southeastern Turkey: Ph. D. dissertation,
    S.U.N.Y.-Albany, 389 pp.

Hempton, M.R. and Savci, G., 1981, Structure and tectonic significance
    of the late Cretaceous Yuksekova island arc complex, SE Turkey:
    Geol. Soc. Am. Annual Meeting, Abstracts with Program, v. 13,
    no. 7, p. 471.

Hempton, M.R. and Savci, G., 1982, Elazig volkanik karmasiginin petrolojik ve yapisal ozellikleri: Bull. Geol. Society of Turkey, v. 25, p. 143-150.

Hobbs, B.E., Means, W.D. and Williams, P.F., 1976, An Outline of Structural Geology, John Willey and Sons, Inc., NY, 571 pp.

Horstink, J., 1971, The late Cretaceous and Tertiary geological evolution of Eastern Turkey: First Petroleum Congress of Turkey, Proceedings, p. 25-41.

Ilhan, E., 1974, Eastern Turkey: in Spencer, A.M., ed., Mesozoic-Cenozoic orogenic belts: Scottish Academy Press: Edinburgh, p. 187-197.

Innocenti, F., Mazzuoli, R., Pasquare, G., Radicati di Brozolo, F. and Villari, ., 1975, The Neogene calc-alkaline volcanism of Central Anatolia: geochronological data on Kayseri-Nigde area: Geol. Magazine, v. 112, p. 349-360.

Innocenti, F., Mazzuoli, R., Pasquare, G., Radicati di Brozolo, F. and Villari, F., 1976, Evolution of the volcanism in the area of interaction between the Arabian, Anatolian and Iranian plates (lake Van, Eastern Turkey): Journal of Volcanology and Geothermal Research, no. 1, p. 103-112.

Jakes, P. and Gill, J., 1970, Rare earth elements and the island arc tholeiitic series: Earth and Planetary Sci. Letters, v. 9, p. 17-28.

Kerr, P.F., 1977, Optical Mineralogy, McGraw Hill, NY, 492 pp.

Ketin, I., 1959, Turkiye'nin orojenik gelismesi: M.T.A. Dergisi, v. 53, p. 78-86.

_____, 1966, Tectonic units of Anatolia: Bull. Min. Res. Expl. Inst. Turkey, v. 66, p. 23-24.

Kines, T., 1971, The geology and the ore mineralization in the Keban area, E. Turkey: Ph.D. dissertation, Durham University.

Kipman, E., 1981, Keban'in jeolojisi ve Keban saryaji: Istanbul Yerbilimleri Mecmuasi, v. 1, p. 75-81.

_____, 1982, Keban volkanitlerinin petrolojisi: Istanbul Yerbilimleri Mecmuasi, v. 2, p. 203-230.

Kovenko, V., 1941, Keban madeni etudu hakkinda rapor: M.T.A. unpublished report no. 1255.

Kumbasar, I., 1964, Keban Bolgesindeki cevherlesmelerin petrografik ve metalojenik etudu: Ph.D. Thesis, I.T.U., Istanbul, 114 pp.

Kuno, H., 1950, Petrology of Hakone volcano and the adjacent areas, Japan: Geol. Society of A. Bull., v. 61, p. 957-1020.

_____, 1959, Origin of Cenozoic petrographic provinces of Japan and surrounding areas: Bull. Volcanol., v. 20/2, p. 37-76.

_____, 1966, Lateral variation of basaltic magma type across continental margins and island arcs: Bull. Volcanol., v. 29, p. 195-222.

_____, 1968, Origin of andesite and its bearing on the island arc structure: Bull. Volcanol., v. 32/2, p. 141-176.

Lambert, R.S.J., Holland, J.G. and Owen, P.F., 1974, Chemical petrology of calcalkaline lavas from Mt. Ararat, Turkey: Jour. Geology, v. 82, p. 419-438.

M.T.A., 1961a, Geological Map of Turkey, scale 1/500,000, Erzurum sheet: M.T.A. Institute, Ankara.

M.T.A., 1961b, Geological Map of Turkey, scale 1/500,000, Sivas sheet: M.T.A. Institute, Ankara.

M.T.A., 1962, Explanatory text of the geological map of Turkey, scale 1/500,000, Diyarbakir sheet, M.T.A. Institute, Ankara, 69 pp.

M.T.A., 1963-1966, Geological Map of Turkey, scale 1/500,000, M.T.A., Ankara.

Maucher, A., 1973, Keban maden zuhurati hakkinda mineralojik rapor: M.T.A. unpublished report no. 406.

Mitchell, A.H. and Reading, H.G., 1969, Continental margins, geosynclines and ocean floor spreading: Jour. Geology, v. 77, p. 629-649.

Miyashiro, A., 1972, Metamorphism and related magmatism in plate tectonics: Am. Jour. Sci., v. 272, p. 629-656.

_____, 1973, Metamorphism and Metamorphic Belts: George Allen and Unwin, London, 492 pp.

_____, 1974, Volcanic rock series in island arcs and active continental margins: Am. Jour. Sci., v. 274, p. 321-355.

Nockolds, S.R., Knox, R.W.O'B. and Chinner, G.A., 1978, Petrology: Cambridge Univ. Press, Cambridge, 435 pp.

Oelsner, 1938, Keban madeni hakkinda rapor: M.T.A. unpublished report.

Ota, R. and Dincel, A., 1975, Volcanic rocks of Turkey: Bull. Geol. Survey of Japan, v. 26, p. 19 (393)-45(419).

Ozgul, N., 1976, Ibroslarin bazi temel jeoloji ozellikleri, Bull. Geol. Society of Turkey, v. 19, p. 65-78.

Ozgul, N., Tursucu, A., Ozyardimci, N., Bingol, I., Senol, N. and Uysal, S., 1982, Munzur daglarinin jeolojisi: M.T.A. unpublished report.

Ozkaya, I., 1972, The Mio-Eugeosynclinal Thrust Interface on Related Petroleum Implications in the Sason-Baykan Area, SE Turkey; Ph.D. dissertation, Univ. of Missouri, Rolla.

_____, 1974, Stratigraphy of Sason and Baykan areas, SE Turkey: Bull. Geol. Society of Turkey, v. 17, p. 51-73.

_____, 1978, Geology of the Yuksekova-Semdinli area: Proc. 4th Petrol. Congr., Turkey, p. 62-81.

_____, 1982, Upper Cretaceous plate rupture and development of leaky transcurrent fault ophiolites in southeast Turkey: Tectonophysics, v. 88, p. 103-116.

Ozpeker, I., 1973, Nemrut yanardaginin volkanolojik incelenmesi: T.B.T.A.K. IV. Bilim Kongresi, p. 1-17.

Passchier, C.W., 1982, Mylonitic Deformation in the Saint-Barthelemy Massif, French Pyrenees, with Emphasis on the Genetic Relationship between ultramylonite and Pseudotachlyte: Ph.D. dissertation, Univ. Amsterdam: Gua Papers of Geology, Series 1, no. 16, 173 pp.

Perincek, D., 1978, Researching petroleum possibilities and geological study of Celikhan-Sincik-Kocali (Adiyaman city) region: Ph.D. dissertation, Univ. Istanbul: T.P.A.O. unpublished report no. 1250, 212 pp. (in Turkish).

_____, 1979a, Palu, Karabegan, Elazig, Sivrice, Malatya alaninin jeolojisi ve petrol imkanlari: T.P.A.O. unpublished report no. 1361, 33 pp.

_____, 1979b, Guidebook for excursion "B" Interrelations of the Arab and Anatolian plates: First Geol. Congr. on Middle East, Ankara, Turkey, 34 pp.

_____, 1980, Sedimentation on the Arabian shelf under the control of tectonic activity in Taurid Belt: Fifth Petroleum Congr. Turkey, Ankara, p. 77-93.

_____ and Ozkaya, I., 1981, Tectonic evolution of the northern margin of Arabian plate: Bull. Institute of Earth Sciences of Hacettepe Univ., Ankara, v. 8, p. 91-101.

Pettijohn, F. J., 1957, Sedimentary rocks : New York, Harper and Row, 628 pp.

Platt, J.P., 1979, Extensional crenulation cleavage: Jour. Structural Geology, v.1, p. 95-96.

Platt, J.P. and Vissers, R.L.M., 1980, Extensional structures in aniso-tropic rocks : Jour. Structural Geology, v.2, p. 397-410.

Powell, M.McA. and Vernon, R.H., 1979, Growth and rotation history of garnet porphyroblasts with inclusion spirals in a Karakoram schist: Tectonophysics, v. 54, p. 25-43.

Ramsay, J.G., 1967, Folding and Fracturing of Rocks: McGraw-Hill, NY, 568 pp.

____, 1980, Shear zone geometry: a review: Jour. Structural Geology, v. 2, p. 83-99.

Ricou, L.E., Argyriadis, I. and Lefevre, R., 1974, Proposition d'une origine interne pour les nappes d'Antalya et le massif d'Alanya (Taurides occidentales, Turquie): Bull. Soc. Geol. Fr., Ser. 7, v. 16, p. 107-111.

Ricou, L.E., Argyriadis, I. and Marcoux, J., 1975, L'Axe calcaire du Taurus, un alignement de fenetres Arabo-Africains sous des nappes radiolaritiques, ophiolitiques et metamorphiques: Bull. Soc. Geol. Fr., Ser. 7, v. 17, p. 1024-1044.

Ricou, L.E., Marcoux, J. and Poisson, A., 1979, L'allochtonie des Bey Daglari orientaux, Reconstruction palinspastique des Taurides occidentales: Bull. Soc. Geol. Fr., Ser. 7, v. 21, p. 125-133.

Rigo de Righi, M. and Cortesini, A., 1964, Gravity tectonics in foothills structure belt of southeastern Turkey: Bull. Am. Ass. Petroleum Geologists, v. 48, p. 1911-1937.

Sagiroglu, G., 1952, Keban volfram zuhurati hakkinda rapor: M.T.A. unpublished report no. 1942.

Savci, G., 1980, Dogu Anadolu volkanizmasinin neotektonik onemi: Yeryuvari ve Insan, v. 5, p. 46-49.

Selley, R.C., 1978, Ancient Sedimentary environments; 2nd edition; Cornell Univ. Press, Ithaca, NY, 287 pp.

Sengor, A.M.C., 1979a, Mid-Mesozoic closure of Permo-Triassic Tethys and its implications: Nature, v. 279, p. 590-593.

____, 1979b, The North Anatolian transform fault: its age, offset and tectonic significance: Jour. Geol. Soc. London, v. 136, p. 269-282.

____, 1980, Turkiye'nin neotektoniginin esaslari: Turkiye Jeoloji Kurumu, Konferanslar Serisi, no. 2, 40 pp.

Sengor, A.M.C. and Burke, K., 1978, Relative timing of rifting and volcanism on earth and its tectonic implications: Geophysical Res. Letters, v. 5, p. 419-421.

Sengor, A.M.C. and Kidd, W.S.F., 1979, Post-collisional tectonic of the Turkish-Iranian Plateau and comparison with Tibet: Tectonophysics, v. 55, p. 361-376.

Sengor, A.M.C. and Yilmaz, Y., 1981, Tethyan evolution of Turkey: a plate tectonic approach: Tectonophysics, v. 75, p. 181-241.

Sengor, A.M.C., White, G.W. and Dewey, J.F., 1979, Tectonic evolution of the Bitlis Suture, southeastern Turkey: implications for the tectonics of the eastern Mediterranean: Rapp. Comm. Int. Mer Medit., v. 25/26-2a, p. 95-97.

Sengor, A.M.C., Yilmaz, Y. and Ketin, I., 1980, Remnants of a pre-Late Jurassic ocean in northern Turkey: Fragments of Permian-Triassic Palaeo-Tethys: Geol. Society of Am. Bull., v. 91, p. 499-609.

Sengor, A.M.C., Yilmaz, Y. and Ketin, I., 1982, Remnants of a pre-Late Jurassic ocean in northern Turkey: Fragments of Permian-Triassic Palaeo-Tethys?: Reply: Geol. Society of Am. Bull., v. 93, p. 932-936.

Sibson, R.H., 1977, Fault rocks and fault mechanisms: Jour. Geol. Soc. London, v. 133, p. 191-213.

Simpson, C., 1983, Strain and shape-fabric variations associated with ductile shear zones: Jour. Structural Geology, v. 5, p. 61-72.

Simpson, C. and Schmid, S.M., in press, Some criteria to deduce the sense of movement in sheared rocks: Geol. Soc. Am. Bull.

Sungurlu, O., 1974, VI. bolge kuzey sahalarinin jeolojisi: in Okay, H. and Dilekoz, E., eds., Second Petroleum Congr. of Turkey, Ankara, p. 85-107.

Sungurlu, O., 1979a, GD Anadolu suruklenim kusagi Kretase suruklenimleri: 33 Turkiye Jeoloji Bilimsel ve Teknik Kurultayi, Bildiri Ozetleri, Ankara, p. 119-120.

_____, 1979b, Guneydogu Anagolis suruklenim kusagi Ust Tersiyer suruklenimleri: 33 Turkiye Jeoloji Bilimsel ve Teknik Kurultayi, Bildiri Ozetleri, Ankara, p. 121-122.

Tilford, N.R. and Ciloglu, I., 1969, Keban baraji temel problemleri: Turkiye'nin En Buyuk Projeleri; Keban ve Asagi Firat (D.S.I.), p. 25-27.

Tolun, N., 1955, Keban'in jeolojik etudu: M.T.A. unpublished report no. 2227.

Travis, R.B., 1955, Classification of Rocks: Quarterly of the Colorado School of Minenes, v. 50, no. 1., 98 pp.

Turner, F.J., 1948, Note on the tectonic significance of deformation lamellae in quartz and calcite: Am. Geophys. Union Trans., v. 29, p. 565-569.

_____, 1953, Nature and dynamic interpretation of deformation lamellae in calcite of three marbles: Am. Jour. Sci., v. 251, p. 276-298.

Turner, F.J. and Weiss, L.E., 1963, Structural analysis of metamorphic tectonites: McGraw-Hill, NY, 545 pp.

Vauchez, A., 1980, Ribbon texture and deformation mechanisms of quartz in a mylonitized granite of Great Kabylie (Algeria): Tectonophysics, v. 67, p. 1-12.

Watts, M.J. and Williams, G.D., 1979, Fault rocks as indicators of progressive shear deformation in the Guingamp region, Brittany: Jour. Structural Geology, v. 1, p. 323-332.

Weiss, L.E. and McIntyre, B., 1957, Structural geometry of Dalradian rocks at Loch Leven, Scottish Highlands: Jour. Geology, v. 65, p. 575-602.

White, S.H., 1979, Grain and sub-grain size variations across a mylonite zone: Contr. Mineral. Petrol., v. 70, p. 193-202.

White, S.H., Evans, D.J. and Zhong, D-L., 1982, Fault rocks of the Moine thrust zone: microstructures and textures of selected mylonites: Textures and Microstructures, v. 5, p. 33-61.

White, S.H., Burrows, S.E., Carreras, J., Shaw, N.D. and Humphreys, F.J., 1980, On mylonites in ductile shear zones: Jour. Structural Geology, v. 2, p. 175-187.

Williams, P.F., 1970, A criticism of the use of style in the study of deformed rocks: Geol. Society of Am. Bull., v. 81, p. 3283-3296.

Wilson, J.T., 1965, A new class of faults and their bearing on continental drift: Nature, v. 207, p. 343-347.

Winkler, H.G.F., 1979, Petrogenesis of Metamorphic Rocks: 5th Edition, Springer-Verlag, NY, 348 pp.

Yalcin, N., 1979, Orta Amanoslarin Jeolojisi ve Petrol Olanaklari: Ph.D. dissertation, Univ. Istanbul, 82 pp.

Yazgan, E., 1981, Dogu Toroslarda etkin bir paleo-kita kenari etudu (Ust Kretase-Orta Eosen) Malatya-Elazig, Dogu Anadolu: Bull. Institute of Earth Sciences of Hacettepe Univ., Ankara, v. 7, p. 83-104.

Yener, H., 1935, Keban madeni hakkinda: M.T.A. unpublished report.

Zusermann, A., 1969, Geological and mining study of Keban maden:
    Etibank Genel Mudurlugu Icin Ozel Rapor.